UNIVERSITY OF CALIFORNIA
RIVERSIDE

Kinematic and Neuromuscular Basis of Arboreal Locomotion in *Anolis* Lizards

A Dissertation submitted in partial satisfaction
of the requirements for the degree of

Doctor of Philosophy

in

Evolution, Ecology, and Organismal Biology

by

Kathleen Lois Foster

June 2016

Dissertation Committee:
Dr. Timothy E. Higham, Chairperson
Dr. Mark A. Chappell
Dr. Scott N. Currie

The Dissertation of Kathleen Lois Foster is approved:

_____

_____

_____

Committee Chairperson

University of California, Riverside

ACKNOWLEDGEMENTS

I would like to thank my supervisor and committee for their guidance and support during the course of my dissertation and Dr. Brian Brown for his input on statistical analyses. Funding was provided by the Natural Sciences and Engineering Research Council of Canada (PGSD-405019-2011), and the University of California, Riverside awarded to KLF as well as start up funds provided by Clemson University and an NSF grant (NSF IOS-1147043) awarded to TEH.

The text of this dissertation, in part, is a reprint of the material as it appears in The Journal of Experimental Biology (July 1, 2012) and Proceedings of the Royal Society B (May 7, 2014). The co-author (Timothy E. Higham) listed in these publications directed and supervised the research, which forms the basis for this dissertation.

ABSTRACT OF THE DISSERTATION

Kinematic and Neuromuscular Basis of Arboreal Locomotion in *Anolis* Lizards

by

Kathleen Lois Foster

Doctor of Philosophy, Graduate Program in Evolution, Ecology, and Organismal Biology
University of California, Riverside, June 2016
Dr. Timothy E. Higham, Chairperson

Locomotion is an integral component of the majority of behaviors that dictate the survival of vertebrates. However, the environments through which animals move are often heterogeneous. The arboreal habitat may be one of the most challenging environments due to its wide variation in substrate incline, diameter, compliance, and texture. This array of structural challenges places extreme and varied demands on the locomotor system that muscles, as the units that power this system, must be able to cope with. Although we have a good understanding of the kinematic and neuromuscular modifications employed by animals encountering different inclines, we know virtually nothing about how other structural challenges affect locomotor behavior and *in vivo* muscle function. In this dissertation, I used a combination of high-speed video, electromyography, *in situ* contractile experiments, and morphology to understand how arboreal *Anolis* lizards modulate their behavior and power cyclical locomotion on surfaces of varying incline and perch diameter. Several significant results emerged. First, the forelimb and hind limb were modulated differently in response to changes in substrate; the forelimb likely adopts a greater propulsive role and the hind limb a more stabilizing role on steeper inclines and narrower surfaces. Second, there was a

decoupling of the response of limb movements and motor patterns to changes in substrate; perch diameter had a stronger effect on kinematics than incline, whereas muscle activity was more strongly affected by incline than by perch diameter. Third, not only does muscle recruitment, operating length, and capacity for force production change with perch diameter to allow the gastrocnemius, a primary ankle extensor, to contribute more to propulsion on broader than on narrower surfaces, but incline appears to alter the relationship between muscle recruitment and efficiency of force production. Finally, hind limb tendons do not appear to have the potential to stretch and store significant elastic energy during cyclical locomotion in *Anolis* lizards. Together these data force us to acknowledge the complex nature of mechanisms that power locomotion in the natural world. The environment can clearly have a profound impact on both the coordinated function of limbs and the neural control and physiology of the muscles that power locomotor behaviors.

Table of Contents

List of Figures

List of Tables

Introduction

Locomotion is one of the most important behaviors contributing to the survival of an animal, being integral for such activities as capturing prey, evading predators, and interacting with conspecifics. However, successful execution of these behaviors requires that the animal interact successfully with their environment, which is often highly heterogeneous. Therefore, as muscles are the functional units responsible for powering movement, it is essential that they be able to function effectively under variable conditions.

Numerous aspects of muscles can impact how they function when performing locomotor activities. For example, in terms of morphology, the force that a muscle can generate is a function of its physiological cross-sectional area (PCSA) because with a greater PCSA, a greater number of muscle fibers can contract simultaneously in parallel to contribute to force, assuming maximal stimulation (Haxton, 1944; Alexander, 1977; Sacks and Roy, 1982; Loeb and Gans, 1986; Zaaf et al., 1999; Herzog, 2000; Allen et al., 2010; Lieber and Ward, 2011). The length of muscle fibers affects total mechanical power (Loeb and Gans, 1986; Gans and de Vree, 1987; Biewener, 1998; Biewener and Roberts, 2000; Allen et al., 2010; Lieber and Ward, 2011) and the origin and insertion points of the muscle relative to the joints across which it acts affects its mechanical advantage (Gans and de Vree, 1987; Richmond, 1998; Rassier et al., 1999; Zaaf et al., 1999; Payne et al., 2006; Wilson and Lichtwark, 2011). Mechanical properties of muscles further interact with these morphological variables to determine locomotor capacity. The force a muscle can generate is both length and velocity dependent. Force

production is highest at intermediate muscle lengths (Blix, 1892, 1893, 1894; Loeb and Gans, 1986; Rassier et al., 1999) and is inversely related to the velocity at which it contracts (Hill, 1922, 1938, 1949, 1951, 1953). In addition to these morphological and physiological properties, the neural control of muscle contraction (i.e. timing and intensity of muscle activation) ultimately determines the nature of the locomotor behavior and how that behavior is modified as the animal moves through different regions of its heterogeneous environment (e.g. Gillis and Biewener, 2002; Higham and Jayne, 2004b; Rivera and Blob, 2010).

The arboreal habitat is one of the most challenging terrestrial environments because of the extraordinary variety of substrate inclines, diameters, compliances, and textures over which species must move. When running up an incline, a greater component of gravity acts to resist forward locomotion, increasing locomotor cost and decreasing performance (Taylor et al., 1972; Huey and Hertz, 1982; Cartmill, 1985; Irschick and Jayne, 1998; Zaaf et al., 2001; Daley and Biewener, 2003; Autumn et al., 2006; Schmidt and Fischer, 2011). Narrow substrates may also negatively affect performance because, with any minor deflection of the center of mass away from the middle of the perch, a greater component of gravity acts tangentially along the perch surface, increasing the toppling moment about the perch and decreasing stability (Cartmill, 1985; Losos and Sinervo, 1989; Losos and Irschick, 1996; Preuschoft, 2002; Vanhooydonck et al., 2006a; but see Schmidt and Fischer, 2010).

Numerous studies have examined how animals cope with moving over surfaces of different incline and perch diameter. For example, when moving up inclines, most

animals will adopt a crouched posture to lower their center of mass, decrease stride length, and increase stride frequency (Vilensky et al., 1994; Irschick and Jayne, 1998; Jayne and Irschick, 1999; Zaaf et al., 2001; Nakano, 2002; Higham and Jayne, 2004a; Spezzano and Jayne, 2004; Schmidt and Fischer, 2011). Further, although the hind limbs are primarily responsible for propulsion on horizontal surfaces, the relative contribution of the forelimbs increase with increasing incline and may produce greater propulsive forces than the hind limbs on vertical surfaces (Autumn et al., 2006; Lammers et al., 2006; Lammers, 2007). To move on narrow substrates, animals tend to lower their center of mass, alter the point of contact between the feet and perch, and increase duty factor in order to reduce peak vertical forces and improve stability (Peterson, 1984; Schmitt, 1994; Higham and Jayne, 2004a; Lammers and Biknevicius, 2004; Franz et al., 2005; Lammers, 2007; Schmidt and Fischer, 2010; Gálvez-López et al., 2011).

In addition to these kinematic changes, muscle activity is also altered in response to changes in substrate. For example, whereas timing of activity does not appear to change with changes in incline, the intensity of muscle activity, which reflects the proportion of the muscle that is active, tends to increase with increasing incline because the muscles have to do more work to combat the increasingly negative effect of gravity on forward locomotion (e.g. Carlson-Kuhta et al., 1998; Gillis and Biewener, 2002; Higham and Jayne, 2004b). However, despite what we know about how incline affects muscle function, how perch diameter and other structural aspects of the arboreal environment impact muscle activity and force output remains unclear.

Anolis lizards have become a model system for a number of fields within biology, including evolution, ecology, and physiology (Losos, 1994, 2009). A primary reason for this interest is that they are a spectacular example of convergent evolution; on each the Greater Antilles Islands, anoles have repeatedly evolved ecomorphs (crown-giant, twig, trunk-crown, trunk, trunk-ground, and grass-bush) that have similar suites of morphological, behavioral, and locomotor performance traits that suit the particular regions of the arboreal environment for which they are named (Williams, 1972; Losos, 1992, 1995; Losos, 2009; Mahler et al., 2010; Alföldi et al., 2011). However, despite the fact that the majority of characteristics that define these ecomorphs relate to aspects of their locomotor morphology, behavior, and performance (Losos et al., 1990; Irschick and Losos, 1999; Higham et al., 2001), it is unknown how their internal muscle morphology, not to mention *in vivo* muscle function, impacts how these animals move successfully in the face of extreme arboreal challenges.

In this dissertation, I examine the relative contribution of the forelimb and hind limb of *Anolis carolinensis* moving on several inclines and perch diameters, testing the hypothesis that shifts in orientation and structure will result in differential modulation of kinematics of the forelimbs and hind limbs (Chapter 1). Next, I measure *in vivo* muscle activity in fore- and hind limb muscles in the same species running on the same substrates to test the hypothesis that muscle activity is modulated in response to external demand such that the changes in limb movements observed in the first chapter are coupled with corresponding shifts in muscle activity (Chapter 2). Finally, I combine video and *in vivo* muscle activity analyses with *in situ* contractile experiments and

dissections to build a comprehensive picture of the function of the gastrocnemius muscle in *Anolis equestris* to test the prediction that the gastrocnemius will be more active and/or generate forces more efficiently on broader surfaces rather than narrower surfaces (Chapter 3).

Chapter 1 - How forelimb and hind limb function changes with incline and perch diameter in the green anole, *Anolis carolinensis*

Abstract

The range of inclines and perch diameters in arboreal habitats pose a number of functional challenges for locomotion. To effectively overcome these challenges, arboreal lizards execute complex locomotor behaviors involving both the fore- and hindlimbs. However, few studies have examined the role of forelimbs in lizard locomotion. To characterize how the fore- and hindlimbs differentially respond to changes in substrate diameter and incline, we obtained three-dimensional high-speed video of green anoles (*Anolis carolinensis*) running on flat (9cm wide) and narrow (1.3cm) perches inclined at 0°, 45°, and 90°. Changes in perch diameter had a greater effect on kinematics than changes in incline, and proximal limb variables were primarily responsible for these kinematic changes. In addition, a number of joint angles exhibited greater excursions on the 45^{o} incline compared to the other inclines. *A. carolinensis* adopted similar strategies to maintain stability as other arboreal vertebrates, increasing limb flexion, stride frequency, and duty factor. However, the humerus and femur exhibited several opposite

kinematic trends with changes in perch diameter. Further, the humerus exhibited a greater range of motion than the femur. A combination of anatomy and behavior resulted in differential kinematics between the fore- and hindlimb, and also a potential shift in the propulsive mechanism with changes in external demand. This suggests that a better understanding of single limb function comes from an assessment of both fore-and hindlimbs. Characterizing fore- and hindlimb movements might reveal interesting functional differences between *Anolis* ecomorphs. Investigations into the physiological mechanisms underlying the functional differences between fore- and hindlimb are needed to fully understand how arboreal animals move in complex habitats.

Introduction

Locomotion is essential to an animal's survival and success, integral to such activities as evading predators and finding suitable mates, prey, and habitat (Garland and Losos, 1994). To successfully perform these tasks, animals must deal with their environment and overcome obstacles and challenges that govern or constrain movement. Terrestrial animals often move over a range of speeds, up or down sloped surfaces, on compliant or smooth surfaces, or may be forced to negotiate a discontinuous environment (e.g. Irschick and Jayne, 1999; Kohlsdorf and Biewener, 2006; Olberding et al., 2012). Compared to terrestrial animals, arboreal animals often face a wider range of challenges, including steep inclines and declines, substrate diameters from flat to extremely narrow (e.g. twigs), and obstacles in the forms of leaves or other branches that force the animal to jump or turn (e.g. Higham et al., 2001; Mattingly and Jayne, 2004). Although

behavioural and/or morphological adaptations are commonly associated with this complex habitat structure, little is known about the detailed three-dimensional limb movements during arboreal locomotion.

Changes in incline and perch diameter are among the greatest challenges that arboreal animals encounter. Moving up an incline increases the cost of locomotion by requiring a greater proportion of the locomotor effort to offset the increased influence of gravity (Taylor et al., 1972; Cartmill, 1985; Farley and Emshwiller, 1996; Roberts et al., 1997; Preuschoft, 2002; Daley and Biewener, 2003; Autumn et al., 2006). This increase in muscle work and overall energetic cost of locomotion often leads to decreased locomotor performance (Huey and Hertz, 1982; Irschick and Jayne, 1998; Zaaf et al., 2001; Schmidt and Fischer, 2011). Based on several studies that have examined the effects of incline on kinematics (Vilensky et al., 1994; Irschick and Jayne, 1998; Jayne and Irschick, 1999; Zaaf et al., 2001; Nakano, 2002; Higham and Jayne, 2004a; Spezzano and Jayne, 2004; Schmidt and Fischer, 2011), kinetics (Autumn et al., 2006; Lammers et al., 2006; Lammers, 2007), and motor patterns (Fowler et al., 1993; Carlson-Kuhta et al., 1998; Gabaldón et al., 2001; Gillis and Biewener, 2002; Higham and Jayne, 2004b; Higham and Nelson, 2008), it is clear that incline has variable effects depending on the species. However, a decrease in the height of the center of mass (CoM) and stride length, more posterior hindlimb placement, and increased stride frequency and muscle activity are common responses to incline in both terrestrial generalists and arboreal specialists. Narrower perches increase the chance of falling by constraining foot placement to a narrower base of support (Cartmill, 1985; Preuschoft, 2002), and often result in decreased

performance (Losos and Sinervo, 1989; Losos and Irschick, 1996; Vanhooydonck et al., 2006a; but see Schmidt and Fischer, 2010). This is likely a result of kinematic changes necessary for increased stability; lowering the CoM by adopting a crouched/sprawled posture through greater limb flexion (Peterson, 1984; Schmitt, 1994; Higham and Jayne, 2004a; Franz et al., 2005; Schmidt and Fischer, 2010), and increasing duty factor (Lammers and Biknevicius, 2004; Franz et al., 2005; Lammers, 2007; Gálvez-López et al., 2011) reduce peak vertical forces and are common strategies for dealing with narrow substrates in a range of vertebrate taxa.

Although the hindlimbs are the key propulsors in terrestrial vertebrates, with the forelimbs absorbing collisional energy and acting primarily as brakes (Lammers and Biknevicius, 2004; Autumn et al., 2006; Lee, 2010; Deban et al., 2012), the coordinated function of the fore- and hindlimbs is poorly understood in arboreal vertebrates. Structural differences between the fore- and hindlimbs have been well documented among vertebrates; the pectoral girdle is generally more mobile than the pelvic girdle and structural differences between the glenoid cavity and acetabulum lead to the potential for greater range of motion in the forelimb than the hindlimb (Haines, 1952; Snyder, 1954; Peterson, 1971, 1973, 1974; Jenkins and Goslow, 1983; Peterson, 1984; Reynolds, 1985; Schmitt, 1994; Larson et al., 2001; Lammers, 2007; Zihlman et al., 2011). In most primates, the shallow glenoid cavity with reduced coracoid and acromion processes in the pectoral girdle compared to the deeper acetabulum of the pelvic girdle are likely related, in part, to the greater weight-bearing function of the hindlimbs relative to the mobile forelimbs (Reynolds, 1985; Zihlman et al., 2011). These structural differences between

fore- and hindlimbs tend to be most exaggerated in arboreal species, including primates (Larson et al., 2000), with some of the most extreme examples found in lizards. Antero-posterior translation of pectoral girdle and greater pectoral girdle rotation permits greater long-axis humerus rotational excursion in chameleons (Peterson, 1971, 1973, 1984; Fischer et al., 2010), anoles (Peterson, 1971, 1974) and varanids (Haines, 1952; Jenkins and Goslow, 1983). Comparative fore- and hindlimb function has been related to incline and perch diameter in a variety of arboreal and terrestrial mammals, with the stabilizing limb taking a more lateral position than the propelling limb, although the limb that dominates a particular function depends on the species (Cartmill, 1985; Nakano, 2002; Lammers and Biknevicius, 2004; Lammers et al., 2006; Lammers, 2007; Schmidt and Fischer, 2010, 2011). Although environmental variables affecting hindlimb kinematics in lizards have been studied extensively, especially in terrestrial species (reviewed in Russell and Bels, 2001a), only two studies have investigated forelimb functional changes with incline in lizards (both with geckos), finding more lateral placement and greater duty factor (Zaaf et al., 2001) and a greater propulsive role of the forelimbs (Autumn et al., 2006).

Lizards are among the most proficient of vertebrate climbers and offer some of the most spectacular examples of arboreal adaptations. In particular, the evolution, morphology, and locomotor behavior and performance of *Anolis* ecomorphs, in relation to habitat structure, have been studied extensively (Pounds, 1988; Losos and Sinervo, 1989; Losos, 1990a, b; Losos, 1994; Losos and Irschick, 1996; Irschick and Losos, 1999; Higham et al., 2001; Perry et al., 2004; Toro et al., 2004; Vanhooydonck et al., 2006a).

However, only a single study has examined three-dimensional kinematics of the hindlimb in response to these challenges (Spezzano and Jayne, 2004). In this study, *A. sagrei* decreased hip height, and increased knee flexion, femur retraction, depression, and long-axis rotation to increase stability on narrower and/or steeper surfaces, although perch diameter had a greater overall effect than incline on kinematics. However, this study looked at only a single species and did not examine the forelimb (Spezzano and Jayne, 2004). Since morphological characteristics of muscle, including mass and moment arms, vary greatly between anole species and ecomorphs (Vanhooydonck et al., 2006b; Herrel et al., 2008a) and between other lizards with divergent ecologies (Zaaf et al., 1999; Aerts et al., 2000), we would expect variation in behavioral and functional changes in response to arboreal challenges. Therefore, investigation of the effects of these variables on forelimb kinematics as well as on hindlimb kinematics in other ecomorphs is needed. We investigated fore- and hindlimb kinematics of the green anole, *A. carolinensis*, which is a trunk-crown ecomorph, encountering a wide range of inclines (0^o to 90^o) and substrate diameters (1cm to flat; Mattingly and Jayne, 2004). It uses its arboreal habitat opportunistically, occupying most arboreal and terrestrial substrates in the absence of other species, but moves higher in the trees when living sympatrically with other species. This is exemplified by the competitive interaction between *A. carolinensis* and *A. sagrei*, a trunk-ground species that prefers slightly larger diameters, in Florida (Collette, 1961; Mattingly and Jayne, 2004; Losos, 2009). Its flexibility and competition with *A. sagrei* makes *A. carolinensis* an ideal subject for understanding the kinematic basis of performance changes in arboreal habitats in both fore- and hindlimbs. Although some

kinematic changes associated with lowering CoM and increasing stability on the more challenging surfaces (e.g. increased elbow/knee flexion and/or humerus/femur elevation) are expected based on previous mammalian and lacertilian literature, we expect *A. carolinensis* to modulate forelimb and hindlimb kinematics differently due to anatomical differences between the limbs. However, we expect *A. carolinensis* to modulate hindlimb kinematics similarly to *A. sagrei*, rotating, retracting, and depressing the femur more, and decreasing stride and step lengths on narrower perches and steeper inclines.

Methods

Subjects

Four adult male *Anolis carolinensis* (mass = 6.1 ± 0.7g; SVL = 6.0 ± 0.2cm) were obtained from commercial suppliers and housed individually in 10-gallon aquaria. The aquaria were heated with 100-watt lights for 12 hours per day, and perches in the aquaria allowed the lizards to behaviorally thermoregulate to their preferred active temperature (28-36^{o}C) (Licht, 1968). Additional lights providing a source of UVB were also places above the aquaria. Lizards were fed vitamin-enriched crickets every other day and were given water *ad libitum*.

While our sample size was limited to 4 individuals, statistical significance can still be determined with confidence if the amount of variation with treatments is less than the variation between treatments (Harmon and Losos, 2005). We calculated the standard deviation within treatments for each variable and divided that by the total standard deviation across treatments for each variable and always found less within-treatment

variation than between-treatment variation (within-treatment variation ranged from 14.2% to 88.2% of between-treatment variation). Therefore, our sample size was sufficient to avoid type I errors.

Prior to running trials, several joints were marked with white nail polish in order to enhance visualization in the video. Points included the shoulder/hip, the elbow/knee, the wrist/ankle, and the base and tip of the third metacarpal/fourth metatarsal. The opposite shoulder/hip joint was also marked as was the midpoint between the shoulders and hips, to aid in determining pectoral/pelvic girdle rotation (Fig. 1.1).

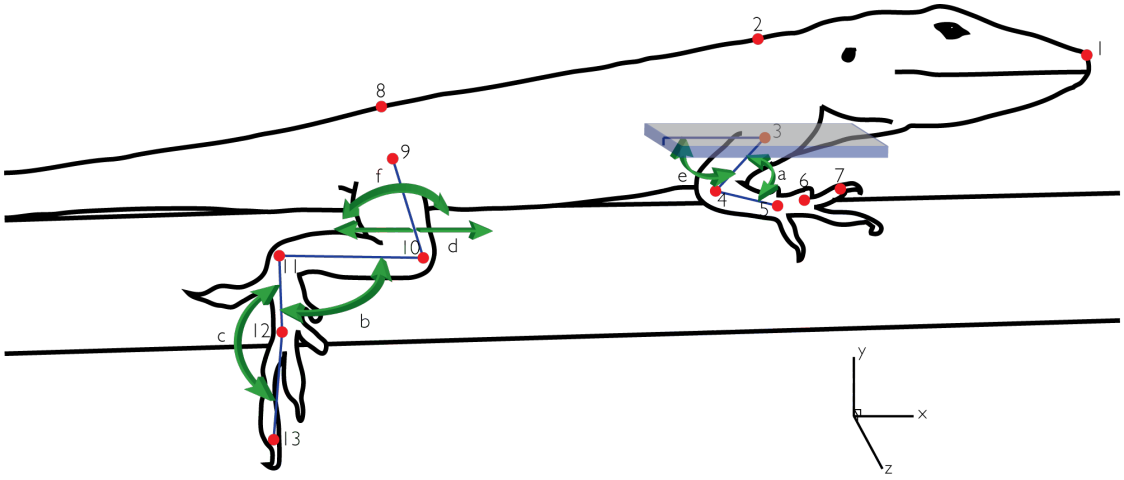

Figure 1.1. Diagram of *Anolis carolinensis*, indicating anatomical landmarks digitized (red dots) and angular variables measured (green arrows) from video analysis. a, elbow/knee, the angle between the humerus/femur and ulna/crus; b, wrist/ankle, the angle between the ulna/crus and third metacarpal/fourth metatarsal; c, metacarpophalangeal/metatarsophalangeal joints, the angle between the third metacarpal/fourth metatarsal and corresponding phalanges; d, humerus/femur retraction, the two dimensional angle, in the horizontal, x-z plane, between the humerus/femur and the line connecting the right and center of the shoulders/hips; e, humerus/ femur depression, the three-dimensional angle between the humerus/femur and a horizontal plane through the shoulder/hip; f, humerus/femur rotation, the three-dimensional angle between a vertical plane through the humerus/femur and a plane containing the upper and lower limbs. 1, nose; 2, center of shoulder; 3, right shoulder; 4, elbow; 5, wrist; 6, third metacarpophalangeal joint; 7, tip of third forelimb phalanx; 8, center of hip; 9, right hip; 10, knee; 11, ankle; 12, fourth metatarsophalangeal joint; 13, tip of fourth hind limb phalanx.

Experimental setup

Lizards ran on 1m long flat (9cm wide) and small (1.3cm diameter) perches that were attached by their ends to a 1x1.2m plywood sheet, which could be rotated on the wall to any angle. Because large diameter surfaces, such as tree trunks or large branches, result in similar hindlimb kinematics as flat surfaces in *A. sagrei* (Spezzano and Jayne, 2004), the flat perch in our study represented a large diameter treatment. The perches were mounted 0.5m from the plywood to discourage the lizards from jumping off the perch, and were suspended 1.1 meters above the ground. Both perches were covered in cork shelf liner to simulate a natural surface and to enhance traction. A mirror was mounted to the plywood above the perches at a 45° angle.

Two high speed Photron APX-RS cameras (Photron USA, Inc., San Diego, CA, USA) were used simultaneously to obtain dorsal (using mirror) and lateral video of the lizards running on the perches. Cameras recorded at 500 frames s^{-1} with a shutter speed of 1/2000 s. We obtained 2-5 strides of steady locomotion for both the hindlimb and forelimb of each individual running on both perches at 0^{o}, 45^{o} and 90^{o}. We selected trials in which 1) both the forelimb and hindlimb were visible 2) the lizard remained on the top of the perch, and 3) the lizard ran steadily through the field of view.

Kinematics

We digitized the sequences using DLT DV 3 custom software (Hedrick, 2008) for MATLAB (version R2009a, The MathWorks, Natick, MA, USA) in order to obtain x, y, and z coordinates. The x-axis described antero-posterior movement, parallel to the

direction of travel, the y-axis described dorso-ventral movement, perpendicular to the perch, and the z-axis described medio-lateral movement perpendicular to the x –y plane. Three-dimensional coordinates were obtained for the following points: tip of nose, right and left shoulder/hip, mid-pectoral/pelvic girdle, elbow/knee, wrist/ankle, base and tip of third metacarpal, and base and tip of fourth metatarsal (Fig. 1.1). Forelimb and hindlimb were analyzed separately and, in each case, the coordinates were transformed to place the shoulder/hip at the origin (0,0,0) to facilitate visualization of the limb such that positive x, y, and z indicated anterior, dorsal, and lateral positions relative to the hip. All calculations based on these coordinates were performed in Microsoft Excel 2010 (Microsoft Corporation, Redmond, WA, USA).

Body speed was calculated for each stride by digitizing a point along the midline of the body (tip of the nose or the middle of the pectoral or pelvic girdles) that showed minimal medio-lateral excursion. The distance traveled by that point between consecutive frames was divided by the duration between frames in order to calculate instantaneous speed. Speed was then standardized by dividing by snout-vent length (SVL).

Stride length was calculated as the two-dimensional (x-y) distance traveled during a complete stride cycle while step length was the distance traveled during stance. Both of these variables were standardized to SVL of the individual. Duty factor was the percentage of the total stride during which the limb of interest was in contact with the ground, and stride frequency was the number of complete strides per second (Hz).

Hip height was calculated as the two dimensional distance between the y-coordinate of the right hip and the perch (set to y=0). From this, minimum and maximum hip height ($Y_{hip\text{-}min}$, $Y_{hip\text{-}max}$), hip height at footfall ($Y_{hip\text{-}FF}$), change in hip height through stance ($Y_{hip\text{-}FF}$-$Y_{hip\text{-}min}$), and total vertical excursion of the hip ($Y_{hip\text{-}EX}$), were determined. Variables for shoulder height were calculated similarly.

Three-dimensional angles were calculated for the elbow/knee, wrist/ankle, and metacarpophalangeal (MCP)/metatarsophalangeal (MTP) joints as described previously (Jayne and Irschick, 1999; Spezzano and Jayne, 2004). Elbow/knee angle was calculated as the three-dimensional angle created by the humerus/femur and ulna/tibia with smaller angles between 0^o and 180^o indicating greater flexion at each joint. Wrist/ankle angle was calculated as the three-dimensional angle created by the ulna/tibia and the third metacarpal/fourth metatarsal, with smaller angles, less than 180^o indicating greater dorsiflexion of fore- and hind-feet. MCP/MTP angle was calculated as the three-dimensional angle created by the third metacarpal/fourth metatarsal and toe tip, with angles greater than 180^o indicating plantar flexion of fore- and hind-toe. Minimum, maximum, excursion, and angle at footfall (FF) and end of stance (ES) were calculated for each of these angular variables (Fig. 1.1).

Three angles described the orientation and movement of the right humerus/femur. Humerus/femur retraction was calculated as the two-dimensional angle (in the x-z plane) between a line connecting the left and right shoulder/hip and the humerus/femur, where positive angles indicate retraction and negative angles indicate protraction, while 0^o indicates the humerus/femur is perpendicular to the antero-posterior axis of the body.

Humerus/femur depression was calculated as the three-dimensional angle between the humerus/femur and a horizontal plane containing the right shoulder/hip such that positive angles indicate depression and negative angles indicate elevation of the elbow/knee relative to the shoulder/hip. Humerus/femur long-axis rotation was calculated as the three-dimensional angle between a vertical plane containing the humerus/femur, and the plane containing the upper and lower limbs, where positive angles indicate clockwise rotation and negative values indicate counter-clockwise rotation. Angles at FF, ES and overall angular excursion were calculated for all three of these variables and minimum and maximum angles were recorded for depression and long-axis rotation (Fig. 1.1). Pectoral/pelvic rotation was calculated as the two-dimensional (x-z) angle between the antero-posterior axis of the body (containing the nose and midpoint of the pectoral/pelvic girdles) and a line connecting both left and right shoulders/hips. Positive angles indicate clockwise rotation where the right shoulder/hip is posterior to the left shoulder/hip, while negative angles indicate the right shoulder/hip is anterior to the left shoulder/hip (counter-clockwise rotation) (Fig. 1.1).

Movement of the skin and/or soft tissue, independent of the underlying skeletal structures may affect the accuracy of the above-mentioned angular variables (e.g. Filipe et al., 2006). Although other techniques, such as three-dimensional x-ray reconstruction of moving morphology (XROMM; Brainerd et al., 2010), would potentially help eliminate some of this error by allowing the skeletal structures to be tracked directly, the extent to which the skin and skeletal elements are decoupled during locomotion in lizards is unclear.

Average angular velocities were calculated during extension (for the elbow/knee, wrist/ankle, and metacarpal/metatarsal joints) and flexion (for knee/elbow joints) during stance, with greater positive values indicating faster extension and greater negative values for the elbow/knee indicating faster flexion. Greater positive and negative values of humerus/femur depression indicate faster depression and elevation, respectively, of the upper limbs. Greater positive and negative values of humerus/femur retraction indicate faster retraction and protraction, respectively, of the upper limbs. Greater positive and negative values of humerus/femur long-axis rotation indicate faster clockwise and counter-clockwise rotation, respectively, of the upper limbs. Angular velocities were calculated in degrees (deg.) s^{-1}.

Lastly, the linear velocity of the distal tip of the metacarpal/metatarsal during swing phase was calculated and standardized to SVL s^{-1} such that greater positive values indicates faster swing in the anterior direction.

Minimum, maximum, and excursions for all variables were determined from the entire stride, except for the velocity variables, which were determined only from the stance portion of the stride. All values reported are means ± s.e.m.

Statistical analyses

All statistical analyses were performed using JMP (version 9.0 SAS Institute Inc., Cary, NC, USA). Because the lizards ran at different speeds depending on treatment (ranging from 2.11-21.24 SVL s^{-1} overall, and averaging 11.89 ± 0.96, 8.42 ± 0.54, and 4.57 ± 0.25 SVL s^{-1} for 0^{o}, 45^{o} and 90^{o}, respectively), the effects of speed were removed

by regressing all the variables individually against body speed (in SVL s^{-1}). The residuals of all variables that exhibited significant relationships with speed (alpha ≤ 0.1) were saved and used for future analyses, while all other variables were kept in their original form. All variables were averaged across strides for each individual prior to further analyses.

Variables associated with time (i.e. velocities, stride frequency, and duty factor) were isolated from the remaining angular and linear distance variables in order to run analyses separately on each set of variables. For the angular set, a principal components analysis (PCA) was used to reduce dimensionality and to isolate the fifteen variables most important for describing the variation in the data. The selected variables were those with the highest loadings chosen from both the first and second principal components (PC), but the number of variables chosen from the first component was proportional to the percentage of variation explained by that axis, with the remaining variables chosen from the second component. For example, if 80% of the variation in the data was explained by the first PC, the top twelve variables, by loading, were chosen from that axis, while the remaining three had the highest loading on the second PC. These fifteen variables were then used in a discriminant function analysis (DFA) in an effort to see if they could predict, and therefore explain, the six treatments tested. Variables that loaded heavily (greater than 0.3) on each axis of the DFA were considered most important in describing the kinematic changes that occurred across treatments (Tables 1.1-1.6). Because fewer variables were included in the velocity and timing variable set, a PCA was not needed to reduce dimensionality and variables were loaded directly into the DFA.

Finally, because the DFA does not allow us to determine which treatments separate significantly from each other, we performed a one-way ANOVA on each DFA axis using treatments as the grouping variable and DFA scores as the dependent variable (Tables 1.7,1.8).

Table 1.1. Loadings from a discriminant function (DF) analysis (F=1.34, P=0.21) of the difference in joint angles between broad and narrow diameter treatments in the forelimb and hind limb of *Anolis carolinensis*.

Variable	DF1 (52.4%)	DF2 (25.6%)
Min. pectoral/pelvic rotation	**-0.30**	-0.07
Ex. pectoral/pelvic rotation	0.20	-0.16
Humerus/femur retraction angle (ES)	**0.58**	**0.43**
Ex. humerus/femur retraction angle	0.14	-0.08
Min. humerus/femur depression angle	**0.50**	0.18
Max. humerus/femur depression angle	**0.33**	-0.01
Humerus/femur depression angle (FF)	0.00	**-0.34**
Humerus/femur depression angle (ES)	**0.81**	**0.36**
Ex. humerus/femur depression angle	0.19	-0.11
Min. humerus/femur rotation angle	**-0.71**	**-0.58**
Max. humerus/femur rotation angle	**-0.55**	**-0.57**
Max. elbow/knee angle	**0.67**	-0.05
Elbow/knee angle (ES)	**0.72**	0.16
Wrist/ankle angle (FF)	**-0.75**	0.10
Ex. wrist/ankle angle	-0.01	0.14

Loadings with a magnitude ≥ 0.3 are in bold.
Positive loadings indicate angles that are greater on broad perches than on narrow perches, while small angles indicate angles that are greater on narrow perches than on broad perches.
Percentages of variation explained by each DF axis indicated in parentheses.
FF, footfall; ES, end of stance; Min, minimum; Max, maximum; Ex, excursion (maximum – minimum).

When variables from both limbs were combined into a single analysis, variation caused by differences between the limbs overwhelmed the majority of the variation within each limb. Therefore, to increase resolution of variables causing within-limb variation, forelimb and hindlimb variables were analyzed separately. For the combined analysis, in order to better visualize the changes that occurred with changes in perch diameter, values obtained on the small diameter perches were subtracted from the values

on the flat perches, for each individual. Therefore, in the combined analyses, variables for which values were greater than zero represented variables that had greater values on flat diameters, while those with values less than zero were variables which increased in value on small diameters.

Table 1.2. Loadings from a discriminant function (DF) analysis (F=2.27, P=0.0032) of the difference in angular velocities between broad and narrow diameter treatments in the forelimb and hind limb of *Anolis carolinensis*.

Variable	DF1 (85.2%)	DF2 (7.2%)
Stride frequency	**0.53**	**0.50**
Duty factor	**0.69**	**-0.38**
Relative swing velocity (limb length/s)	**0.80**	-0.28
Humerus/femur retraction velocity	-0.14	-0.07
Humerus/femur depression velocity	**-0.45**	0.26
Humerus/femur rotation velocity	-0.05	**0.43**
Elbow/knee angle flexion velocity	-0.14	**0.63**
Elbow/knee angle extension velocity	-0.18	**0.78**
Elbow/knkle angle extension velocity	0.11	**0.54**
Toe angle extension velocity	**-0.35**	-0.11

Loadings with a magnitude ≥ 0.3 are in bold.
Positive loadings indicate angles that are greater on broad perches than on narrow perches, while small angles indicate angles that are greater on narrow perches than on broad perches.
Percentages of variation explained by each DF axis indicated in parentheses.

Results

General description and overall differences in forelimb and hindlimb kinematics

At footfall (FF), the femur was protracted 30°or more, depressed between 2 and 16°, and rotated, clockwise, by at least 20° (Fig. 1.2). The knee was generally anterior and ventral to the hip and was extended more than 90° on flat perches, but was flexed to 50-60° on small diameters. Ankle angle was, on average, obtuse on flat perches and acute on small diameters. The fourth toe was always extended more than 120° at FF (Fig. 1.2).

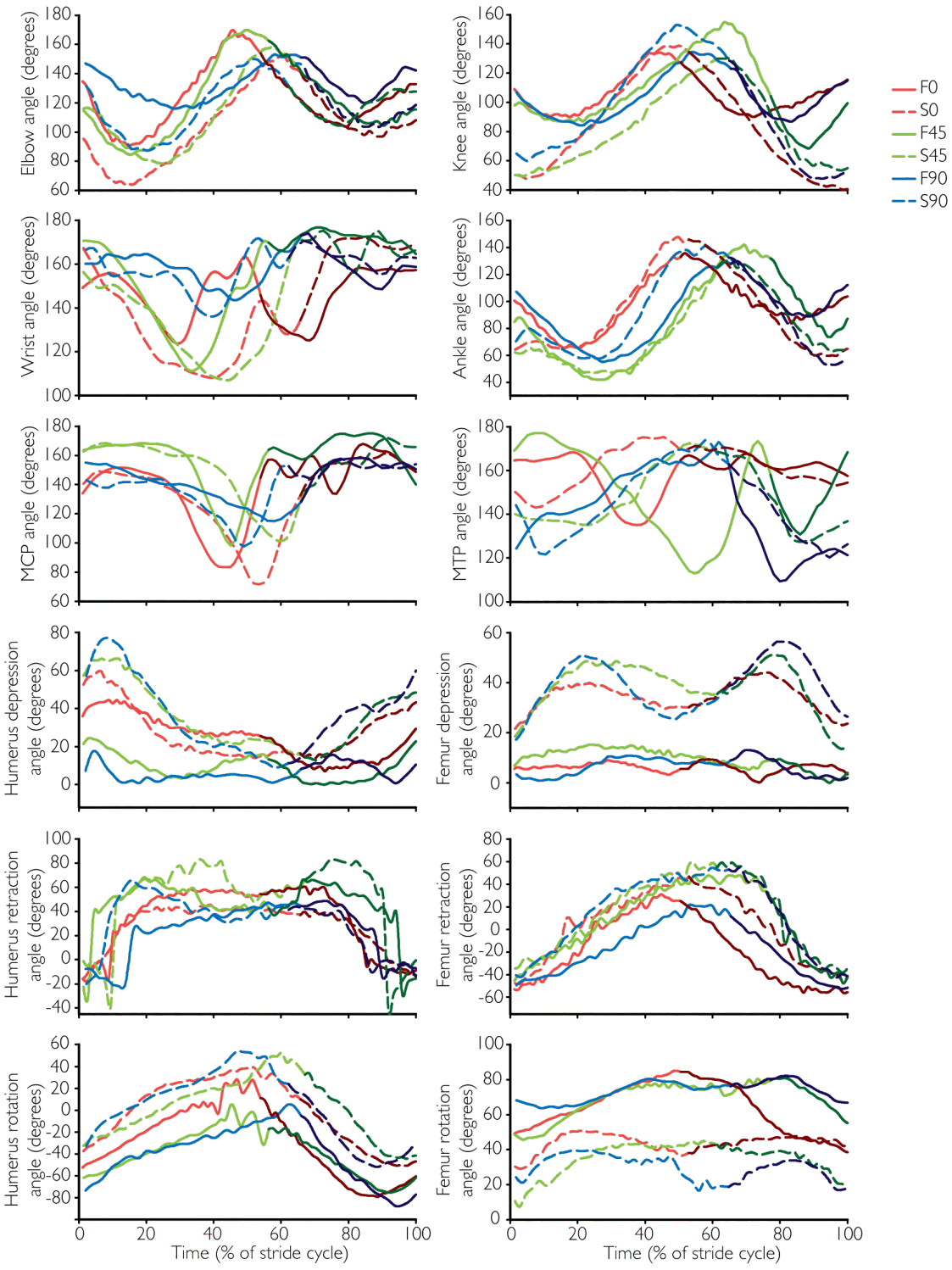

Figure 1.2. Angles of forelimb (left) and hind limb(right) joints versus time (as a percentage of stride cycle) for a single stride of a representative *Anolis carolinensis*. Red, 0 deg; green, 45 deg; blue, 90 deg; solid line, broad perch; dashes, narrow perch. Footfall begins at 0% and the transition from brighter to darker shades indicates the end of stance.

At FF, the humerus was generally protracted slightly, was more depressed (between 12 and 43°, on average) than the femur, and was rotated counter-clockwise by at least 45°. The elbow was generally anterior and ventral to the shoulder at FF and the elbow, wrist and third toe were all extended beyond 90° at FF (Fig. 1.2).

Table 1.3. Loadings from a discriminant function (DF) analysis (F=1.52, P=0.13) of joint angles in the forelimb of *Anolis carolinensis* in response to broad and narrow diameter treatments at 0, 45, and 90 deg.

Variable	DF1 (60.7%)	DF2 (20.6%)
Min. shoulder height	**0.37**	-0.07
Max. shoulder height	**0.45**	-0.08
Humerus retraction angle (ES)	-0.07	-0.18
Min. humerus depression angle	**-0.39**	-0.29
Max. humerus depression angle	**-0.45**	**-0.43**
Humerus depression angle (FF)	**-0.43**	**-0.37**
Ex. humerus depression angle	**-0.44**	**-0.44**
Min. humerus rotation angle	**-0.69**	-0.29
Max. humerus rotation angle	**-0.47**	**-0.37**
Humerus rotation angle (FF)	**-0.42**	**-0.32**
Humerus rotation angle (ES)	**-0.36**	**-0.39**
Min. elbow angle	**0.73**	0.03
Min. wrist angle	**0.56**	**0.44**
Ex. wrist angle	**-0.54**	**-0.41**
Toe angle (FF)	-0.28	**-0.35**

Loadings with a magnitude ≥ 0.3 are in bold.
Percentages of variation explained by each DF axis indicated in parentheses.
FF, footfall; ES, end of stance; Min, minimum; Max, maximum; Ex, excursion (maximum – minimum).

The wrist and ankle were located in a position lateral to the elbow and knee, respectively, on flat perches, but the ankle was placed more medially under the knee on small diameters. The third metacarpal, fourth metatarsal, and the toes were consistently oriented laterally relative to the long axis of the perch throughout the stride on the level surfaces, regardless of perch diameter, but they became oriented more medially, in line with the wrist/ankle, on the small diameter at steeper inclines, especially at 90°.

Table 1.4. Loadings from a discriminant function (DF) analysis (F=1.72, P=0.035) of angular velocities in the forelimb of *Anolis carolinensis* in response to broad and narrow diameter perches at 0, 45, and 90 deg.

Variable	DF1 (70.4%)	DF2 (19.3%)
Stride frequency	**0.49**	**-0.32**
Duty factor	**0.56**	-0.03
Relative swing velocity (limb length/s)	**0.91**	0.09
Humerus retraction velocity	0.18	**0.59**
Humerus depression velocity	**-0.44**	0.14
Humerus rotation velocity	**0.39**	-0.03
Elbow angle flexion velocity	0.04	0.28
Elbow angle extension velocity	**0.54**	0.04
Wrist angle extension velocity	0.26	0.09
Toe angle extension velocity	-0.05	0.05

Loadings with a magnitude ≥ 0.3 are in bold.
Percentages of variation explained by each DF axis indicated in parentheses.

The humerus and femur retracted during the majority of stance, usually achieving maximum retraction at ES, although the humerus often had an additional period of retraction immediately following toe-off. Both the humerus and femur underwent clockwise long-axis rotation through the entire duration of stance but the humerus rotated over a greater range than the femur (83.96±3.18° and 31.23±1.64° in humerus and femur, respectively). The femur usually achieved greatest rotation at ES, but the humerus achieved maximal rotation 5-10% before the ES. Humeral rotation and retraction were generally faster (rotation: 0.29±0.02 deg. s^{-1}, retraction: 0.75±0.12 deg. s^{-1}) than for the femur (rotation: 0.13±0.01 deg. s^{-1}, retraction: 0.35±0.03 deg. s^{-1}). The femur usually depressed during the first half of stance before being elevated almost back to the original position during the second half of stance. The humerus, however, was elevated for most of stance, reaching a more elevated position at ES (12.46±1.24° below horizontal) compared to FF (29.57±3.21° below horizontal, Fig. 1.2).

Table 1.5. Loadings from a discriminant function (DF) analysis (F=2.90, P=0.0026) of joint angles in the hind limb of *Anolis carolinensis* in response to broad and narrow diameter perches at 0, 45, and 90 deg.

Variable	DF1 (76.0%)	DF2 (14.6%)
Relative stride length (SVL)	**0.87**	-0.29
Relative step length (SVL)	**0.91**	-0.26
Femur retraction angle (ES)	**-0.37**	**0.74**
Min. femur depression angle	**-0.51**	**0.50**
Max. femur depression angle	**-0.43**	**0.64**
Femur depression angle (FF)	**-0.53**	**0.46**
Femur depression angle (ES)	**-0.46**	**0.67**
Ex. femur depression angle	**-0.35**	**0.68**
Min. femur rotation angle	0.28	**-0.73**
Max. femur rotation angle	**0.42**	**-0.63**
Femur rotation angle (FF)	0.23	**-0.66**
Femur rotation angle (ES)	**0.45**	**-0.67**
Max. knee angle	0.12	**0.35**
Knee angle (FF)	**0.67**	**-0.50**
Ankle angle (FF)	**0.43**	**-0.49**

Loadings with a magnitude ≥ 0.3 are in bold.
Percentages of variation explained by each DF axis indicated in parentheses.
FF, footfall; ES, end of stance; Min, minimum; Max, maximum; Ex, excursion (maximum – minimum).

The femur and humerus protracted and rotated counter-clockwise through most of swing and the knee and elbow flexed and then extended in the first and second halves of swing. However, the ankle and fourth hind-toe spent most of swing flexing with a brief extension at the end of swing, contrasting with the wrist and third toe of the forelimb, which generally maintained constant angles or extended during swing. The femur depressed during the first half of swing and elevated during the second half, causing the knee to describe an arc as the hindlimb came into position at the end of swing. The elbow, however, tended to trace a linear path dorsally and anteriorly as the humerus elevated through swing (Fig. 1.2). Swing phase velocity was slower in the forelimb (14.56±1.13 SVL s^{-1}) than in the hindlimb (18.36±1.01 SVL s^{-1}).

Table 1.6. Loadings from a discriminant function (DF) analysis (F=2.40, P=0.0018) of angular velocities in the hind limb of *Anolis carolinensis* in response to broad and narrow diameter treatments at 0, 45, and 90 deg.

Variable	DF1 (47.2%)	DF2 (28.6%)
Stride frequency	-0.08	**0.61**
Duty factor	-0.02	**-0.54**
Relative swing velocity (limb length/s)	**0.75**	-0.19
Femur retraction velocity	**0.39**	**0.75**
Femur depression velocity	-0.18	**0.62**
Femur rotation velocity	0.18	**0.78**
Knee angle flexion velocity	**-0.64**	**0.47**
Knee angle extension velocity	-0.10	**0.85**
Ankle angle extension velocity	0.10	**0.63**
Toe angle extension velocity	**0.45**	**-0.40**

Loadings with a magnitude ≥ 0.3 are in bold.
Percentages of variation explained by each DF axis indicated in parentheses.

Effects of surface diameter and incline

With the exception of the combined and forelimb DFA's of the angular variables (Figs 1.3a and c, respectively), all DFA's were significant (Tables 1.1-1.6). However, as only one misclassification occurred (the hindlimb of one individual running at 90° was classified with the 0° treatment in the combined DFA), we have confidence in the ability of the chosen variables to define treatments.

Decreasing perch diameter significantly affected more variables than increasing incline (41 and 28 variables affected by diameter and incline, respectively; Figs 1.3c-f, Tables 1.3-1.6). In addition, the kinematics of the proximal joints (shoulder/hip, humerus/femur) were more affected than distal joints (40/50 and 19/40 of proximal and distal variables, respectively; chi-squared goodness-of-fit test, Pearson χ^2=13.03, DF=1, P=0.0003) and, in many instances, there were opposite trends in kinematics between the limbs (see below).

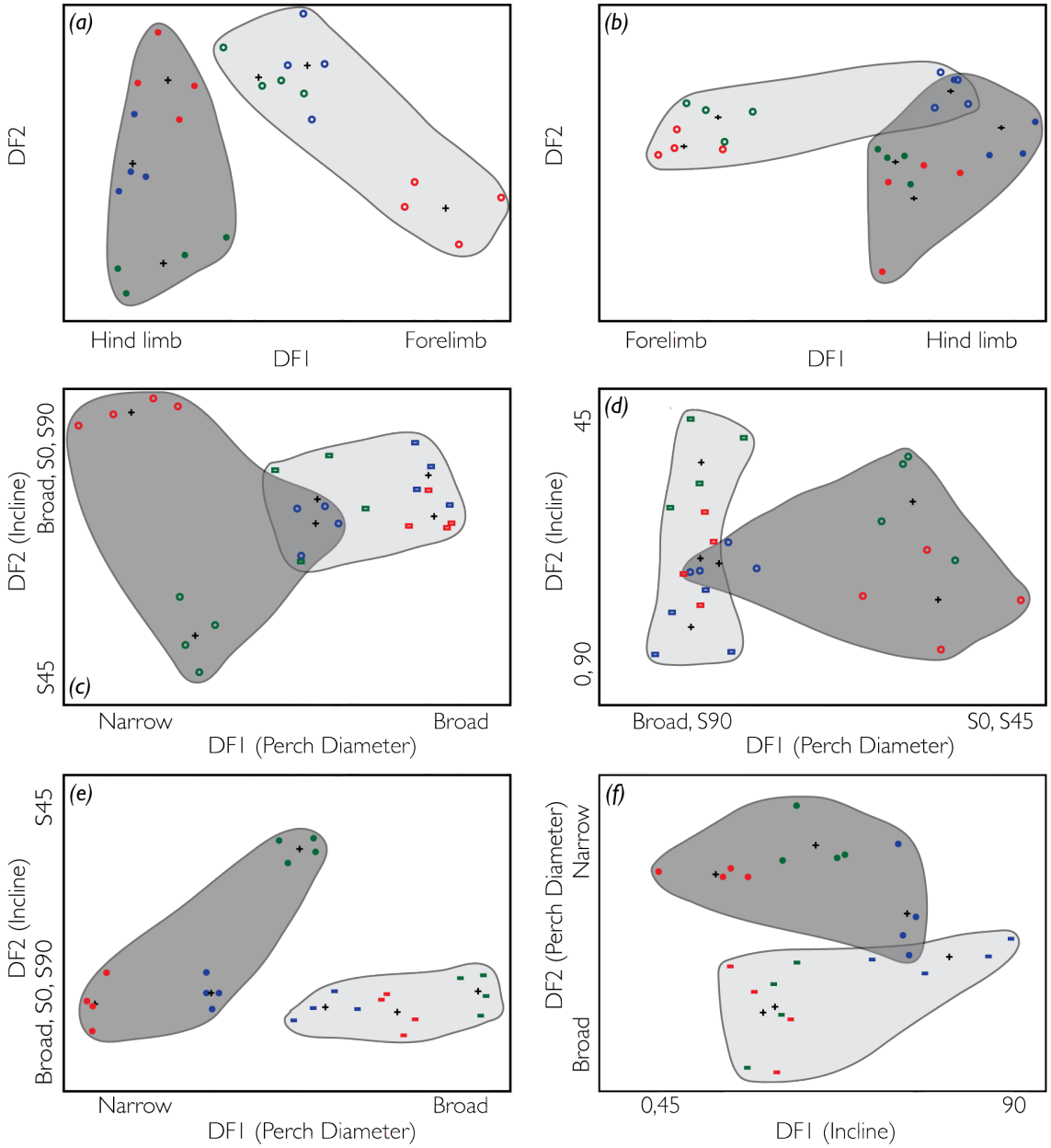

Figure 1.3. First two axes of discriminant function analyses of combined forelimb and hind limb joint angles (a) and angular velocities (b), forelimb joint angles (c) and angular velocities (d), and hind limb joint angles (e) and angular velocities (f) of *Anolis carolinensis*. For panels (a) and (b), each point represents the difference between broad and narrow perch diameter treatments, averaged across strides for each individual, at 0 deg (red), 45 deg (green), and 90 deg (blue) inclines. Variables loading heavily on the same side of the axis as the points on the DFA indicate inclines at which angles are greater on the broad perch than on the narrow perch. Forelimb and hind limb points are shaded in light and dark grey, respectively. Canonical loadings on each axis can be seen in tables 1.1 and 1.2. Open circles, forelimb, closed circles, hind limb. For panels (c)-(f), points represent individuals (strides averaged within each treatment) on broad (rectangles) and narrow (circles) perches at 0 deg (red), 45 deg (green), and 90 deg (blue) inclines. Broad and narrow points are shaded in light and dark grey, respectively. Canonical loadings on each axis can be seen in tables 1.3 and 1.4 for panels (c) and (d), and tables 1.5 and 1.6 for panels (e) and (f).

Table 1.7. Results of one-way ANOVAs showing significant separation of treatments on each axis of forelimb and hind limb DFAs.

	Forelimb DFA joint angles		Forelimb DFA angular velocities		Hind limb DFA joint angles		Hind limb DFA angular velocities	
Treatment	DF1 (76.45)	DF2 (25.93)	DF1 (38.5)	DF2 (10.58)	DF1 (277.68)	DF2 (53.23)	DF1 (25.69)	DF2 (15.56)
Broad; 0 deg	A	B	B	B,C	B	B	B,C	C
Broad; 45 deg	B	B	B	A	A	B	B,C	C
Broad; 90 deg	A	A,B	B	C	C	B	A	B,C
Narrow; 0 deg	D	A	A	C	E	B	C	A
Narrow; 45 deg	C	C	A	A,B	C	A	B	A
Narrow; 90 deg	B	B	B	B,C	D	B	A	A,B

F-values are in parentheses, d.f=5,23, $P<0.0001$ for all ANOVAs.
Treatments that do not share letters are significantly different.

Changes in forelimb kinematics with perch diameter and incline

Forelimb stride frequency increased on the small diameter perch at 0° (flat: 7.79±1.69 Hz, small: 9.44±0.77 Hz) and 45° (flat: 6.56±0.85 Hz, small: 7.53±0.21 Hz), but decreased at 90° (flat: 6.08±0.87 Hz, small: 5.63±0.80 Hz; Figs 1.3b and d). Forelimb swing phase velocity was significantly faster on the small perch (17.09±1.85 SVL s^{-1}) than on flat (12.04±0.87 SVL s^{-1}), resulting in increased duty factor (small: 0.68±0.02, flat: 0.54±0.05; Figs 1.3b and d). The shoulders were significantly closer to the surface and rotated slightly more on the smaller diameter perch (min. height: 4.27±0.87 mm, min. rotation: -37.51±3.89^{o}) than on the flat perch (min. height: 8.53±0.66 mm, min. rotation: -37.45±2.03^{o}; Figs 1.3a and c).

Long-axis humeral rotation, but not retraction, was significantly greater on the smaller perch diameter (max. rotation: 29.58±6.25^{o}, ES retraction: 54.78±4.16^{o}) than the flat treatment (max. rotation: -0.12±4.96^{o}, ES retraction: 53.81±3.45^{o}), especially at 45° (Figs 1.3a and c). Depression and vertical excursion were greater on the small perch

diameter (max: 51.05±5.57°, excursion: 44.78±4.22°) than on the flat surface (max: 25.89±1.56°, excursion: 24.97±1.32°), especially at 45°, and elevation generally increased with incline on flat surfaces (Fig. 1.3c). Retraction of the humerus was faster on the smaller perch (0.77±0.16 deg. s^{-1}) than on the flat surface (0.72±0.18 deg. s^{-1}), and at 45° (1.14±0.25 deg. s^{-1}) than at the other two inclines (0°: 0.72±0.10 deg. s^{-1}, 90°: 0.38±0.15 deg. s^{-1}). The humerus elevated faster on the small diameter than on flat at 0° (small: -0.28±0.05 deg. s^{-1}, flat: -0.23±0.04 deg. s^{-1}) and 45° (small: -0.21±0.04 deg. s^{-1}, flat: -0.15±0.01 deg. s^{-1}), but slower at 90° (small: -0.15±0.05 deg. s^{-1}, flat: -0.15±0.03 deg. s^{-1}; Figs 1.3b and d).

Table 1.8. Results of one-way ANOVAs showing significant separation of treatments on each axis of combined DFAs.

Treatment	Combined DFA joint angles		Combined DFA angular velocities	
	DF1 (54.49)	DF2 (26.62)	DF1 (85.86)	DF2 (7.24)
Forelimb; 0 deg	A	B,C	C	A,B,C
Forelimb; 45 deg	B	A	C	A,B
Forelimb; 90 deg	B	A	A,B	A
Hind limb; 0 deg	C	A	B	C
Hind limb; 45 deg	C	C	B	B,C
Hind limb; 90 deg	C	B	A	A,B

F-values are in parentheses, d.f.=5,23, *P*<0.001 for all ANOVAs.
Treatments that do not share letters are significantly different.

Elbow flexion was greater on the small diameter than on the flat surface (Table 1.9). Similarly, wrist flexion and angular excursion were greater on the small diameter than on the flat surface and at 45° than on the other two inclines (Table 1.9). However, wrist extension at FF was greater on the small diameter perch than on the flat surface (Table 1.9). Lastly, MCP extension at FF was greater on the small perch at 45° (166.14±1.28°) than in all other treatments and slower on the small diameter than the flat

surface at 0° (small: 1.55±0.31 deg. s^{-1}, flat: 2.14±0.43 deg. s^{-1}) and 45° (small: 0.97±0.08 deg. s^{-1}, flat: 1.48±0.18 deg. s^{-1}; Figs 1.3b and d).

Table 1.9. Selected significant variables for distal joints in the forelimb and hind limb of *Anolis carolinensis*

	Perch Diameter		Incline		
	Narrow	Broad	0 deg	45 deg	90 deg
Forelimb					
Min. elbow angle	74.81±3.16	87.7±2.71			
Min. wrist angle	112.79±3.72	62.18±3.72	118.40±3.86	109.05±3.04	124.86±3.60
Ex. wrist angle	122.08±2.37	53.99±2.70	56.01±3.94	67.42±2.85	50.82±3.57
Wrist angle (FF)	163.54±1.61	157.10±6.99			
Max. knee angle	137.67±3.06	135.62±3.89			
Hind limb					
Knee angle (FF)	52.74±2.26	96.35±4.78			
V. Knee extension	0.37±0.04	0.29±0.03			
V. knee flexion	-0.13±0.01	-0.28±0.06	-0.30±0.09	-0.18±0.03	-0.15±0.02
Ankle angle (FF)	72.83±4.03	101.67±5.04			

Angles and angular velocities are given in deg and deg. s^{-1}.
FF, footfall; Min, minimum; Max, maximum; Ex, excursion.; V., velocity.
Values are means ± s.e.m.

Changes in hindlimb kinematics with perch diameter and incline

Hindlimb stride frequency was greater on the small diameter perch compared to the flat surface at 0° (small: 9.44±0.94 Hz, flat: 8.94±0.83 Hz) and 45° (small: 7.44±0.26 Hz, flat: 6.40±0.81 Hz) but was generally lower on the small diameter at 90° (small: 5.48±0.95 Hz, flat: 6.08±0.90 Hz; Fig. 1.3b). Both stride and step lengths decreased on the small diameter (stride length: 0.96±0.03 SVL, step length: 0.59±0.01 SVL) compared to the flat surface (stride length: 1.28±0.09 SVL, step length: 0.80±0.04 SVL; Fig. 1.3e). Hindlimb swing phase velocity was slower on the smaller perch (15.98±0.80 SVL s^{-1}) than on flat (20.74±1.62 SVL s^{-1}) and duty factor was lower on the smaller diameter (small: 0.61±0.02, flat: 0.64±0.02; Figs 1.3b and f). Also, pelvic girdle rotation was

greater on the smaller diameter perch (min. rotation: -30.94±3.87^{o}) than on the flat surface (min. rotation: -24.76±2.12^{o}; Fig. 1.3a).

Femur retraction was greatest, and rotation least, on the small diameter at 45° (ES retraction: 68.58±4.43^{o}, min. rotation: 12.48±8.17^{o}; Figs 1.3a and e). Femur depression and vertical excursion were greater on the small perch diameter (max. depression: 42.10±4.71^{o}, excursion: 30.12±3.07^{o}) than the flat surface (max. depression: 13.26±0.81^{o}, excursion: 12.97±0.79^{o}), especially at 45° (Figs 1.3a and e). Femur elevation was generally greater with incline on flat surfaces (Figs 1.3a). In addition, the femur rotated, retracted, and depressed faster on the small diameter (rotation: 0.13±0.01 deg. s^{-1}, retraction: 0.38±0.04 deg. s^{-1}, depression: 0.20±0.03 deg. s^{-1}) than on the flat surface (rotation: 0.12±0.02 deg. s^{-1}, retraction: 0.32±0.03 deg. s^{-1}, depression: 0.08±0.01 deg. s^{-1}; Figs 1.3b and f).

Knee extension was greater on the small diameter perch than on the flat surface (Table 1.9) and at end of stance was greatest on the small perch diameter at 45^{o} (137.81±6.51^{o}; Figs 1.3a and e). However, knee flexion at FF was greater on the small diameter perch (Table 1.9; Figs 1.3a and e). The knee extended faster, but flexed slower on the smaller diameter than on the flat and flexed slower at 90° than at the other two inclines (Table 1.9; Fig. 1.3e). In addition, ankle flexion at FF was greater on the small diameter compared to the flat surface (Table 1.9; Figs 1.3a and e) and was greatest at 45^{o} (67.67±5.87^{o}). Lastly, the MTP extension was slower on the smaller diameter than on the flat surface at 0^{o} (small: 0.25±0.02 deg. s^{-1}, flat: 0.74±0.20 deg. s^{-1}) and 45^{o} (small:

0.15±0.12 deg. s^{-1}, flat: 0.54±0.14 deg. s^{-1}), but not on smaller diameters at 90° (small: 0.12±0.02 deg. s^{-1}, flat: 0.12±0.02 deg. s^{-1}; Figs 1.3b and f).

Discussion

A. carolinensis adopted similar strategies for dealing with changes in incline and perch diameter as other vertebrates, increasing stride frequency to increase dynamic stability, and increasing limb flexion to lower the CoM and reduce torque and the tendency to topple (Schmitt, 1994; Higham and Jayne, 2004a; Franz et al., 2005; Schmidt and Fischer, 2010; Gálvez-López et al., 2011; Lammers and Zurcher, 2011). However, kinematics generally differed between the fore- and hindlimbs and limb function was modulated differently in response to changes in habitat structure (Fig. 1.3). A key conclusion is that, when dealing with a small diameter perch, the forelimb and hindlimb exhibited opposite kinematic trends (Fig. 1.3), suggesting that the propulsive mechanisms in anoles shift with external demand. Additionally, the humerus exhibited a greater range of motion than the femur in all treatments. This might allow the humerus to be more functionally plastic.

Of the functional demands that we manipulated in this study, perch diameter had the greatest impact on limb kinematics. Interestingly, of the variables affected by incline, the majority revealed a difference between the 45^{o} treatment and the other two treatments (0 and 90°), which were similar. The proximal joints (shoulder/hip and humerus/femur) appeared to be primarily responsible for these changes in kinematics across treatments. Despite the added energetic cost associated with moving up inclined surfaces (Taylor et

al., 1972; Farley and Emshwiller, 1996; Roberts et al., 1997), the greater impact of perch diameter on kinematics in our study may be explained by the constraints that narrow surfaces impose on foot placement.

Forelimbs and hindlimbs in vertebrate locomotion

Independent of treatment, the humerus of *A. carolinensis* in our study was protracted more and exhibited a greater range of rotation than the femur, which remained rotated in a more clockwise orientation than the humerus. In addition, the wrist was extended more than the ankle. These angular differences may be explained by anatomical differences between the limbs (Humphry, 1876; Russell and Bauer, 2008) and girdles (Haines, 1952; Snyder, 1954; Peterson, 1971, 1973, 1974; Jenkins and Goslow, 1983; Peterson, 1984; Reynolds, 1985; Schmitt, 1994; Zihlman et al., 2011). The forelimb girdle of habitual climbers is adapted to allow a greater range of motion to meet the demands for flexibility in arboreal habitats (Reynolds, 1985; Zihlman et al., 2011). Anoles and chameleons lack or modify the attachment of the clavicle, which braces the anterior edge of the pectoral girdle in terrestrial species, and possess girdle musculature oriented to facilitate rotation and antero-posterior translation of the girdle (Peterson, 1971, 1973, 1974, 1984). Rotation and translation of the scapulocoracoid, in addition to a sagitally-oriented coracosternal orientation and modified glenoid cavity, allows a greater degree of humerus protraction/retraction and long-axis rotation than is possible in the femur (Jenkins and Goslow, 1983).

Terrestrial vertebrates generally exhibit a division in function between the forelimbs (braking) and the hindlimbs (propulsion; Deban et al., 2012). Kimura et al. (1979) argued that primates were hindlimb driven while non-primate mammals were forelimb driven, linking these differences in function with differences in placement of the CoM (posterior in primates and anterior in non-primate mammals). However, Demes et al. (1994) found that differences in CoM position translated into differences in peak vertical forces, not propulsive forces. With few exceptions, forelimbs exert net braking forces while hindlimbs exert net propulsive forces in variety of primates and non-primate mammals (e.g. horses, cats, dogs, chipmunks, Demes et al., 1994; Lammers and Biknevicius, 2004). Similarly, lizard hindlimbs are often the primary propulsors on terrestrial surfaces (e.g. Autumn et al., 2006), resulting in few studies examining forelimb function (Russell and Bels, 2001a). Despite the functional dichotomy between fore- and hindlimbs in terrestrial systems, the relative importance of forelimbs for propelling an animal commonly increases in arboreal situations to assist in overcoming the greater propulsive challenges of the system (Arnold, 1998; Zaaf et al., 1999; Autumn et al., 2006). The greater flexibility, anatomically and kinematically, of the forelimb of arboreal specialists, may make it a particularly effective structure for propulsion and stabilization in complex arboreal situations, where a greater range of motion is beneficial (Reynolds, 1985; Zihlman et al., 2011). Because pulling the CoM would assist in keeping the animal against arboreal surfaces, propulsion from the forelimbs likely increases locomotor stability relative to the pushing motion seen in hindlimbs. Although it appears from our study that anoles exhibit greater kinematic flexibility of forelimb

compared to the hindlimb, measurements of forces exerted by *A. carolinensis* running on a range of inclines and perch diameters are needed to confirm the shift in the propulsive roles of the fore- and hindlimbs.

Changes with incline and perch diameter

Climbing up steeper surfaces or narrower branches presents a number of functional challenges for arboreal species. Steeper inclines increase resistance to locomotion by increasing the proportion of gravity acting parallel to the surface and reducing the proportion holding the animal against the substrate (Cartmill, 1985; Preuschoft, 2002). In addition, the gravitational force acting on the animal is shifted downwards, towards the hindlimb when climbing and towards the forelimb when descending, head-first (Preuschoft, 2002). As a result of this weight shift, individual leg function changes. On level surfaces, forelimbs of a wide range of animals exert net braking forces and posterior limbs push against the substrate towards the midline of the body (Full et al., 1991; Demes et al., 1994; Lammers and Biknevicius, 2004; Schmitt and Bonnono, 2009). On inclines, however, substrate reaction force data indicate that all four limbs pull the body upwards, towards the point of contact between the feet and substrate (Autumn et al., 2006; Goldman et al., 2006; Schmitt and Bonnono, 2009). Thus, the relative propulsive contribution of the forelimb is dependent, at least partially, on the orientation of the animal, likely increasing in importance with increasing slope. Perches of narrow diameter increase the likelihood of toppling because the sloped sides and the narrow base of support increase the proportion of the gravitational force acting

tangentially to the perch, creating a toppling moment that increases with deflection of the CoM away from the perch (Preuschoft, 2002; Lammers and Biknevicius, 2004; Lammers and Gauntner, 2008). Although claws and adhesive structures of lizards help grip and maintain contact with the surface in the face of these challenges (Zani, 2000), both sets of limbs must undergo changes in posture and function to contribute to overcoming the greater challenges for propulsion and stability. One way arboreal animals can circumvent, to some extent, the negative impacts of a smaller diameter substrate involves placing the foot more laterally on the perch. This increases the angle of the arc subtended by the limbs, reducing the tangential component of the adduction force and increasing the normal component, aiding with grip maintenance (Cartmill, 1985; Schmidt and Fischer, 2010). However, lateral foot placement in small mammals correlates with a reduced propulsive component of force due to a greater proportion of force being directed medially to maintain grip (Lammers and Biknevicius, 2004; Lammers, 2007; Schmidt and Fischer, 2010, 2011). Forelimbs can assume a greater propulsive role than the hindlimbs on small diameters (opossums, Lammers and Biknevicius, 2004) or on inclines (geckos, Autumn et al., 2006; opossums, Lammers, 2007). Our study supports the idea that forelimbs become increasingly important for propulsion in arboreal circumstances; *A. carolinensis* placed the hindlimb laterally on narrow perches, maintaining a medial forelimb position, indicating the forelimb may adopt a more propulsive role while the hindlimb assists in stabilization (Lammers and Biknevicius, 2004; Schmidt and Fischer, 2010). Although lateral foot placement indicates an increased role in stabilization in the hindlimb, a number of other variables that contribute to stability (e.g. swing phase

velocity) did not change as expected (Lammers and Biknevicius, 2004; Franz et al., 2005; Lammers, 2007; Gálvez-López et al., 2011). However, whether the functional correlation between foot position and role in propulsion is similar in mammals and lizards remains to be investigated.

A. carolinensis modulated its kinematics to aid with stability in several ways. Forelimb stride frequency, duty factor, and swing phase velocity were all greater on the small diameter perch compared to the flat surface (Figs 1.3b and d). Combinations of these strategies have been observed in a number of other vertebrates moving on small diameter surfaces and are thought to increase dynamic stability and reduce peak vertical forces by applying force over a greater proportion of the stride (Lammers and Biknevicius, 2004; Franz et al., 2005; Lammers, 2007; Schmidt and Fischer, 2010; Gálvez-López et al., 2011; Lammers and Zurcher, 2011). In addition, *A. carolinensis* increased both elbow and knee flexion to decrease the height of the shoulder and hip above the surface (Figs 1.3c and e). However, the decrease in hip height on small diameters was not significant, likely because femur depression also increased to assist in lateral placement of the hind feet on the perch (Fig. 1.3a). Limb flexion lowers the CoM, decreasing the gravitational component acting to destabilize or slow locomotion on both inclines and narrow perches (Cartmill, 1985; Arnold, 1998). This also allows a greater proportion of force to act parallel to the surface and aid in propulsion, and may reduce peak vertical forces by reducing vertical oscillations of the CoM, a factor that becomes especially important on compliant surfaces (Schmitt, 1994; Arnold, 1998; Lammers and Biknevicius, 2004; Gálvez-López et al., 2011). However, it is also possible that greater

knee flexion has a negative impact on limb muscle function by shifting the operating lengths of the muscles. Future work examining how muscle function in *Anolis* lizards responds to changes in habitat structure would reveal any shifts in function.

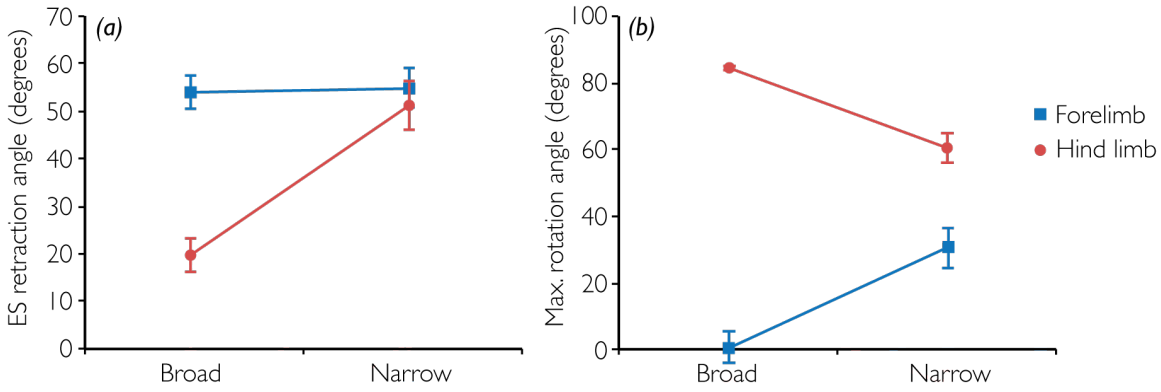

Figure 1.4. Mean end of stance retraction angle (a) and maximum rotation angle (b) of the humerus (blue) and femur (red) on broad and narrow perches. Variables chosen were identified as significant in discriminant function analyses (Fig. 1.3). ES, end of stance. Values are means ± s.e.m.

Increased limb flexion reduces effective limb length and thus has a negative impact on step length and stance duration; further kinematic adjustments occurring at the shoulder and hip joints may help mitigate this in *A. carolinensis*. We found significant increases in humerus rotation, but decreases in humerus retraction on small diameters (Figs 1.3a, c, and 1.4). In contrast, femur rotation decreased while retraction increased (Figs 1.3a, e, and 1.4). Increasing rotation and retraction are two mechanisms that can contribute to increasing step length in lizards (for a general discussion see Russell and Bauer, 2008). It is interesting, however, that the fore- and hindlimbs in *A. carolinensis* appear to use different mechanisms to overcome the reduction in effective limb length. The forelimb is capable of a greater range of motion, especially long-axis humerus rotation, due to anatomical specialization of the *Anolis* pectoral girdle that is not seen in the pelvic girdle (Peterson, 1971, 1973, 1974). In addition, the pectoral girdle rotated

more on the small diameter compared to the flat surface, allowing a further increase in long-axis humerus rotation. This contrasts with the reduction in long-axis femur rotation on the small diameter despite the increase in pelvic rotation (Fig. 1.3a). While increased pelvic rotation may contribute to instability by increasing lateral displacement of the CoM (Peterson, 1984; Preuschoft, 2002; Lammers and Gauntner, 2008), increasing pelvic rotation may be important to increase antero-posterior excursion of the femur (Peterson, 1984; Fischer et al., 2010). In contrast, rotation of the pectoral girdle is unlikely to have as great an effect on stability and therefore may allow a greater reliance on rotation as the primary forelimb propulsive mechanism. Further, excessive forelimb retraction may increase the possibility of interference between forelimb at ES and the ipsilateral hindlimb at FF since these events often occur at approximately the same time.

The variables impacted by the small diameter perch were exaggerated at 45^{o}, resulting in a distinction between 45^{o} and the 0^{o} and 90^{o} treatments. The humerus rotated most at 45^{o} while the femur further reduced long-axis rotation, but both the humerus and femur depressed more on this incline (Figs 1.3a, c, and e). Greater depression of the humerus and femur may increase the range of antero-posterior as well as rotational movement by altering the orientation of these limb segments in the glenoid/acetabular cavities (Peterson, 1973). Thus, when combined with increases in wrist extension at FF, humerus rotation, knee extension at ES, and ankle flexion at FF, greater humerus and femur depression may indicate an effort to increase step length at 45^{o}. Compared to the 45^{o} treatment, the range of limb movement appears to be more restricted at 0^{o} and 90^{o}, suggesting possible behavioral and/or biomechanical constraints on step length on these

two inclines. Therefore, 45^{o} may be a preferable incline for effective locomotion in *A. carolinensis*, although this species appears to use inclines randomly in its environment, showing no particular preference for a specific incline (Mattingly and Jayne, 2004). Determining whether the 45^{o} treatment results in optimal limb function requires further investigation.

Climbing in Anolis ecomorphs

Changes in perch diameter and incline resulted in similar changes in hindlimb kinematics in *A. carolinensis* and *A. sagrei* (Spezzano and Jayne, 2004). *Anolis sagrei* was affected more by perch diameter than by incline, the femur retracted and depressed more, the knee flexed more, contributing to a decrease in hip height, and stride and step lengths decreased on small diameters (Spezzano and Jayne, 2004). However, unlike A. *carolinensis*, *A. sagrei* increased femur rotation with decreasing perch diameter and increasing incline (Spezzano and Jayne, 2004). Further, pelvic rotation was not affected by perch diameter in *A. sagrei* (Spezzano and Jayne, 2004). Average minimum, maximum, and excursion of femur retraction appeared to be similar or greater in *A. carolinensis* than *A. sagrei*, but there was considerably less long-axis femur rotation in *A. carolinensis*. Therefore, the reduction in long-axis femur rotation by *A. carolinensis* on small diameters may be the result of a preferential increase in femur retraction allowed by greater pelvic rotation. That *A. sagrei* appears to maintain a similar pelvic rotation regardless of treatment, may indicate a greater sensitivity to instability caused by lateral undulation on these small diameters. In addition, as limb length has been correlated with

preference of perch diameter in *Anolis* (Losos, 1990a, b; Mattingly and Jayne, 2004), it is unsurprising that the longer-legged *A. sagrei* (relative leg length approx. 84% of SVL; Spezzano and Jayne, 2004), a trunk-ground species, appears to use greater perch diameters than are available on average in its environment (Mattingly and Jayne, 2004) and exhibits greater limb flexion on small diameters (Spezzano and Jayne, 2004) than *A. carolinensis* (relative leg length approx. 58% of SVL). However, *A. carolinensis*, a trunk-crown species, demonstrates an inconsistent preference for perch diameters, using substrates in proportion to what is available in its habitat in the Bahamas (Mattingly and Jayne, 2004), yet showing a preference for larger diameters in several habitats in Louisiana (Irschick et al., 2005a,b). Thus, *A. sagrei*'s preference for larger diameters may stem from longer relative leg lengths, which renders locomotion on narrower perches less stable, whereas the shorter relative leg lengths in *A. carolinensis* may facilitate the greater flexibility in habitat preference that is observed in some populations. As these considerations likely affect pelvic and hindlimb angles and excursions, locomotor kinematics may contribute to habitat use distinctions among *Anolis* ecomorphs.

Morphological differences between ecomorphs, especially in body size (ranging from 130-191mm in crown giants and 33-51mm in grass bush species) and relative leg length (smallest in twig ecomorphs and longest in grass-bush and trunk-ground ecomorphs) have been related to sprinting and jumping performance such that longer-legged species can sprint faster and jump further on larger diameters, but are more negatively affected by decreases in perch diameter than shorter-legged species (Losos

and Sinervo, 1989; Losos, 1990a, b; Irschick and Losos, 1999). Our data suggest possible kinematic explanations for these patterns. Similarly, shorter limbs keep the body closer to the substrate surface, which aids in stability (Schmitt, 1994; Higham and Jayne, 2004a; Franz et al., 2005; Schmidt and Fischer, 2010). Therefore, species with shorter limbs may be expected to exhibit fewer and less extreme changes in kinematics as diameter changes. This may explain, in part, the relatively consistent performance observed in species with shorter limbs (Losos and Sinervo, 1989).

Further experimentation on other ecomorphs is necessary to test these predictions and to clarify the underlying kinematic and biomechanical changes that explain the correlation between morphology and performance in this system. Furthermore, the forelimb has the potential to augment stabilization and/or propulsion during arboreal locomotion, potentially relieving functional restrictions in the hindlimb. Therefore, kinematic data of the forelimb of other ecomorphs is an essential component for understanding differences in arboreal locomotion and performance in *Anolis*.

Conclusions

A. carolinensis not only moves its fore- and hindlimbs differently under a specific condition, but also modulates fore- and hindlimb function differently with changes in perch incline and diameter. Although the majority of these differences can be explained by anatomy, their functional consequences are less clear. We found that both forelimb and hindlimb angular velocities generally increased on the small diameter perch relative to the flat surface (the femur and humerus rotated and retracted faster, the elbow and knee

extended faster, and the knee flexed faster; Figs 1.3b, d, and f), but these faster angular velocities may have been caused by either increased muscle recruitment or passive collapse/extension of the joints caused by the shift in weight distribution as the body moved over the joints. In order to determine the relative contributions of the fore- and hindlimbs to propulsion, ground reaction force (GRF) and patterns of *in vivo* muscle function are needed. Ground reaction force data from a variety of vertebrate taxa indicate that perch diameter and incline can affect whether the forelimb or the hindlimb adopts the primary propulsive role (Lammers and Biknevicius, 2004; Autumn et al., 2006; Lammers, 2007; Schmidt and Fischer, 2010). A single study has examined the neuromuscular responses to changes in arboreal structure, but this study focused on a lizard (*Chamaeleo calyptratus*) with a highly-specialized gripping mechanism (Higham and Jayne, 2004b). They found that the hindlimbs can be used to both pull (early stance) and push (latter half of stance) when moving up an incline. Whether this is common across lizards is not fully understood. In addition, different groups of lizards utilize very different morphological features during locomotion. For example, *Anolis* lizards employ an adhesive system, which is not actively modulated to the degree observed in other pad-bearing lizards (Russell and Bels, 2001b), and this might result in very different patterns of neuromuscular modulation. Understanding how this morphological diversity relates to the underlying physiological control of locomotion might reveal key functional axes of variation among groups of arboreal lizards. Further experimentation assessing both GRF and *in vivo* muscle function, therefore, is essential for understanding arboreal locomotion in lizards.

Chapter 2 - Context-dependent changes in motor control and kinematics during locomotion: modulation and decoupling

Abstract

Successful locomotion through complex, heterogeneous environments requires the muscles that power locomotion to function effectively under a wide variety of conditions. Although considerable data exist on how animals modulate both kinematics and motor pattern when confronted with orientation (i.e. incline) demands, little is known about the modulation of muscle function in response to changes in structural demands like substrate diameter, compliance, and texture. Here, we used high-speed videography and electromyography to examine how substrate incline and perch diameter affected the kinematics and muscle function of both the forelimb and hindlimb in the green anole (*Anolis carolinensis*). Surprisingly, we found a decoupling of the modulation of kinematics and motor activity, with kinematics being more affected by perch diameter than by incline, and muscle function being more affected by incline than by perch diameter. Also, muscle activity was most stereotyped on the broad, vertical condition, suggesting that, despite being classified as a trunk-crown ecomorph, this species may prefer trunks. These data emphasize the complex interactions between the processes that underlie animal movement and the importance of examining muscle function when considering both the evolution of locomotion and the impacts of ecology on function.

Introduction

Animals necessarily interact with their environment when performing activities necessary for survival. Perhaps the most important examples involve locomotion, which is almost always important for capturing prey, evading predators, and interacting with conspecifics. However, the environment through which animals move is often highly heterogeneous. Therefore, in order to be successful, species must be able to effectively perform locomotor behaviors under a variety of conditions. Further, as muscles are the contractile units that generate movement, they, too, must be able to function effectively to power diverse behaviors under variable conditions.

Although morphological properties of muscle, such as physiological cross-sectional area (Haxton, 1944; Alexander, 1977; Loeb and Gans, 1986; Lieber and Ward, 2011), fiber length (Loeb and Gans, 1986; Gans and de Vree, 1987; Biewener and Roberts, 2000; Lieber and Ward, 2011), and moment arm (Gans and de Vree, 1987; Rassier et al., 1999; Wilson and Lichtwark, 2011), can impact overall muscle function, studies of the *in vivo* function of muscle are necessary to determine the actual role of muscles in generating observed movements. Although there is extensive support for a link between locomotor kinematics and motor control patterns in a variety of species (e.g. Walmsley et al., 1978; De Leon et al., 1994; Olson and Marsh, 1998; Higham and Biewener, 2008), this relationship may not always hold, despite the fact that muscles often power locomotion. Changes in the activity of specific muscles may not always result in changes in the kinematics of the corresponding joint or limb segment if the muscle activity changes are used to counteract changes in external forces acting on the

animal or changes in the activity of other antagonistic muscle groups. For example, despite ample evidence that increases in incline require significant increases in muscle work (either through increased muscle recruitment or length change; e.g. Carlson-Kuhta et al., 1998; Gillis and Biewener, 2002; Higham and Jayne, 2004b), extensive changes in kinematics are not always observed (e.g. Foster and Higham, 2012). Similarly, changes in kinematics that are necessitated by changes in the external environment, such as habitat structure, may not alter the demand placed on the muscles. Thus, despite their dependent relationship, motor control patterns may not be affected when locomotor kinematics are determined by extrinsic rather than intrinsic factors. The additional complexity of this potential decoupling between kinematics and motor control patterns, as well as the potential influence of substrate structure on this decoupling, emphasizes the importance of simultaneous measurement of *in vivo* muscle activity and locomotor movements, especially in the context of varying environmental demand.

Most locomotor challenges that animals face as they move through heterogeneous habitats can be divided into two types, orientational and structural demand. The orientation of a substrate determines the relative impact of gravity on stability and forward locomotion and thus can profoundly impact the cost of locomotion and overall locomotor performance (e.g. Huey and Hertz, 1982; Cartmill, 1985; Irschick and Jayne, 1998; Daley and Biewener, 2003). Whereas the timing of muscle activity is fairly consistent with changes in incline, muscle recruitment tends to increase with increasing incline (e.g. Carlson-Kuhta et al., 1998; Gillis and Biewener, 2002; Higham and Jayne, 2004b). However, there are many other kinds of demands in terrestrial habitats (e.g.

perch diameter, substrate rugosity and texture, compliance, three-dimensional clutter), all of which can be placed into the broad category of structural demands. Although kinematics and kinetics have been shown to change in response to at least some of these structural demands (e.g. Franz et al., 2005; Foster and Higham, 2012; Gilman et al., 2012), how these types of challenges impact motor patterns is poorly understood.

Anolis, containing nearly 400 species, is among the best studied of lizard genera and has become a model system for a number of facets of biology (reviewed in Losos, 1994, 2009). Despite extensive research into differences in locomotor performance, morphology, and behavior in the different *Anolis* ecomorphs (e.g. Losos, 1990b; Irschick and Losos, 1999; Higham et al., 2001), we know nothing about how variation in habitat structure influences the muscles that power locomotion in these species. We examined the *in vivo* muscle activity patterns and relevant limb kinematics of the green anole, *Anolis carolinensis*, running on two different inclines (0^o and 90^o) and perch diameters (1cm and flat). This species is a trunk-crown ecomorph that regularly utilizes a wide range of substrate diameters and inclines, in proportion to what is available in its habitat (Mattingly and Jayne, 2004). We determined the function of the focal muscles based on hypotheses from the literature (Herrel et al., 2008a), and we tested the hypothesis that, as is the case with kinematics, muscle function will be modulated in response to changes in demand, resulting in a coupling of physiology and kinematics. Specifically, we expected that anoles would increase the intensity of motor unit recruitment in response to steeper inclines. On narrow perches, we expected increased recruitment in all of the muscles

examined in this study given that they are associated with moving in the more crouched posture that is associated with narrow perches [16,30].

Methods

Subjects

Research was conducted in accordance with the University of California, Riverside Animal Care and Use Protocol no. A-20110038E. Seven adult male *Anolis carolinensis* Voigt 1832 [mass=5.9± 0.4g; snout-vent length (SVL)=6.1±0.2cm] were obtained from commercial suppliers. Anoles were not fed within the 12 hours prior to surgery to minimize the effect of undigested food on anaesthetized subjects.

Based on previous kinematic data (Foster and Higham, 2012) and hypothesized muscle function from the literature (Table 2.1; Herrel et al., 2008a), six muscles were chosen for electromyography (EMG) implantation: biceps, caudofemoralis (CF), puboischiotibialis (PIT), ambiens pars dorsalis (AMB), peroneus longus (PL), and peroneus brevis (PB) (Fig. 2.1). These last two muscles were chosen instead of the synergistic gastrocnemius (Herrel et al., 2008a) because their position on the lateral, posterior side of the crus facilitated successful implantation and reduced the likelihood that electrodes would be pulled out during experimentation. Four points on the forelimb (shoulder, elbow, wrist, and center of the pectoral girdle) and five points on the hindlimb (hip, knee, ankle, base of the third metatarsal, and center of the pelvic girdle) were used to visualize the joints for subsequent kinematic analysis.

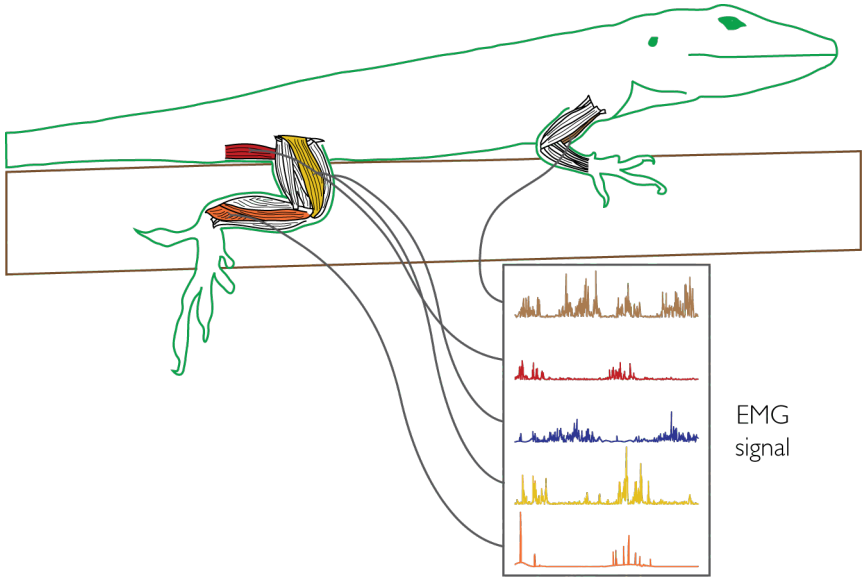

Figure 2.1. Schematic showing location of five of the six muscles implanted with electromyography (EMG) electrodes. Brown, biceps; red, caudofemoralis; blue, puboischiotibialis (located on ventral surface of proximal hind limb); yellow, ambiens; orange, peroneus brevis/longus.

Surgery and experimental protocol

These procedures follow those of Higham and Jayne (2004a). Prior to surgery anoles were anaesthetized with an intramuscular injection of Ketamine (100mg/kg). Bipolar EMG electrodes, constructed from 0.051mm diameter polycoated stainless-steel wire (California Fine Wire Co., Grover Beach, CA, USA), were implanted through the skin into the mid-bellies of each muscle using a 26-guage hypodermic needle. To reduce the possibility of electrodes pulling out during the course of the experiment, EMG wires were individually sutured to the skin, immediately proximal to the implantation point and again on the dorsal surface of the lizard's back, using 5-0 coated vicryl suture (Ethicon, Inc., Somerville, NJ, USA). After surgery, lizards were placed in clean 10-gallon aquaria and allowed to recover from anaesthesia for 6-12 hours.

Table 2.1. Muscles implanted with electromyography electrodes in *Anolis carolinensis* and their hypothesized function

	Hypothesized function
Forelimb	
Biceps pars dorsalis/ventralis[7]	Elbow flexion
Hind limb	
Caudofemoralis[8]	Femur retraction, rotation, knee flexion
Puboischiotibialis[9]	Femur depression, knee flexion
Ambiens pars dorsalis[5]	Knee extension
Peroneus longus[3]	Ankle extension
Peroneus brevis[4]	Ankle extension

Superscript, # individuals successfully implanted and analyzed.
Hypothesized function based on Herrel *et al*. (2008).

Running trials took place on an apparatus identical to that described previously (Foster and Higham, 2012). Lizards ran on 1 m long trackways at two perch diameters, a 9 cm wide flat perch, representing the large diameter treatment (Spezzano and Jayne, 2004; Foster and Higham, 2012), and a narrow, 1.3 cm diameter perch. Perches were covered with cork shelf liner to enhance traction and were inclined at 0^{o} and 90^{o}. To allow calculation of 3D kinematics, perches were mounted below a mirror inclined at 45^{o}. EMG wires were suspended below the perch and were long enough to ensure unobstructed forward locomotion.

Dorsal and lateral videos of the running anoles were obtained simultaneously with two high speed Photron APX-RS cameras (Photron USA, San Diego, CA, USA) at 500 frames s^{-1}. EMG signals were amplified 10000 times using GRASS QP511 quad and P55 AC amplifiers (Natus Neurology Inc., Warwick, RI, USA) with a 60Hz notch filter and low- and high-bandpass filters of 0.1Hz and 3000Hz, respectively. Signals were recorded at 5000 samples s^{-1} using a BIOPAC MP150 data acquisition system with the UIM100C module and Acqknowledge (version 4.0) software (BIOPAC Systems, Inc., Goleta, CA, USA). An external trigger was used to sync EMG and video data. Trials were

considered for analysis if anoles ran steadily through the field of view, on top of the perch.

After experimentation was complete, anoles were euthanized with an overdose of sodium pentobarbital (300mg/kg intraperitoneal injection). Post-mortem dissections were performed to verify electrode placement and all the muscles of the hindlimb and proximal forelimb were removed for mass and fascicle length measurements (Table 2.2).

Table 2.2. Mean limb muscle fascicle lengths and masses for *Anolis carolinensis*

	Fascicle Length (cm)	Mass (mg)
Proximal Forelimb		
Biceps pars dorsalis*	0.76±0.02	16.87±1.14
Biceps pars ventralis*	0.81±0.03	
Coracobranchialis longus	0.94±0.04	5.89±0.52
Coracobranchialis brevis	0.47±0.04	2.66±0.37
Triceps pars humerus anterior and posterior	0.79±0.03	23.91±12.03
Triceps pars scapularis	0.73±0.03	5.48±0.38
Triceps pars scapulohumeralis	0.64±0.04	3.16±0.56
Proximal Hind limb		
Puboischiotibialis*	1.36±0.04	18.91±1.60
Flexor tibialis internus	1.01±0.04	9.38±0.89
Flexor tibialis externus	1.13±0.03	12.91±0.08
Pubofibularis	1.04±0.05	5.80±0.53
Femorotibialis pars dorsalis	0.78±0.04	6.27±0.86
Femorotibialis pars ventralis	0.62±0.03	4.80±0.58
Ambiens pars dorsalis*	0.88±0.05	13.30±1.15
Ambiens pars ventralis	0.84±0.03	13.24±1.13
Iliofibularis	1.10±0.03	11.08±0.92
Ilioischiotibialis	0.91±0.05	9.40±1.24
Adductor femoris	0.88±0.04	8.08±1.20
Ilioischiofibularis	1.08±0.09	11.99±1.86
Distal Hind limb		
Tibialis anterior	0.83±0.04	4.33±0.40
Flexor digitorum communis	0.82±0.02	6.63±0.84
Peroneus longus*	0.84±0.08	3.66±0.29
Peroneus brevis*	0.74±0.04	4.10±0.38
Extensor digitorum longus	1.00±0.05	4.54±0.54
Gastrocnemius pars fibularis pars minor	0.63±0.07	3.59±0.50
Gastrocnemius pars fibularis pars major	0.98±0.04	13.62±1.34
Caudofemoralis*	1.30±0.04	81.27±6.00

Caudofemoralis muscle length=2.12±0.07cm.
Mean body mass=5.87±0.44g; mean snout-vent length=6.13±0.17cm.
*, implanted with electromyography electrodes.
Sample size for all dissected muscles, 9.
Values are means ± s.e.m.

Electromyography

Prior to all analyses, EMG signals were bandpass filtered (2500Hz and 70Hz high and low bandpass filtered, respectively) and rectified. Seven variables were calculated from these signals: onset and offset time, burst duration, magnitude and timing of peak burst amplitude, total rectified integrated area (RIA) during the stance phase, and the time during each burst at which half of the burst RIA was achieved. All calculations were performed using custom code written for MATLAB (written by K.L.F.).

Burst onset and offset times were calculated following the method described in Roberts and Gabaldón (2008). A signal envelope was obtained through additional smoothing using a lowpass filter (300Hz). The boundaries of the burst were defined as occurring when signal envelope exceeded a cutoff value of twice the standard deviation of an inactive section. Burst duration was the time between burst onset and offset. Both burst onset time and duration were standardized by stride duration and onset time was expressed relative to footfall prior to statistical analyses.

Before any calculations using EMG amplitude data, signal noise was subtracted from the rectified EMG signal. The maximum activity observed in each burst was identified and the time at which that peak occurred was expressed relative to footfall and standardized by stride duration. The total RIA during stance phase was the product of EMG amplitude and time and reflected the relative proportion of the muscle that was active during the period of time for which it was calculated. Both amplitude variables (i.e. peak burst amplitude and total stance RIA) were expressed relative to the maximum amplitude ever observed for that muscle per individual. To approximate the shape of the

EMG burst, we calculated the time at which half of the total burst RIA was achieved (sensu Roberts et al., 2007) and expressed this value relative to burst duration.

To confirm the hypothesized function of the muscles (Table 2.1), EMG signals from strides of different length were averaged. To facilitate this, signal amplitudes during stance and swing phases were divided into 40 and 20 equal-duration bins, respectively, to be consistent with the average duty factor of 66%. These binned amplitudes were expressed relative to the maximum amplitude observed for each individual and muscle to allow data to be pooled across individuals. The resulting trace for each muscle was then compared to the binned kinematic data for the joint at which each muscle was expected to act (e.g. Figs. 2.2-2.4).

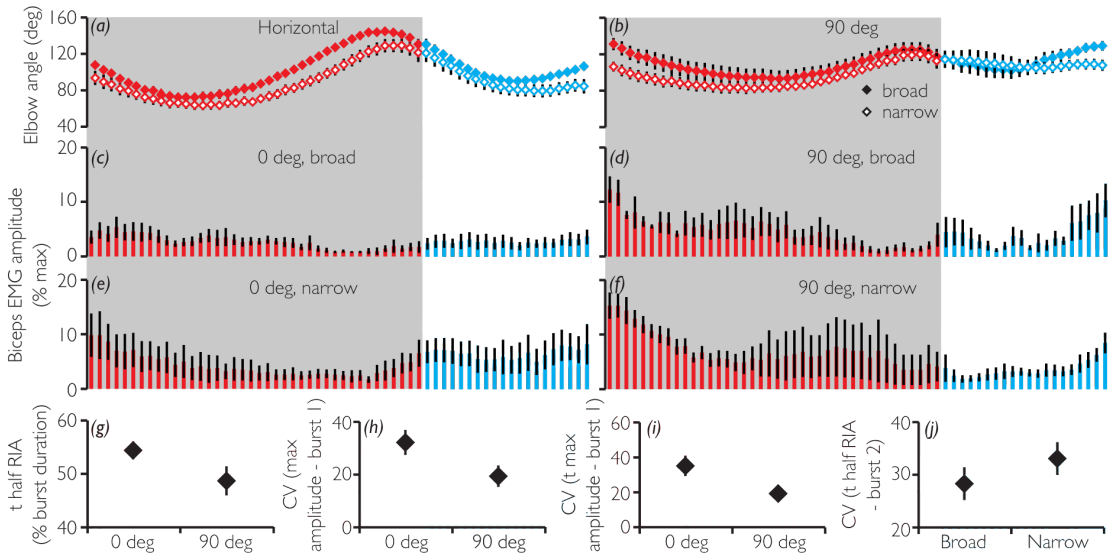

Figure 2.2. Binned joint angle (a,b), binned electromyography (EMG) amplitude (c-f), and significant relationships (g-j) for the biceps on the various conditions. (a-b): closed, broad perch; open, narrow perch. (a-f): shaded region (red data), stance phase; unshaded region (blue data), swing phase. CV, coefficient of variation; t, time; RIA, rectified integrated area; max, maximum. Values are mean ± s.e.m.

Kinematics

We obtained *x*, *y*, and *z* coordinates for each point (see above) using DLT DV 5 custom software (Hedrick, 2008) for MATLAB (version R2010a, The MathWorks, Natick, MA, USA). The *x*-axis represented fore-aft movement, the *y*-axis described dorso-ventral movement, and the *z*-axis represented medio-lateral movement perpendicular to the *x*-*y* plane. These points were used to calculate body speed, femur depression, retraction, and rotation angles, and elbow, knee and ankle angles as previously described in detail (Spezzano and Jayne, 2004; Foster and Higham, 2012). Briefly, body speed was calculated separately for each limb, dividing the distance traveled by the point at the center of the pectoral/pelvic girdles during the stride by the duration of the stride. Although body size did not correlate significantly with speed, speed was standardized (divided by SVL) to facilitate comparisons with other individuals and species in past and future studies.

Although these kinematic variables have already been measured for this species on similar substrates (Foster and Higham, 2012), the data reported here are from separate experiments in which the animals were implanted with EMG electrodes. Thus, a comparison can be made between unimplanted individuals (Foster and Higham, 2012) and implanted individuals (this paper) to ensure that behavior was not significantly altered by surgical procedures.

To facilitate comparisons with muscle activity data, angular data were binned as described for the EMG analysis. Minimum, maximum, and excursion of the angular data were obtained for the entire stride for input into statistical analyses.

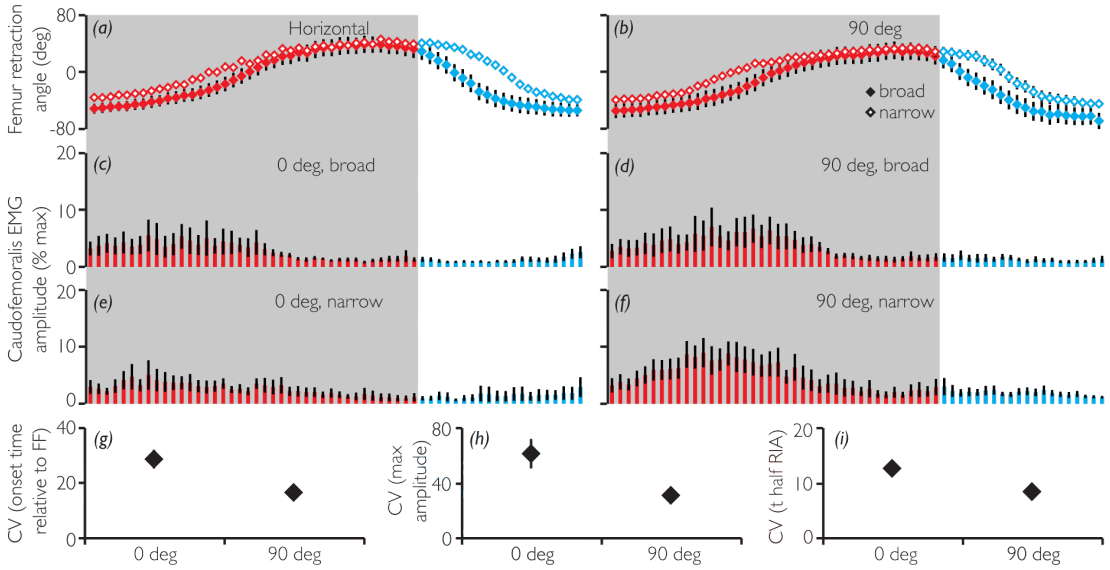

Figure 2.3. Binned joint angle (a,b), binned electromyography (EMG) amplitude (c-f), and significant relationships (g-i) for the caudofemoralis on the various conditions. (a-b): closed, broad perch; open, narrow perch. (a-f): shaded region (red data), stance phase; unshaded region (blue data), swing phase. CV, coefficient of variation; t, time; RIA, rectified integrated area; max, maximum. Values are mean ± s.e.m.

Statistical analyses

JMP (version 9.0, SAS Institute Inc., Cary, NC, USA) was used to perform all statistical analyses. The effect of speed (SVL s^{-1}) was removed prior to all analyses by regressing all kinematic and EMG variables individually against speed and saving residuals of the variables that showed a significant ($\alpha \pm 0.1$) relationship with speed.

The kinematic analyses performed were similar to those performed on previously published data (Foster and Higham, 2012) in order to confirm that EMG implantation did not interfere with normal movement. Briefly, temporal (angular velocities, stride frequency, and duty factor) and angular variables (minimum, maximum, and excursion of joint angles) were separated and input into separate discriminant function analyses (DFA). The variables that loaded heavily (greater than 0.3) on each of the first two DF axes were considered important for explaining the differences in kinematics between

treatments. A similar DFA was performed on temporal data. For a more detailed explanation of these statistical methods, see (Foster and Higham, 2012). As the kinematic changes between treatments were similar in these data as in individuals that were not implanted with EMG electrodes, the surgery did not affect our results.

Statistical analyses for each EMG variable were performed separately for each muscle. To test for significant differences between mean values of the treatments, mixed-model analyses of variance (ANOVAs) were performed in which individual was a random factor and incline and perch diameter were fixed factors. As there was never a significant interaction between incline and perch diameter, this interaction was removed from all analyses. The correct F-values and degrees of freedom for perch diameter and incline effects were obtained using the mean squares of the two-way interaction between fixed and individual factors as the denominator of each fixed factor (Zar, 1999).

In addition to testing for differences between mean EMG values, we tested for differences in the coefficient of variation (CV) of each variable between treatments using a two-way ANOVA in which incline and perch diameters were fixed effects. As above, the interaction between incline and perch diameter was never significant and so was removed from analyses.

Results

Overall, the experimental treatments affected kinematics much more strongly than they affected muscle activity patterns. Of the 32 kinematic variables examined, 63% were affected by the treatments whereas only 10% of the 100 muscle activity variables were affected. However, although more of the kinematic variables were affected by

perch diameter (47%) than by incline (25%), the opposite trend was seen in the muscle activity data (2% and 8% significant for perch diameter and incline, respectively). These relationships were not affected by the use of different statistical tests on the two datasets.

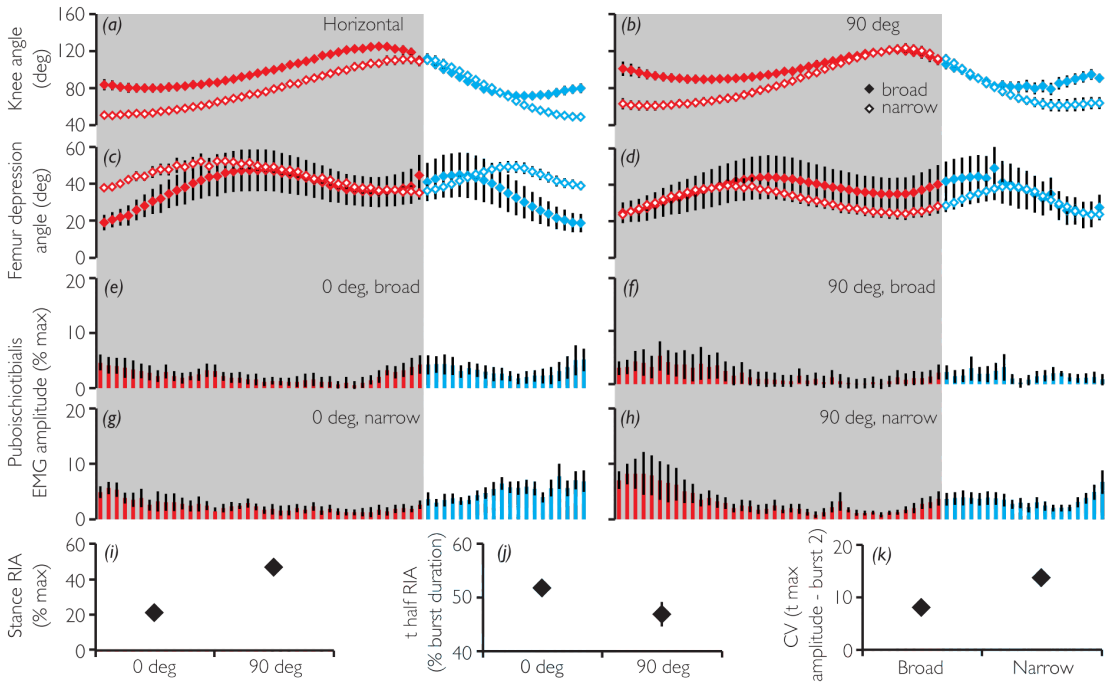

Figure 2.4. Binned joint angle (a-d), binned electromyography (EMG) amplitude (e-h), and significant relationships (i-k) for the puboischiotibialis on the various conditions. (a-d): closed, broad perch; open, narrow perch. (a-h): shaded region (red data), stance phase; unshaded region (blue data), swing phase. CV, coefficient of variation; t, time; RIA, rectified integrated area; max, maximum. Values are mean ± s.e.m.

Changes in kinematics with perch diameter and incline

Detailed descriptions of limb movements of this species on a variety of inclines and perch diameters have been published elsewhere using different individuals from the current study (Foster and Higham, 2012). We refer interested readers to those descriptions and here focus on highlighting the significant differences relevant to the focal muscles of this study.

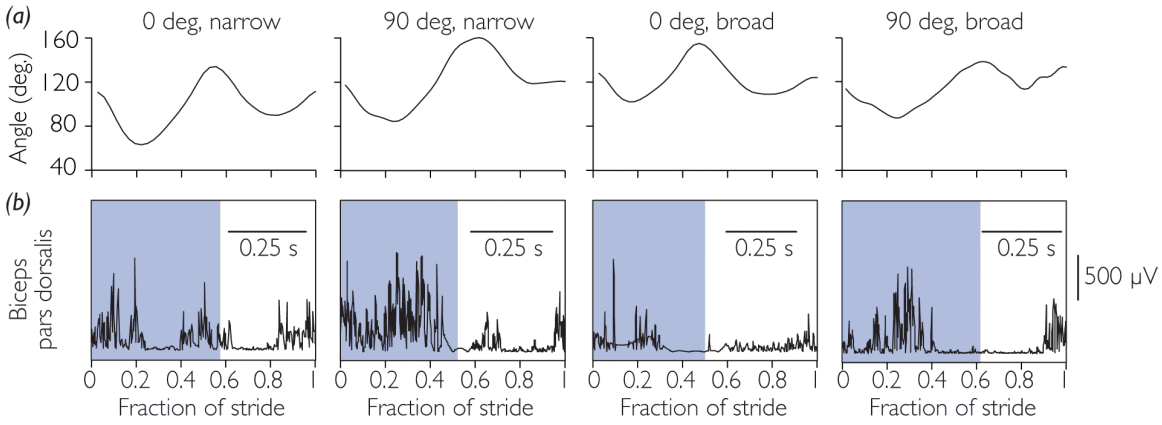

Figure 2.5. Elbow angle (a) and biceps electromyography trace (b) for a representative stride in each condition. Shaded area represents stance phase.

Table 2.3. Joint angle (Pillai's Trace F=2.75, P=0.029, describing 96.45% of total variation) and angular velocity (Pillai's Trace F=2.18, P=0.011, describing 93.43% of total variation) variables that loaded heavily (>0.3) on the first two axes of discriminant function analyses for *Anolis carolinensis*.

	Perch diameter		Incline	
	Narrow	Broad	0 deg	90 deg
Joint angle				
Max. elbow angle (FF)	106.53±5.75	123.44±5.00	103.73±5.46	126.24±5.29
Min. elbow angle			66.46±5.17	80.97±6.31
Ex. elbow angle			74.68±2.77	47.49±6.60
Ex. femur rotation			11.65±4.39	14.04±2.25
Min. femur retraction	-49.77±7.39	-63.28±11.75		
Max. femur retraction	49.46±7.91	40.69±4.28		
Min. femur depression	27.66±2.28	19.18±5.77		
Max. knee angle (FF)	73.67±7.34	97.44±6.40	79.09±6.36	92.03±7.39
Min. knee angle	54.71±4.09	84.85±5.40	63.96±3.88	75.60±5.61
Max. knee angle (ES)			122.09±3.86	126.54±4.27
Ex. knee angle	66.47±7.20	42.68±6.19		
Max. ankle angle	121.27±3.76	132.43±5.22		
Ex. ankle angle	59.10±6.25	71.42±5.26		
Joint angular velocity				
Stride frequency (strides s^{-1})	5.69±0.38	5.56±0.34		
Duty factor	0.63±0.02	0.71±0.03		
V. femur rotation	2.76±1.35	2.01±.89		
V. femur retraction	40.56±20.29	17.20±2.70		
V. femur depression	7.38±1.91	6.39±1.43		
V. knee flexion			-8.85±.95	-8.38±2.10
V. knee extension	12.90±3.61	9.46±2.49		
V. ankle extension	13.95±3.36	19.39±4.47		

Angles and angular velocities are given in deg and deg. s^{-1}.
FF, footfall; ES, end of stance; Min, minimum; Max, maximum; Ex, excursion; V, velocity.
Values are means ± s.e.m.

Of the kinematic variables considered in this study, approximately twice as many variables were significantly affected by changes in perch diameter than by changes in incline (Table 2.3). In general, individuals had a faster stride frequency and a lower duty factor on the narrow perch than on the flat perch (Table 2.3). In the forelimb, the elbow had a smaller excursion and was generally held more extended on the vertical treatment than on the level treatment but flexed more on the small diameter perch than on the flat perch (Table 2.3). In the hindlimb, the femur had a greater rotational excursion on the vertical than on the horizontal treatment but was more retracted and depressed on the small diameter perch than on the flat perch (Table 2.3). The femur also rotated, retracted, and depressed faster on the narrow perch than on the flat perch (Table 2.3). Like the elbow, the knee was held in a more extended posture at 90^{o} than at 0^{o} but it was generally more flexed and had a greater angular excursion on the small diameter than on the flat perch (Table 2.3). However, it extended faster on the narrow perch than on the flat perch (Table 2.3). Finally, the ankle extended less at end of stance, had less angular excursion, and extended slower on the small diameter perch than on the flat perch (Table 2.3).

Overall, joint kinematics of the anoles in this study were similar to the kinematics of individuals that had not been surgically implanted with EMG electrodes (Foster and Higham, 2012). Therefore, we conclude that electrode implantation did not alter normal movement.

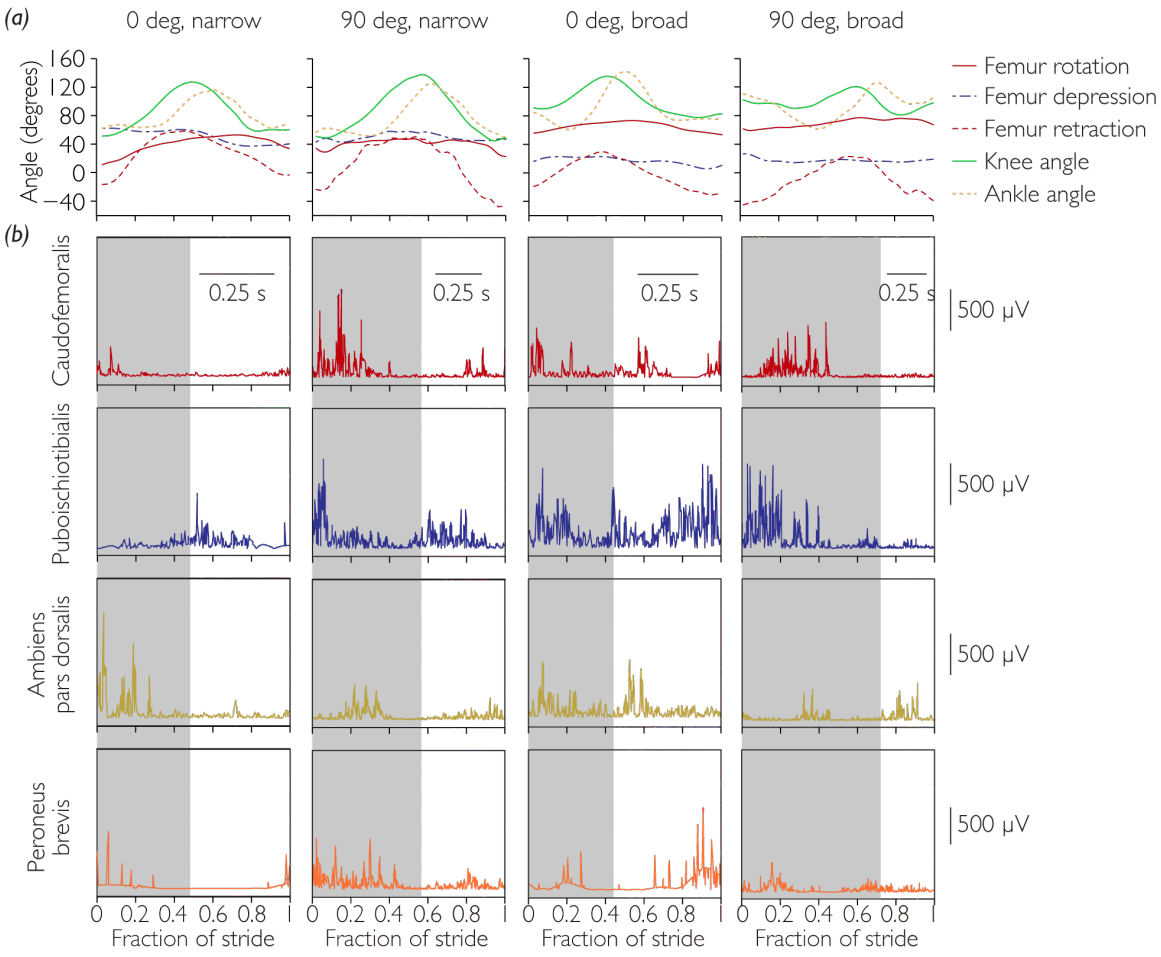

Figure 2.6. Joint angle (a) and electromyography traces (b) for the hind limb muscles and corresponding joints. Shaded area represents stance phase. Femur retraction/rotation = caudofemoralis; femur depression, knee flexion = puboischiotibialis; knee extension = ambiens; ankle angle = peroneus brevis.

General description of muscle activity patterns

The overall timing of muscle activity appeared to coincide with hypothesized functions of the muscles (Table 2.1, Figs. 2.2-2.6). The biceps had two bursts of activity during the stride. The first burst occurred during the entire period of stance phase elbow flexion. It began immediately prior to footfall, although sometimes as early as half of the way through swing phase, and generally ended ½ to ⅔ of the way through stance phase, generally after the end of elbow flexion (Figs. 2.2a-f,2.5). The beginning of second,

smaller burst approximately coincided with the end of elbow extension towards the end of stance phase and continued briefly during the first ¼ of swing phase as the elbow was flexing during the first portion of limb recovery (Figs. 2.2a-f,2.5).

The CF was generally characterized by a single prolonged burst of activity. Activity began shortly before footfall, often in the last ¾ of swing phase, and generally ended ½ to ⅔ of the way through stance (Figs. 2.3a-f,2.6). However, in some trials, CF activity continued through all of stance and ended shortly after the beginning of swing. The PIT generally had a double burst, a high amplitude, short burst centered around footfall and coinciding with a small amount of femur depression at the beginning of stance phase, and a lower amplitude, longer burst centered around end of stance, coincident with the end of knee extension and the beginning of knee flexion as the limb is brought forward in recovery during the swing phase (Figs. 2.4a-h,2.6). The AMB also had two bursts of activity. The first burst was generally larger in amplitude and occurred during knee extension, beginning shortly after footfall and ending around ⅔ of stance phase (Fig. 2.6). The second, smaller burst occurred during swing phase in the last ½ to ⅓ of knee flexion (Fig. 2.6). The PB and PL both had double bursts, the first beginning in late swing phase and ending shortly after footfall, and the second burst generally occurring in the second half of stance during the major propulsive period of ankle extension (Fig. 2.6).

Changes in muscle activity with perch diameter and incline

Overall, changes in incline had a stronger impact on muscle activity patterns than changes in perch diameter; a total of 8 variables, from the biceps, CF, and PIT, were

significantly affected by incline whereas only 2 variables, one each from the biceps and PIT, were affected by perch diameter.

Substrate diameter did not significantly affect the means of any of the variables considered here. However, the shape of the second burst of the biceps, as measured by the time, relative to the beginning of the burst, at which half RIA was achieved, was more variable on the small diameter perch (CV=33.40±2.92) than on the flat perch (CV=28.31±3.06; $F_{1,14}$=4.82, P=0.046; Fig. 2.2j). Similarly, the time, relative to footfall, at which the maximum amplitude of the second burst of the PIT was reached was more variable on the narrower perch (CV=13.56±1.68) than on the flat perch (CV=7.83±1.32; $F_{1,19}$=4.82, P=0.041; Fig. 2.4k).

Mean differences in muscle activity patterns, in response to changes in incline, were only observed in the biceps and PIT. The first burst of the biceps ($F_{1,4}$=8.17, P=0.046; Fig. 2.2g) and the second burst of the PIT ($F_{1,4}$=12.26, P=0.025; Fig. 2.4j) had a more front-loaded shape on the vertical (time to half RIA, relative to FF, as % of burst duration; biceps=48.77±2.57; PIT=46.98±2.23) than on the horizontal treatment (biceps=54.30±1.60; PIT=51.95±1.44) and the PIT had a greater total recruitment during stance on 90^o (RIA, as % max=46.48±4.40) than on 0^o (RIA, as % max=20.96±2.29; $F_{1,4}$=23.52, P=0.0083; Fig. 2.4i). The remaining variables that were affected by incline all showed a significant increase in variability on the level treatment compared to the vertical treatment. These variables included the maximum amplitude (0^o CV=32.10±4.64, 90^o CV=19.19±3.97; F1,15=4.73, P=0.046; Fig. 2.2h) and the time, relative to FF, at which that max. amplitude was achieved (0^o CV=35.05±5.70, 90^o

CV=19.34±2.85; F1,15=5.08, P=0.04; Fig. 2.2i) for the first burst of the biceps, and the onset time (0^o CV=28.69±3.39, 90^o CV=16.61±2.37; F1,20=7.80, P=0.011; Fig. 2.3g), maximum amplitude (0^o CV=61.61±10.65, 90^o CV=31.44±5.39; F1,20=6.69, P=0.018; Fig. 2.3h), and shape (0^o CV=12.76±1.31, 90^o CV=8.47±1.27; F1,20=5.93, P=0.024; Fig. 2.3i) of the CF burst.

Discussion

We assessed simultaneous changes in 3D limb kinematics and motor control of a lizard moving in a simulated arboreal environment with varying inclines and perch diameters. Limb kinematics were impacted more than muscle activity patterns in response to our treatments, and both were more strongly affected by different substrate characteristics; more kinematic variables were significantly affected by perch diameter than by incline (Table 2.3; Foster and Higham, 2012), whereas more EMG variables were significantly affected by incline than by perch diameter (Figs. 2.2-2.4). This decoupling of kinematics and muscle activity suggests that muscles and limb movements do not respond to changes in substrate in the same way, and that a given pattern of neural control can result in different kinematic patterns (possibly impacted by external factors rather than internal control). Further, different variables were found to be significantly different with changes in perch diameter than with changes in incline, indicating that these substrate variables pose distinct functional challenges.

Temporal heterogeneity of function within muscles

All muscles examined in this study, with the exception of the CF, were characterized by two bursts during a single stride cycle. Timing of these bursts relative to angular changes at the corresponding joints (Figs. 2.2-2.6) indicate that, contrary to what has been hypothesized based on anatomical position, these muscles likely have more than one function. For example, although the first, mid-stance burst in the AMB and the second, late-stance burst in the PL and PB both support the hypothesized functions of these muscles (Table 2.1), the remaining bursts of activity in these muscles seem to occur during knee and ankle flexion, respectively. As these muscles act to resist flexion when active, they likely are performing a stabilizing function in these instances. In contrast with this additional antagonistic function, the two bursts of the PIT appear to temporally segregate the dual function of this muscle, with femur depression occurring during the first, early-stance burst and knee flexion occurring during the second, late-stance burst. These patterns of muscle activity suggest an added complexity to muscle function that cannot be gleaned from morphological dissections alone. Further, double bursts are not unheard-of in vertebrates (e.g. De Leon et al., 1994; Ashley-Ross, 1995; Higham and Jayne, 2004b), but it is worthwhile to consider that such activity patterns may be important for temporally separating multiple functions of a single muscle. This temporal segregation, in addition to the recent research that has identified spatial segregation of function within muscles during locomotion [10], highlights the complex function of muscles under dynamic conditions.

Effect of substrate on muscle activity

As incline increases, an increasing component of gravity acts to resist forward locomotion (Cartmill, 1985; Preuschoft, 2002), necessitating an increase in muscle work. Based on studies examining the effects of incline on vertebrate muscle activity (Carlson-Kuhta et al., 1998; Gabaldón et al., 2001; Gillis and Biewener, 2002; Daley and Biewener, 2003; Higham and Jayne, 2004b), it is common for animals to increase intensity, rather than altering timing of muscle activity to increase muscle work on steeper inclines. In our study, the PIT was the only muscle with greater stance phase recruitment on steeper inclines, despite the fact that we examined multiple propulsive muscles. In addition, temporal aspects of the biceps and PIT muscles were altered, with greater front-loading of the muscle bursts on vertical than on level treatments. Although the onset time of these bursts did not differ significantly across treatments, this change in burst shape indicates that a greater number of motor units were being recruited earlier in the burst to facilitate a more rapid initiation of movement at the beginning of the stride on the steeper incline. Whether or not this also indicates changes in the recruitment timing of different fiber-types remains to be determined.

Interestingly, the majority of the EMG variables that were affected by substrate were significant for changes in CV rather than differences in mean values. Within-individual variability was always significantly greater on the level than on the vertical incline, and on the narrow perch diameter than on the broad surface. The degree of stereotypy of locomotion is a reflection of the degree to which an animal is specialized for that particular locomotor mode in its preferred habitat (Klopfer and MacArthur, 1960;

Sanderson, 1990). Therefore, although *A. carolinensis* is commonly observed in all areas of the arboreal habitat, and on the ground (Mattingly and Jayne, 2004), the decreased variability in muscle activity patterns observed on steep, broad substrates may indicate a functional preference for tree trunks. However, future work on more species with varying degrees of specialization will be needed to determine if there is a link between substrate preference and stereotypy of muscle activity patterns.

Decoupled kinematics and muscle activity in response to substrate

Surprisingly, kinematics and muscle activity exhibited a decoupled response to changes in substrate, particularly perch diameter. Despite considerable differences in limb posture and movement on the different substrate diameters (Table 2.3; Foster and Higham, 2012), there were no changes in mean values for any of the EMG variables examined and only two changes in variability (Figs. 2.2,2.4). The significant changes in kinematics, namely increases in limb flexion, depression, and retraction on the narrower substrate than on the broad surface, likely require a change in the length of the muscle-tendon units of most muscles investigated here (a possible exception is the biarticular PL, which may have minimal net length change through simultaneous knee and ankle flexion). As *A. carolinensis* is very small and these muscles insert via short tendons (biceps, CF, and PL/PB) or no tendon at all (PIT and AMB; Herrel et al., 2008a), these changes in limb posture likely result primarily in changes of the muscle length itself. If these operating lengths became suboptimal, muscle force generation would decrease, requiring a compensatory increase in fiber recruitment in order to maintain a similar force

output (Loeb and Gans, 1986; Rassier et al., 1999). The absence of any change in muscle intensity with substrate diameter may reflect the opportunistic nature of this species' habitat use; the expected changes may be more evident in ecomorphs with a more specialized habitat preference, in which optimal muscle lengths may have become adapted for the preferred substrate condition. However, this hypothesis remains to be tested. Interestingly, populations of green anoles differ in habitat use in Louisiana, USA (Irschick et al., 2005). Populations that occupy habitat dominated by broad leaves use broader surfaces, on average, than populations living in habitat dominated by narrower substrates (Irschick et al., 2005). However, within each of these populations, anoles generally preferred to use broader surfaces than were available on average (Irschick et al., 2005), potentially indicating the challenges of instability and its negative impact on locomotor performance on suboptimal, narrow perches. A comparison of kinematics and muscle activation in these populations may reveal the basis for this preference. Although it is possible that other muscles not examined may have been impacted, this is not likely given that we implanted most of the important propulsive muscles in the limbs. In addition, simultaneously recording from every muscle in the limbs is not feasible given the limited size of the animals.

In summary, despite considerable changes in limb kinematics with substrate, and perch diameter in particular (Foster and Higham, 2012), there were few significant changes in muscle activity patterns. This apparent decoupling of the response of muscle and limb movement to substrate highlights the complex nature of animal locomotion and how little we understand about muscle function in ecologically relevant contexts. It is

evident that biomechanical and neuromechanical studies must use caution when interpreting observed changes in kinematics and motor control signals since altered kinematics do not necessarily imply active modulation and muscle activity patterns cannot be used in isolation when attempting to infer movement. Further, the possibility that different physiological and biomechanical variables can be decoupled in their contribution to locomotion may complicate our theories about the evolution of different locomotor modes or how locomotor adaptation for demanding substrates may have been achieved. The fact that kinematics can change significantly without corresponding changes in motor control is intriguing, and might be widespread among vertebrates that live in complex habitats. Examination of more specialized *Anolis* ecomorphs to see if they exhibit a similar decoupling of movement and motor control may be a promising and fruitful next step in the investigation of the evolution of kinematic flexibility for a single motor pattern.

Habitat complexity stretches beyond consideration of incline and perch diameter in isolation. Arboreal habitats are characterized by numerous challenges that must be dealt with or circumvented such as substrate compliance, rugosity, swaying caused by wind or animal movement, obstacles, sharp turns, and gaps that must be bridged. These and other variables occur in various combinations and arboreal animals must deal with or circumvent each of them, often in quick succession. Given that the forelimbs are likely the first to contact a new surface first during a transition, much of the modulation might stem from feedback following this initial footfall. Examining the role of combinations of

these challenges, as well as transitioning between combinations during a locomotor event, would be a highly interesting avenue of future research.

Chapter 3 - Integrating gastrocnemius force-length properties, *in vivo* activation, and muscle-tendon unit length reveals how *Anolis* deals with varying ecological conditions

Abstract

Locomotion through heterogeneous environments often requires moving on substrates that constrain foot placement. This likely affects not only limb posture, but also muscle operating lengths and forces. Although many studies have examined the impact of substrate incline on vertebrate locomotor behavior, motor control, and force production, very little is known about how these variables are affected by structural demands like substrate diameter. Thus, how substrate shape impacts *in vivo* muscle function remains an important, but neglected question in muscle ecophysiology. Here, we used high-speed videography, electromyography, *in situ* contractile experiments, and dissection to build a comprehensive picture of gastrocnemius muscle function during arboreal locomotion in the Cuban knight anole, (*Anolis equestris*). Muscle recruitment, operating lengths, and potential force all indicate that the gastrocnemius contributes more to the propulsive effort on broad surfaces than narrow surfaces. Surprisingly, substrate inclination affected the relationship between the maximum potential force and fiber recruitment of the gastrocnemius; the trade-off that was present between these variables on horizontal

conditions became a positive relationship on inclined surfaces. Further, hind limb tendons are incapable of undergoing significant strain during cyclical locomotion in this species. Finally, the biarticular nature of the gastrocnemius appears to allow the muscle to generate forces isometrically, regardless of condition, despite the lack of tendon strain. These results emphasize that ecology can impact numerous aspects of muscle function and the necessity of examining both behavioral and physiological properties of muscles to build a comprehensive picture of how animals move successfully in their environment.

Introduction

How animals function within the context of environmental demand determines their successful performance at numerous tasks integral for survival. The majority of these tasks, which include evading predators, capturing prey, defending territories, and attracting mates, require locomotion and occur in highly heterogeneous environments. Muscles, as the fundamental units responsible for powering locomotion, must, therefore, have the morphological, behavioral, and/or physiological flexibility to generate movement in the face of these varying conditions.

There are several mechanisms by which muscle function can theoretically shift to allow animals to meet environmental demands. Changes in the morphological arrangement of muscles can impact the magnitude and effective transmission of forces to the environment. For example, species that commonly move on steep inclines tend to have greater propulsive muscle moment arms (Zaaf et al., 1999; Herrel et al., 2008b; Herrel et al., 2008a) whereas species that oscillate their limbs through wide ranges in

amplitude do so with muscles with longer fibers (Loeb and Gans, 1986; Biewener, 1998; Biewener and Gillis, 1999; Daley and Biewener, 2003). Although the time scale of such changes in morphology may be long, short term alterations in muscle activation and operating length may have considerable impact on muscle force production. Muscle recruitment may increase to meet an increased demand for muscle work (e.g. on an incline; Carlson-Kuhta et al., 1998; Gillis and Biewener, 2002; Daley and Biewener, 2003; Higham and Jayne, 2004b; Foster and Higham, 2014) or the lengths over which the muscle is generating force may be altered, impacting the amount of force and/or work it generates because of where it is active on its force-length and/or force-velocity curves (e.g. Johnston, 1991; Roberts et al., 1997; Olson and Marsh, 1998; Gabaldón et al., 2004).

Anolis lizards from the Greater Antilles islands in the Caribbean are small, arboreal lizards that have repeatedly and rapidly evolved ecomorphs that differ moprhologically and behaviorally based on the region of the arboreal environment on which they specialize (Losos, 1994, 2009). They are extremely adept at moving through the highly complex arboreal environment, making them an excellent system to study how muscles function in the face of extreme structural (e.g. perch diameter, compliance, substrate rugosity) and orientational (i.e. incline) challenges. The extreme shifts in limb kinematics required for these animals to move on arboreal surfaces, particularly different diameter perches, make it likely that shifts in motor recruitment (Foster and Higham, 2014) and/or operating length will alter the efficacy of force production on these different surfaces. Although recent work has begun to investigate how motor patterns shift as

these animals move on surfaces of different incline and perch diameter (Foster and Higham, 2014), thus far we have been unable to place such shifts in motor control into a broader context of how muscle function (i.e. force production) is impacted by the demands of the arboreal environment.

Tendons are well recognized as an integral component in the locomotor system because of their ability to store elastic energy via stretch and recoil. However, in small animals, tendons are unlikely to be able to play such a role in energy conservation during steady locomotion because there is insufficient time to employ a catch mechanism and the muscle forces and body mass are too small to deform the tendon without that catch mechanism (Biewener et al., 1981; Biewener and Blickhan, 1988; Pollock and Shadwick, 1994b; Astley and Roberts, 2012). If we can show that tendons are incapable deforming during cyclical, non-ballistic locomotion in Anolis lizards, we will be able to infer *in vivo* muscle length from three-dimensional joint kinematics. The utility of using kinematics to infer *in vivo* muscle length has been demonstrated previously in other systems (e.g. fishes; Katz and Shadwick, 1998; Shadwick et al., 1998; Donley and Shadwick, 2003) and will allow us to link *in vivo* muscle activation patterns and three-dimensional joint kinematics to *in situ* force-length contractile properties. This indirect approach is essential for understanding muscle function in these small animals because their muscles and tendons are too small to enable the use of traditional techniques (i.e. sonomicrometry and tendon force-buckles) to measure *in vivo* muscle length and force directly. Here, we use the muscle and tendon of the gastrocnemius pars fibularis pars major (a prominent ankle extensor and hereafter referred to as gastrocnemius, for simplicity) in *Anolis*

equestris to test whether tendons are capable of deformation during cyclical locomotion in this species using both calculations based on dissections of hind limb muscles and tendons as well as evidence derived from *in situ* contractile experiments. Thus, when combined with *in vivo* kinematics, *in vivo* muscle activation data, and *in situ* force-length properties, we will be able to address the fundamental questions of whether small arboreal animals have muscles that operate at or near the plateau of the force-length curve and how muscle function shifts in the face of changes in environmental demand.

We predict that the gastrocnemius will have greater muscle recruitment and/or function at a more optimal position on the force-length curve on broad rather than narrow surfaces since the geometry of the surface means the position of the foot (on top of the surface rather than on the side) should allow ankle extension to contribute more to propulsion (Foster and Higham, 2014). Further, we expect to see a trade-off between potential force (force predicted by the *in situ* force-length curve) and muscle recruitment. This is because as the lengths at which a muscle is activated become more optimal causing the muscle to generate forces at a position closer to the plateau of the force-length curve (i.e. the muscle becomes more effective), the muscle theoretically shouldn't need to recruit as many fibers to generate a given amount of force. Alternatively, it is possible that there may be no relationship or a positive relationship between potential force and muscle recruitment if there is a shift in demand necessitating the use of multiple mechanisms to achieve increased amounts of force.

Methods

Seven adult male *Anolis equestris* Merrem 1820 (mass = 58.5 ± 5.8g; snout-vent length = 14.3 ± 0.5cm) were purchased from commercial suppliers and housed individually in 10-gallon aquaria illuminated with a combination of 100W incandescent and UVB lights for 12h per day. Lizards were provided and water *ad libitum* and fed vitamin-enriched crickets every day, except the day of experimentation.

Six of the seven individuals were used in a succession of 4 procedures that were combined to create a comprehensive picture of the function of the gastrocnemius in *A. equestris* (Fig. 3.1): 1) electromyography (EMG) experiments to obtain muscle activity data *in vivo* as animals ran on 4 different surfaces varying in incline and perch diameter, 2) *in situ* experiments to characterize force-length properties of the gastrocnemius, 3) post-mortem manipulation of hind limbs with muscles exposed to quantify the relationship between joint angle and muscle length, and 4) detailed dissection and morphometric analysis of the muscles and tendons of the hind limb to calculate maximum potential for tendon strain during cyclical locomotion in these animals. Each of these procedures are described in detail below. Due to problems with maintaining EMG implantation in the seventh individual, this individual was only used for the 4th (morphological) portion of the project.

Table 3.1. Hind limb muscle and tendon morphology for *Anolis equestris*.

		Individual						
	Variable	1	2	3	4	5	6	7
External morphology	Body mass	63.92	60.33	78.32	74.58	40.35	52.89	39.12
	SVL	15.1	15	16.1	15	12.5	14.1	12.3
	Total L.	39	37.7	46.1	29.5	28.5	38.4	34.6
	Humerus L.	2.5	2.5	2.5	2.1	2.4	2.7	2.1
	Radius L.	2.3	2	2.5	2.1	2	2.1	1.7
	Metacarpal L.	0.9	0.9	1	0.8	0.6	0.6	0.6
	3rd finger L.	1	1	1	0.9	0.8	1	0.9
	Femur L.	3.5	3	3.3	2.8	2.7	2.6	2.6
	Tibia L.	3.1	2.9	3.4	2.8	2.9	2.9	2.5
	Metatarsal L.	1.9	2	2.1	1.7	1.5	1.8	1.3
	4th toe L.	1.8	1.9	2.1	1.9	1.5	1.7	1.4
Puboischiotibialis	Fascicle L.	3.3	3.8	3.1	3.7	3.3	3.4	2.8
	Tendon L.	0.2	0.2	0.5	0.4	0.2	0.5	0.4
	Tendon mass for L.=0.2cm	0.0018	0.0029	0.0028	0.001	0.001	0.0013	0.0018
	Insertion on tibia (cm from knee)	0.3-0.7	0.4-0.8	0.5-0.9	0.3-0.6	0.5-0.8	0.4-0.8	0.3-0.6
	Origin on pelvic girdle (cm from hip)	0.5	0.7	0.4	0.6	0.6	0.6	0.4
	Mass	0.3058	0.3096	0.5094	0.404	0.2323	0.3547	0.2253
Flexor tibialis internus	Fascicle L.	3	2.7	2.6	2.5	2.4	2.2	2
	Tendon L.	0.2	0.2	0.5	0.4	0.2	0.5	0.4
	Tendon mass for L.=0.2cm	0.0018	0.0029	0.0028	0.001	0.001	0.0013	0.0018
	Insertion on tibia (cm from knee)	0.7	0.8	0.9	0.6	0.8	0.8	0.6
	Mass	0.1191	0.1127	0.1737	0.1533	0.0863	0.1234	0.0742
Flexor tibialis externus	Fascicle L.	3.1	3	2.9	2.7	2.5	2.6	2.3
	Insertion on tibia (cm from knee)	0.4	0.3	0.3	0.3	0.3	0.3	0.3
	Mass	0.1062	0.1399	0.2736	0.1896	0.1065	0.1474	0.1332
Pubofibularis	Fascicle L.	2.5	2.5	2.7	2.5	2.3	2.3	2
	Insertion on fibula (cm from knee)	0.25	0.3	0.2	0.2	0.3	0.3	0.3
	MTU L.	3.1	3.1	2.9	2.8	2.6	2.7	2.4
	Tendon mass for L.=0.2cm	0.0004	0.0004	0.0005	0.0004	0.0006	0.0002	0.0008

	Mass	0.0668	0.0769	0.0987	0.1021	0.0514	0.068	0.0511
Femorotibialis pars ventralis	Avg fascicle L.	1.7	1.7	1.9	2.1	1.4	1.6	1.3
	Insertion on tibia (cm from knee)	0	0	0	0	0	0	0
	Mass	0.0764	0.0741	0.1243	0.0875	0.0844	0.1224	0.0958
Ambiens pars ventralis	Fascicle L.	2.6	2.6	2.4	2.4	2.4	2.3	1.9
	Insertion on tibia (cm from knee)	0.25	0.2	0.3	0.2	0.2	0.2	0.2
	Mass	0.1532	0.1916	0.2912	0.2202	0.1437	0.2102	0.1532
Ambiens pars dorsalis	Fascicle L.	2.2	2	2.5	2.3	1.4	1.8	1.4
	Insertion on tibia (cm from knee)	0.25	0.2	0.3	0.2	0.2	0.2	0.2
	Tendon L.	0.9	1	0.8	0.7	0.6	0.7	0.7
	Tendon mass for L.=0.3cm	0.009	0.0063	0.004	0.0041	0.0029	0.003	0.0017
	Mass	0.1555	0.1522	0.223	0.1768	0.0939	0.1643	0.1169
Iliofibularis	Fascicle L.	2.9	3	3.3	2.7	2.7	2.7	2.3
	Insertion on fibula (cm from knee)	0.6-0.8	0.7-0.9	0.9-1.1	0.6-0.8	0.5-0.7	0.5-0.7	0.4-0.6
	Mass	0.1791	0.1764	0.2788	0.223	0.1333	0.2187	0.1536
Ilioischiotibialis	Fascicle L.	2.4	2.3	2.2	2.2	2	2	1.7
	Insertion on tibia (cm from knee)	0.7	0.7	0.6	0.6	0.6	0.6	0.5
	MTU L.	2.8	2.7	2.5	2.7	2.5	2.5	2.1
	Tendon mass for L.=0.2cm	0.0007	0.0007	0.0003	0.0004	0.0003	0.0004	0.0002
	Mass	0.1247	0.1044	0.174	0.1645	0.0789	0.1318	0.1056
Femorotibialis pars dorsalis	Fascicle L.	1	1	1.1	1.1	1.1	1.1	1.1
	Insertion on tibia (cm from knee)	0	0	0	0	0	0	0
	Pennation angle	28	24	25	20	22	25	25
	Mass	0.1718	0.1392	0.241	0.1301	0.1151	0.1919	0.1427
Adductor femoris	Fascicle L.	1.8	1.7	1.8	1.7	1.4	1.4	1.4
	Pennation angle	12	12	11	13	14	13	14
	Mass	0.1949	0.2236	0.2985	0.2688	0.1575	0.2854	0.2046
Ilioischiofibularis	Fascicle L.	1.4	1.4	1.4	1.4	1.4	1.4	1.4
	Insertion on fibula (cm from knee)	0.4	0.4	0.4	0.4	0.4	0.4	0.4
	MTU L.	2.2	2.2	2.2	2.4	2.2	2.1	2.2

	Tendon mass for L.=0.3cm	0.0002	0.0002	0.0004	0.0006	0.0002	0.0005	0.0001
	Pennation angle	10	10	10	10	10	10	10
	Mass	0.0696	0.0472	0.0715	0.1022	0.0457	0.0637	0.0927
Tibialis anterior	Fascicle L.	1.3	1.2	1.2	1.2	1.1	1.1	1
	Insertion on metatarsals (cm from ankle)	0.1-0.3	0.1-0.3	0.1-0.3	0.1-0.3	0.1-0.3	0.1-0.3	0.1-0.3
	Pennation angle	5	7	9	9	8	9	9
	Mass	0.0795	0.0876	0.098	0.0903	0.0512	0.1091	0.0693
Flexor digitorum communis	Fascicle L.	1.3	1.4	1.3	1.2	1.1	1.1	1.1
	Insertion on metatarsals (cm from ankle)	0.2	0.2	0.2	0.2	0.2	0.2	0.2
	MTU L.	1.5	1.6	1.5	1.5	1.5	1.7	1.5
	Tendon mass for L.=0.3cm	0.0001	0.0013	0.0019	0.002	0.0014	0.0038	0.0008
	Mass	0.0226	0.0458	0.0544	0.0501	0.0347	0.1415	0.0323
Peroneus longus	Fascicle L.	2.1	1.9	2.1	1.8	1.7	1.6	1.6
	MTU L.	2.9	2.9	2.9	2.7	2.6	2.7	2.4
	Insertion on metatarsals (cm from ankle)	0.3	0.3	0.4	0.4	0.4	0.3	0.2
	Tendon mass for L.=0.45cm	0.0011	0.0015	0.0015	0.0013	0.0009	0.0005	0.0014
	Mass (g)	0.0462	0.0532	0.0708	0.0435	0.0312	0.0587	0.0494
Peroneus brevis	Fascicle L.	0.5	0.5	0.5	0.5	0.5	0.5	0.5
	MTU L.	2.8	2.4	2.4	2.2	1.9	2	1.9
	Insertion on metatarsals (cm from ankle)	0.1	0.1	0.1	0.1	0.1	0.1	0.1
	Tendon mass for L.=0.3cm	0.001	0.0016	0.002	0.0013	0.0009	0.0005	0.0008
	Pennation angle	15	17	15	18	13	18	16
	Mass	0.0491	0.0481	0.0746	0.0585	0.0359	0.059	0.0465
Extensor digitorum longus	Fascicle L.	2.6	2.3	2.2	2	1.9	2	1.9
	Femoral tendon L.	1.2	1.4	1.2	1	1	1	0.9
	Mass femoral	0.0004	0.0003	0.0008	0.0004	0.0004	0.0007	0.0006

	tendon for L.=0.25cm							
	Origin on femur (cm from knee)	0.1	0.1	0.1	0.1	0.1	0.1	0.1
	MTP tendon L.	0.9	1.2	1	0.9	0.9	0.8	0.8
	Mass MTP tendon for L.=0.3	0.0004	0.0005	0.0008	0.0004	0.0003	0.0004	0.0007
	Insertion on metatarsals (cm from ankle)	0.3	0.5	0.6	0.4	0.3	0.4	0.4
	Mass	0.0497	0.0648	0.0781	0.0695	0.0366	0.0704	0.0753
Gastrocnemius pars fibularis pars minor	Fascicle L.	1.4	1.2	1.2	1.2	1	1	1
	Insertion on metatarsals (cm from ankle)	0.4	0.4	0.4	0.4	0.4	0.4	0.4
	Origin on femur (cm from knee)	0.2	0.4	0.3	0.4	0.3	0.3	0.3
	Pennation angle	14	12	14	14	13	15	13
	MTU L.	3.3	3.5	3.3	2.9	2.5	2.8	2.6
	Tendon mass for L.=0.3cm	0.003	0.0027	0.0024	0.0034	0.0022	0.001	0.0019
	Mass	0.1282	0.1331	0.1723	0.1729	0.0874	0.1228	0.1067
Gastrocnemius pars fibularis pars major	Fascicle L.	2.2	2.3	2.1	2.2	2	2.2	2.1
	Insertion on metatarsals (cm from angle)	0.4	0.4	0.4	0.4	0.4	0.4	0.4
	Origin on femur (cm from knee)	0.2	0.4	0.3	0.4	0.3	0.4	0.3
	MTU L.	3	3.2	3	2.9	2.5	2.7	2.5
	Tendon mass for L.=0.3cm	0.0044	0.0043	0.0084	0.0057	0.0032	0.006	0.0026
	Mass	0.1303	0.1496	0.2877	0.2237	0.0955	0.1784	0.1418
Caudofemoralis longus	Muscle L.	6.2	6.5	6.8	7.1	5.7	5.8	5.5
	Avg fascicle L.	1.9	2.1	2	1.9	1.8	1.8	1.8
	MTU L.	6.8	7.1	7.3	7.6	6.2	6.3	6
	Pennation angle	20	17	20	16	15	15	15
	Femoral tendon mass for	0.0041	0.0055	0.0044	0.0052	0.0031	0.0045	0.0062

L.=0.5cm							
Mass	0.7325	0.8505	1.233	1.0221	0.5983	0.7314	0.9384

L., length; SVL, snout-vent length; MTU, muscle-tendon unit; MTP, metatarsalphalangeal; Avg, average.
All lengths given in cm; all masses given in g.

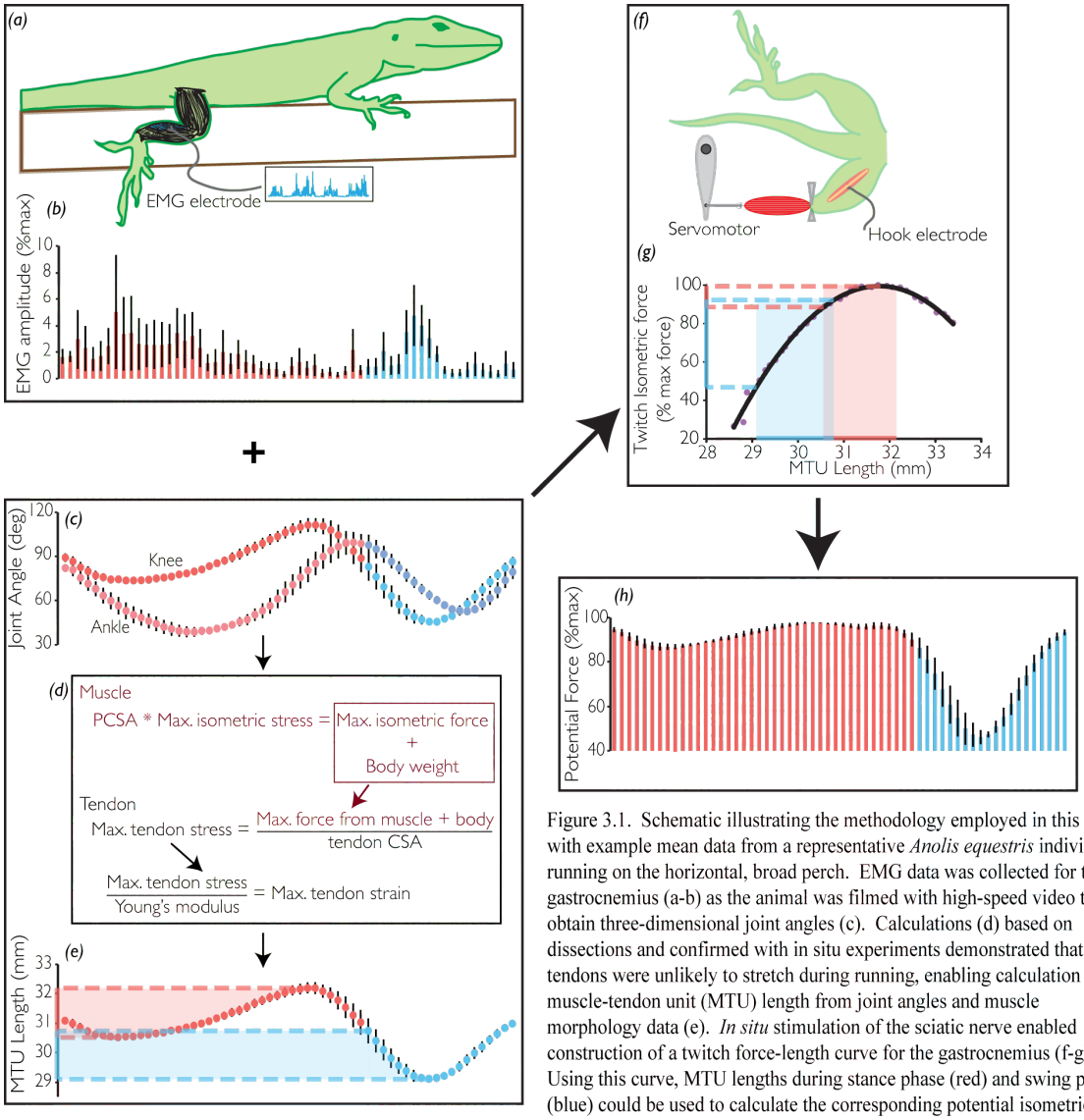

Figure 3.1. Schematic illustrating the methodology employed in this study, with example mean data from a representative *Anolis equestris* individual running on the horizontal, broad perch. EMG data was collected for the gastrocnemius (a-b) as the animal was filmed with high-speed video to obtain three-dimensional joint angles (c). Calculations (d) based on dissections and confirmed with in situ experiments demonstrated that tendons were unlikely to stretch during running, enabling calculation of muscle-tendon unit (MTU) length from joint angles and muscle morphology data (e). *In situ* stimulation of the sciatic nerve enabled construction of a twitch force-length curve for the gastrocnemius (f-g). Using this curve, MTU lengths during stance phase (red) and swing phase (blue) could be used to calculate the corresponding potential isometric force (h). Max., maximum. Values are mean ± s.e.m.

Electromyography experiments

As described previously (Higham and Jayne, 2004b; Foster and Higham, 2014), *A. equestris* were anaesthetized with an intramuscular injection of ketamine (100 mg kg^{-1}) into the left hind limb prior to the percutaneous implantation of a bipolar 0.051 mm diameter polycoated stainless-steel EMG electrode (California Fine Wire Co., Grover Beach, CA, USA) into the mid-belly of the right gastrocnemius pars fibularis pars major

(following Herrel et al., 2008a and hereafter referred to as gastrocnemius for simplicity). Because of the large mass of the individuals used in this study, EMG wires were sutured to the skin in three positions on the limb and back using 5-0 coated vicryl suture (Ethicon, Inc., Somerville, NJ, USA) in order to reduce the chance that electrodes pulled out during running trials (Foster and Higham, 2014). Once surgery was completed, the center of each hind limb joint was painted with white and black dots to facilitate digitizing for kinematic analyses. Animals were allowed to recover from anaesthesia in clean 10-gallon aquaria for 18-24 h prior to running trials.

Animals ran along 4 different 1 m long trackways, each representing a combination of 2 different inclines (0 and 30 deg) and perch diameters (a broad 30 cm wide flat perch and a narrow 5 cm diameter perch). Trials were considered for analysis only if the animals ran steadily through the stride and remained on the dorsal surface of the perch. The trackways were covered in cork shelf liner to facilitate greater traction (Schmidt and Fischer, 2010; Foster and Higham, 2012, 2014). Two high-speed cameras (Phantom Miro M150, Vision Research Inc., Wayne, NJ, USA), operating at 1000 frames s^{-1} were used to obtain dorsal and lateral video of the animals while simultaneously recording EMG data at 5000 samples s-1 using a BIOPAC MP150 data acquisition system with the UIM100C module and ACQKNOWLEDGE (v. 4.0) software (BIOPAC Systems, Inc., Goleta, CA, USA). Video and EMG recordings were synchronized using an external trigger. During recording, EMG signals were amplified 10000 times and filtered with a 60 Hz notch filter using a GRASS QU511 quad amplifier (Natus Neurology Inc., Warwick, RI, USA).

Electromyography analyses

All EMG analyses followed (Foster and Higham, 2014). Briefly, EMG signals were rectified and filtered using low (70 Hz) and high (2500 Hz) bandpass filters prior to calculating burst onset and offset time, burst duration, magnitude and timing of peak burst amplitude, total rectified integrated area (RIA) during stance phase, and the time at which half of the burst RIA was achieved. See Foster and Higham (2014) for greater detail. Calculations were performed using custom code written for MATLAB (R2012a, The MathWorks, Natick, MA, USA) by K.L.F.

To facilitate the averaging of data across strides and trials as well as subsequent calculations incorporating kinematic data, EMG amplitudes were divided into 40 bins for activity occurring during stance phase and 20 bins for swing phase activity (e.g. Fig. 3.1b) as in (Foster and Higham, 2014). Given the variation between electrode placement and the length of exposed electrode tips, all amplitudes were expressed relative to the maximum amplitude ever observed for each individual.

Kinematic analyses

Three-dimensional coordinates for each joint of the hind limb were obtained using DLT DV5 custom software (Hedrick, 2008) for MATLAB and then used to calculate body speed and magnitudes and velocities of femur depression, retraction and rotation, and knee and ankle angles using custom MATLAB code written by Aleksandra Birn-Jeffrey (Birn-Jeffery and Higham, 2014). Calculations followed (Spezzano and Jayne, 2004; Foster and Higham, 2012). Trajectories of joint kinematics were binned as

described for the EMG analyses (e.g. Fig. 3.1c) in order to facilitate subsequent calculations and comparisons across trials and individuals.

In situ force-length experiments

Following the EMG experiments, individuals were anaesthetized with an intramuscular injection of ketamine (300 mg kg^{-1}) and monitored to ensure continued, deep anaesthesia throughout the duration of the surgery and *in situ* experiments. An incision was made on the ventral surface of the proximal half of the femoral segment of the right hind limb to isolate the sciatic nerve proximal to its first branching point. Any connective tissue surrounding the nerve was removed to ensure maximal contact between the nerve and electrode, although very little connective tissue was present. Once isolated, a bipolar platinum hook electrode was hooked around the nerve and mineral oil was dropped onto the site to help maintain hydration of the nerve and minimize any voltage dissipation during stimulation (Fig. 3.1F; Nelson et al., 2004). More mineral oil was reapplied at several points during experimentation to ensure consistent signal transmission. The other end of the hook electrode was attached to a Grass S48 Stimulator (Natus Neurology Inc., Warwick, RI, USA) for muscle stimulation.

Next, the skin was removed from the distal hind limb and the gastrocnemius muscle was carefully isolated from the rest of the muscles of the hind limb. To anchor the proximal end of the gastrocnemius, the femur was anchored in place using machine screws built into the *in situ* apparatus and the distal end of the gastrocnemius was fastened to a servomotor (Aurora 300C, Aurora Scientific Inc., Aurora, ON, Canada) via

a short (approx. 1 cm long) piece of silk suture tied around the proximal end of the gastrocnemius tendon which was then attached to steel wire. The length of the silk suture was minimized to reduce the possibility of stretch occurring between the muscle and servomotor. Because the tendon of the gastrocnemius is very short and slender in this species, a number of measures were taken to ensure that the suture tied around the tendon at the distal end of the muscle could not slide during experimentation (verified with high-speed video). The majority of the crus, along with all other distal limb muscles were removed by severing the limb just above the ankle and just below the knee after a piece of suture was tied below the knee as a tourniquet to reduce blood loss. Further, the weight at the distal end was minimized by removing all the toes of the foot. Virtually no blood was lost during this procedure. This arrangement meant that the ankle joint could be used as an added anchor past which the suture fastened to the distal gastrocnemius could not slide. This also ensured that no other muscles could contract and interfere the gastrocnemius during sciatic nerve stimulation. A small drop of contact cement was placed on the knot tied around the tendon to prevent the knot from loosening and to further reduce the possibility that the suture could slide along the tendon.

Since the gastrocnemius of this species was too small to hold sonomicrometry crystals in place during contraction, the length of the muscle prior to each stimulation event was measured using digital calipers (error ± 0.005mm) and the length during contraction was monitored using the Aurora dual-mode lever system. All force and length signals from the Aurora lever system were sent to the same BIOPAC MP150 data acquisition system and ACQKNOWLEDGE software as used for the EMG experiments.

Before constructing force-length curves (FLC) for the gastrocnemius, it was necessary to determine a voltage at which we could be sure of stimulating all available motor units and thus generate maximum forces. To do this, the force generated during a twitch contraction was measured when the sciatic nerve was stimulated at a series of voltages, beginning at 1 V and increasing in increments of 0.5 V. Once no further increase in twitch force was observed, the stimulation voltage was increased by 1 V to ensure supramaximal stimulation, which was used for all subsequent twitch and tetanic contractions.

To construct the twitch FLC, a single 0.2 ms pulse at the supramaximal stimulation voltage was sent to the sciatic nerve at each muscle length and the resulting force was recorded. For the four individuals for which we obtained tetanic FLC, the nerve was stimulated for 500 ms at a stimulation rate sufficient to allow good summation of the 0.2 ms pulses (with 0.01 ms delay between pulses) into a tetanic contraction. This stimulation rate varied slightly between individuals, but ranged between 17 and 26 pulses s^{-1}. As tetanic contractions can result in fatigue of the muscle, 5 minutes of rest, during which all external tension was removed from the muscle, was provided between each successive stimulation event. In all cases, twitch FLC were constructed prior to tetanic FLC, in order to minimize the potential for fatigue or nerve degradation.

Calculation of maximum tendon strain

As noted above, the muscle was too small for sonomicrometry crystal implantation, so we had to rely on the combination of instantaneous joint angles from our

kinematic data and detailed morphology (i.e. muscle-tendon unit length and moment arm) in order to estimate the instantaneous muscle length *in vivo*. However, because changes in the length of the muscle-tendon unit (MTU) can be caused by changes in the length of the muscle, changes in the length of the tendon, or a combination of the two (Higham and Nelson, 2008), it was necessary to first establish whether the tendon could be stretching during normal, cyclical locomotion in these animals. To determine this, we performed detailed dissections to measure mass, fascicle length, whole muscle length, pennation angle, and origin and insertion point of each muscle of the proximal hind limb and crus, as well as the mass and length of any associated tendons (Table 3.1). These measurements were used in a series of calculations (Fig. 3.1d) to determine the maximum amount of tendon strain. Briefly, we calculated the maximum amount of force each hind limb muscle could generate by multiplying the physiological cross-sectional area (PCSA) by maximum isometric stress for vertebrate muscle (0.3 MPa; Wells, 1965; Medler, 2002). Next, we added body weight to this muscle force to create a worst-case scenario in which the focal muscle is responsible for propelling the entire body mass. Thus, the resulting force represents an overestimation of the maximum amount of force the focal tendon could possibly experience during cyclical locomotion. We divided this force by tendon CSA to determine the maximum stress the tendon could experience. Finally, although there is some debate about how elastic properties vary among vertebrates (Bennett et al., 1986; Pollock and Shadwick, 1994b; Matson et al., 2012), we chose to divide tendon stress by an elastic modulus of 1.5 GPa (Bennett et al., 1986), which is within the range of values reported by these papers, to calculate maximum tendon strain.

In order to confirm these calculations, high-speed video was obtained for two individuals during maximal tetanic *in situ* contractions similar to those described above. For these two individuals, after both twitch and tetanic FLC had been obtained, the suture tied around the proximal end of the gastrocnemius tendon was removed and retied around the distal-most end of the tendon, just proximal to the insertion point on the pes. No damage to the tendon was visible.

Both the calculations and *in situ* experiments suggested it is very unlikely that the gastrocnemius tendon or any other tendon in the hind limb is capable of deforming significantly during normal cyclical locomotion in these animals (Table 3.2; see results section for details).

Table 3.2. Mean muscle-tendon unit (MTU) length and tendon length change in mm and as a percentage of MTU length for all the hind limb muscles of the femur and crus that have tendons.

Muscle	Tendon length change (mm)	MTU length (mm)	Tendon length change (% of MTU length)
Puboischiotibialis	0.014	36.8	0.038
Flexor tibialis internus	0.008	2.8	0.294
Pubofibularis	0.026	28	0.094
Ambiens pars ventralis	0.017	31.4	0.053
Ambiens pars dorsalis	0.016	27.1	0.060
Ilioischiotibialis	0.048	25.4	0.189
Ilioischiofibularis	0.191	22.1	0.863
Flexor digitorum communis	0.018	15.4	0.115
Peroneus longus	0.051	27.3	0.187
Peroneus brevis	0.029	22.3	0.132
Extersor digitorum longus	0.076	41.6	0.182
Gastrocnemius pars fibularis pars minor	0.038	29.9	0.125
Gastrocnemius pars fibularis pars major	0.011	28.3	0.037
Caudofemoralis longus	0.069	67.6	0.103

Calculation of in vivo muscle length

Once it was established that the gastrocnemius tendon was not likely to be changing length *A. equestris* ran, it was possible to generate a calibration curve, which

converted instantaneous joint angles into instantaneous muscle lengths. To generate this calibration curve, the skin was removed from the left hind limb and the thin connective tissue linking the gastrocnemius to the other muscles of the crus was severed along the entire length of the muscle and tendon. This allowed the gastrocnemius to stretch and slide easily relative to the other muscles in the limb as the knee and ankle were manipulated. The knee and ankle joints and origin and insertion points of the gastrocnemius muscle and tendon were painted with black nail polish to facilitate visualization in video. The limb was manipulated with forceps through the entire range of hip, knee, and ankle angles normally observed during running in these animals. These manipulations were filmed with two high-speed video cameras and the resulting video was digitized in MATLAB with DLT DV5 as described for the EMG analyses above. The MTU length was calculated from the resulting three-dimensional coordinates. Because the gastrocnemius is biarticular, crossing both the knee and ankle joints, a multiple regression was used to obtain the calibration curve that converted the instantaneous knee and ankle joints from the video of the EMG trials into instantaneous muscle lengths (Fig 3.1e; custom MATLAB code written by K.L.F.). To facilitate visual comparison of EMG amplitudes and instantaneous muscle lengths, we generated binned trajectories of muscle strain as described above (Fig. 3.2a-b). These muscle strain values were expressed as a percentage of resting muscle length, which was defined as the length of the muscle when the limb was positioned with the knee and ankle angles at 90 deg.

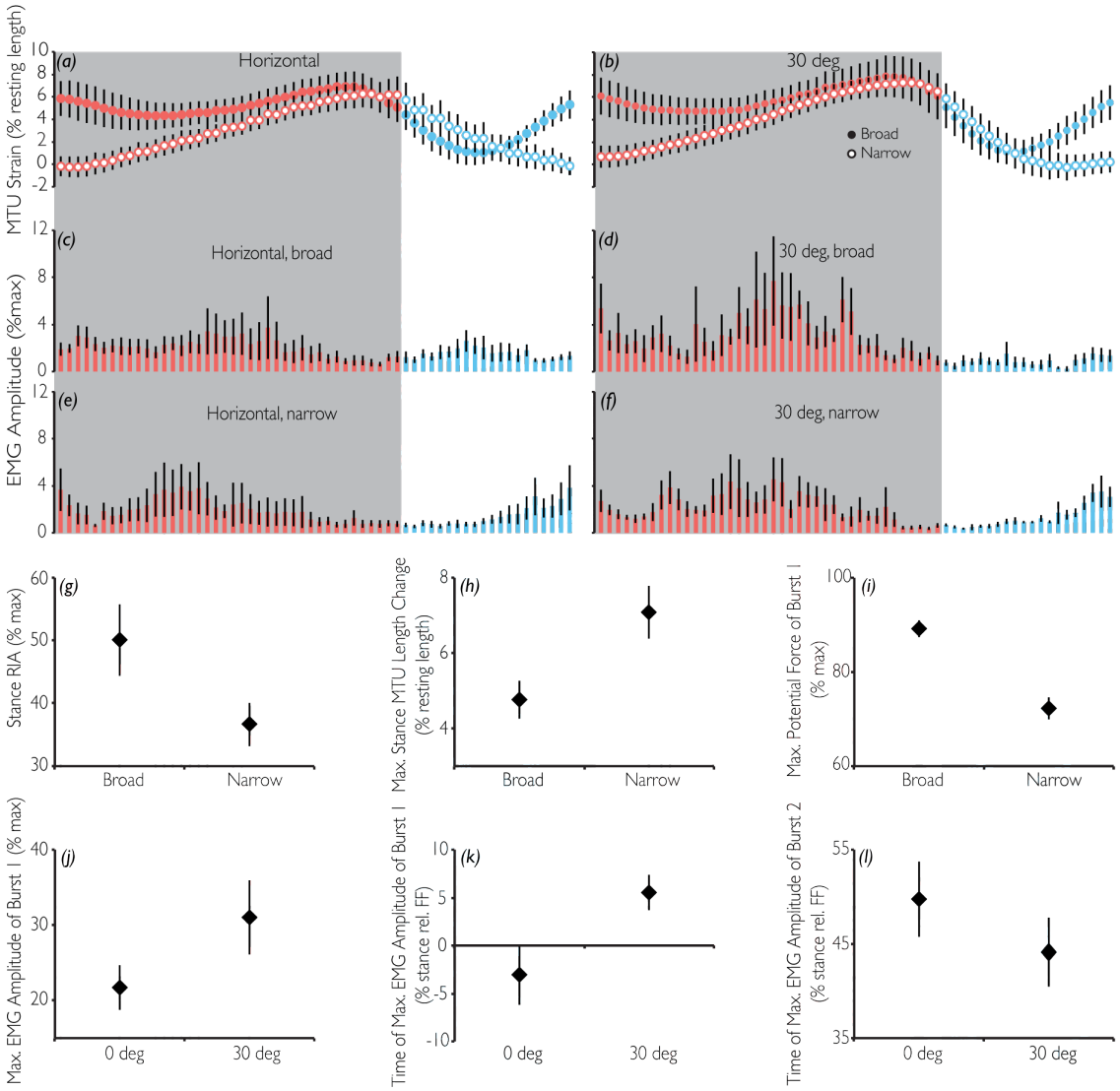

Figure 3.2. Binned muscle-tendon unit length trajectories (a-b), binned EMG amplitude (c-f), and significant relationships on perches of different diameter (g-i) and incline (j-l). (a-f) Closed symbols, broad perch; open symbols, narrow perch. Shaded region (red data), stance phase; unshaded region (blue data), swing phase. MTU, muscle-tendon unit; RIA, rectified integrated area; max., maximum; FF, footfall. Values are mean ± s.e.m.

Calculation of potential force

We defined potential force as the force that the gastrocnemius muscle could theoretically generate under isometric conditions as defined by the twitch FLC. Although we generated tetanic FLC as well, we viewed the twitch curves more biologically relevant since tetanic contractions are not observed in these animals during natural

behaviors. Therefore, we used the formula for the third order polynomial that fit the twitch FLC of each individual to calculate the PF that corresponded to any given MTU length for that individual. This process is illustrated in Figure 3.1g, which shows the range of MTU lengths and corresponding PFs during the stance (red) and swing (blue) phases. These forces could then be used to generate a trajectory of PFs through time (Fig. 3.1h). Finally, we used the onset and offset times of EMG bursts to determine the portions of the twitch FLC that corresponded to periods of activity of the muscle (i.e. locate the active portion of the FLC). From these regions, we identified the minimum and maximum PFs within each burst, as well as the minimum and maximum PFs generated during both periods of activity.

Statistical analyses

Prior to all analyses, the effect of speed (SVL s^{-1}) was removed by regressing it against all kinematic, EMG, and force variables and saving the residuals of those variables that had a significant ($r>0.15$, $p<0.01$) relationship with speed. Principal component and discriminant function analyses used to analyze the kinematic data were performed in JMP (version 11, SAS Institute Inc., Cary, NC, USA). All other statistical analyses (i.e. mixed-model analyses of variance) were performed with SYSTAT (version 13, Systat Software, Inc., San Jose, CA, USA).

Table 3.3. Loadings from a discriminant function (DF) analysis (Wilks' Lambda F=1.87, p=0.0466) of hind limb joint angles in *Anolis equestris*. As only DF1 was significant, DF2 is not shown.

Variable	DF1 (94.6%)
Femur depression angle (ES)	**0.9431**
Max. swing femur depression angle	**0.9417**
Mid swing femur depression angle	**0.9311**
Femur rotation angle (ES)	**-0.9104**
Knee angle (FF)	**-0.9083**
Max. femur depression angle	**0.8611**
t. max. femur rotation angle (% swing)	**0.8152**
Femur depression angle (MS)	**0.7668**
t. min. knee angle (% stance)	**-0.7656**
Pelvic girdle rotation angle (MS)	**0.4865**
Pelvic girdle rotation angle (ES)	**0.3729**
Max. swing ankle angle	0.0684

Loadings with a magnitude ≥ 0.3 are in bold.
Percentage of variation explained by DF1 axis is indicated in parentheses.
FF, footfall; MS, mid stance; ES, end of stance; T, time; Max., maximum; Min., minimum.

As described in detail previously (Foster and Higham, 2012), kinematic variables were separated into temporal (angular velocities, stride frequency, duty factor) and angular (magnitudes of joint angles observed at beginning, middle, and end of stance, as well as minimum, maximum and excursion of angles) variables before being inserted into a principal components analysis (PCA) to reduce dimensionality and identify the 12 variables most important for generating the majority of the variation between treatments. The number of variables chosen from each of the first two PC axes corresponded to the proportion of variance explained by those axes (Foster and Higham, 2012). These variables were then loaded into a discriminant function analysis (DFA; Fig. 3.3) and those variables that loaded heavily (greater than ±0.3) on a significant axis were considered significant and important for explaining kinematic differences between treatments (Tables 3.3 and 3.4). Finally, post-hoc one-way analyses of variance

(ANOVAs) were performed on DFA scores to determine which treatments were significantly different from each other.

Force and EMG data were analyzed using mixed-model ANOVAs in which individual was a random factor and perch diameter and incline were fixed factors, as described previously (Foster and Higham, 2014). To obtain the correct F values for incline and perch diameter in this design, the mean squares for each of these factors were divided by the mean squares of the interaction between individual and each fixed factor, and the corrected denominator for the degrees of freedom was the degrees of freedom of this interaction (Zar, 1999).

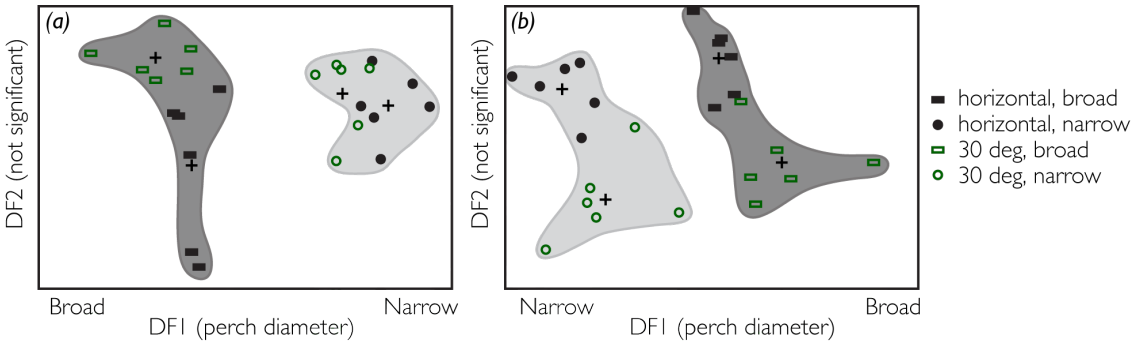

Figure 3.3. First two axes of discriminant function (DF) of hind limb joint angles (a) and angular velocities (b) of *Anolis equestris*. The mean for each treatment is indicated by a + symbol. Closed, black symbols, horizontal treatment; open, green symbols; 30° incline. Rectangles, broad perch; circles, narrow perch. Regions occuped by broad and narrow treatments are shaded in dark and light grey, respectively. DF2 was not significant in either DF analysis. Cannonical loadings on each axis are given in Tables 3 and 4.

Results

Changes in kinematics with perch diameter and incline

As has been observed previously for *Anolis carolinensis* (Foster and Higham, 2012, 2014), changes in perch diameter had a much more profound impact than changes in incline on hindlimb kinematics. For both angular and velocity DFAs, only the first discriminant axis, which described perch diameter, was significant (Fig. 3.3, Tables 3.3

and 3.4). Therefore, all significant changes in kinematics described here are associated with changes in perch diameter.

The majority of the angular variables that were affected by changes in perch diameter were associated with the proximal joints (i.e. pelvic girdle and hip; Table 3.3). The pelvic girdle was less rotated and the femur was more depressed on the narrow perch than on the broad perch (Table 3.5). Further, the femur rotated less and achieved its maximum long-axis rotation later in swing phase on the narrow perch than on the broad perch (Table 3.5). Further, the knee achieved its greatest flexion earlier in stance phase on the narrow perch than on the broad perch (Table 3.5).

Table 3.4. Loadings from a discriminant function (DF) analysis (Wilks' Lambda F=2.04, p=0.028) of hind limb angular velocities in *Anolis equestris*. As only DF1 was significant, DF2 is not shown.

Variable	DF1 (64.3%)
Max. swing knee angle velocity (residuals)	**0.8093**
Mid swing knee angle velocity	**0.8087**
Avg. swing femur rotation velocity (residuals)	**-0.8081**
Avg. swing knee angle velocity	**0.7475**
Max. swing ankle angle velocity (residuals)	**0.7429**
Avg. stance knee angle velocity	**-0.665**
Avg. stance ankle angle velocity (residuals)	**-0.6262**
Max. stance femur depression velocity	0.1951
Femur depression velocity (MS)	0.1631
Min. swing femur depression velocity	-0.1519
Avg. stance femur depression velocity	-0.1331
Min. swing ankle angle velocity (residuals)	0.1128

Loadings with a magnitude ≥ 0.3 are in bold.
Percentage of variation explained by DF1 axis is indicated in parentheses.
Variables that were loaded as residuals because they regressed significantly with body speed are indicated in parentheses.
MS, mid stance; Max., maximum; Min., minimum; Avg., average.

In contrast with the angular variables, changes in joint angular velocities with perch diameter were generally associated with the distal joints (i.e. knee and ankle; Table 3.4). During stance phase, both the knee and the ankle extended faster on the narrow

perch than on the broad perch (Table 3.5). The average angular velocity of the knee during swing phase indicated that it was generally extending (positive angular velocity) during recovery on the broad perch but flexing (negative angular velocity) during recover on the narrow perch (Table 3.5). Also, during swing phase, both ankle extension and femur long-axis rotation (in the counter-clockwise [i.e. negative] direction) occurred slower on the narrow perch compared to the broad perch (Table 3.5).

Table 3.5. Hind limb joint angle and angular velocity variables that loaded heavily (≥ 0.3) on the first axis of discriminant function analyses (Fig. 3, Tables 3,4) for *Anolis equestris*.

	Perch Diameter	
	Narrow	Broad
Joint Angle		
Femur depression angle (ES)	38.43±2.30	9.49±1.68
Max. swing femur depression angle	40.23±2.45	9.42±1.83
Mid swing femur depression angle	33.53±2.75	-3.92±2.33
Femur rotation angle (ES)	50.50±2.38	76.24±1.39
Knee angle (FF)	48.36±3.23	88.77±2.09
Max. femur depression angle	42.85±2.28	19.73±2.50
t. max. femur rotation angle (% swing)	45.03±5.19	9.88±2.17
Femur depression angle (MS)	35.68±2.83	11.50±2.85
t. min. knee angle (% stance)	9.77±2.85	42.28±4.75
Pelvic girdle rotation angle (MS)	-2.67±1.83	-12.72±2.94
Pelvic girdle rotation angle (ES)	-0.67±2.62	-8.57±2.78
Joint angular velocity		
Max. swing knee angle velocity	308.01±75.08	955.63±140.35
Mid swing knee angle velocity	-480.66±76.01	247.44±115.90
Avg. swing femur rotation velocity	-45.80±19.34	-180.21±20.58
Avg. swing knee angle velocity	-422.71±66.36	17.11±47.26
Max. swing ankle angle velocity	276.54±84.58	892.83±127.37
Avg. stance knee angle velocity	217.19±37.67	11.00±26.16
Avg. stance ankle angle velocity	247.13±46.68	96.46±28.11

Angles and angular velocities are given in deg and deg. s^{-1}.
FF, footfall; MS, mid stance; ES, end of stance; t., time; Max., maximum; Min., minimum; Avg., average.
Values are means ± s.e.m.

Tendon function during cyclical locomotion

Calculations based on morphological data reveal that the most any hind limb tendon could be expected to stretch during non-ballistic, cyclical locomotion in *A.*

equestris is 0.191mm, or 0.863% of MTU length in the tendon of the ilioishiofibularis (Table 3.2). In contrast, the tendon of the gastrocnemius, the focal muscle in this study, could stretch only 0.037% of MTU length (Table 3.2), which reflects a maximum strain energy storage of 0.000239 J/kg. This value is several orders of magnitude lower than the strain energy storage seen in the Tamar wallaby (0.3125 J/kg; Biewener and Baudinette, 1995), which is known for using elastic energy storage for hopping. Further, in situ experiments performed under conditions of maximal tetanic stimulation, high-speed video of the muscle-tendon unit revealed no visible change in tendon length or length of the entire muscle-tendon unit. Thus, it is reasonable to assume that neither the tendon of the gastrocnemius nor any other hind limb tendon is capable of deforming during cyclical locomotion in *A. equestris*.

Changes in gastrocnemius muscle function with perch diameter and incline

Regardless of experimental treatment, muscle activity in the gastrocnemius was similar in general pattern to that seen in the peroneus longus and brevis in *Anolis carolinensis* (Foster and Higham, 2014). It was generally characterized by two bursts per stride, the first centered around footfall and the second occurring in mid to late stance phase. Surprisingly, we saw very little change in muscle length during stance phase in the gastrocnemius during the propulsive stance phase; it appeared to be functioning nearly isometrically, with changes in muscle strain during stance phase ranging from an average of 4.77 ± 0.5% resting length on broad surfaces to 7.10 ± 0.70% resting length on

narrow surfaces. Further, gastrocnemius activity for all individuals occurred on the ascending and plateau regions of the FLC (see Fig. 3.1g for a representative example).

Although there were significant alterations in muscle activity patterns with changes in both incline and perch diameter, only perch diameter seemed to elicit significant shifts in the operating length and potential force generated by the gastrocnemius. Total rectified integrated area (i.e. muscle recruitment) during stance phase was lower on the narrow perch (36.62 ± 3.45% max. amplitude) than on the broad surface (50.11 ± 5.74% max. amplitude, p=0.039; Fig. 3.1g). Further, the maximum range of lengths over which the MTU operated was larger on the narrow perch (7.10 ± 0.70% resting length) than on the broad perch (4.77 ± 0.5% resting length, p=0.019; Fig. 3.1h), primarily due to lower values of strain at the beginning of stance on the narrow perch compared to the small diameter perch (Fig. 3.2a,b). Finally both the minimum and maximum (Fig. 3.2i) potential force the first burst of the gastrocnemius could be generating was lower (min. p=0.030; max. p=0.016) on the narrow surface (min. potential force=52.70 ± 4.08% max. force; max. potential force=72.27±2.37% max. force) compared to the broad surface (min. potential force=72.44 ± 2.52% max. force; max. potential force=89.13±1.77% max. force).

On the steeper incline, the maximum EMG amplitude of burst 1 was greater (31.02 ± 4.92% max. amplitude) than on the horizontal treatment (21.68 ± 2.99% max. amplitude, p=0.020; Fig. 3.1j). Further, this peak activity occurred later (after footfall rather than before footfall) on the 30 deg treatment (5.53 ± 1.86% from beginning of stride) than on the horizontal treatment (-3.03 ± 3.14% before beginning of stride,

p=0.041; Fig. 3.1k). In contrast, the time of peak burst 2 amplitude occurred earlier in stance phase on the 30 deg incline (44.11 ± 3.68% from beginning of stride) than on the horizontal condition (49.75 ± 4.02% from beginning of stride p=0.043; Fig. 3.1l). Interestingly, although changes in incline did not appear to elicit shifts in either operating lengths or potential forces, incline had a significant impact on the relationship between potential force and muscle recruitment during stance (t=2.20, df=20, p=0.04; Fig. 3.4). On horizontal treatments there was a negative relationship between potential force and stance RIA (slope=-1.12, r^2=0.16) whereas on the inclined surfaces this relationship was positive (slope=1.32, r^2=0.23).

Discussion

By combining *in vivo* and *in situ* techniques with gross morphological dissection this study is the first to successfully gain a comprehensive understanding of how altering not only incline, but also perch diameter impacts both muscle activation and force generation capacity in a small lizard (*Anolis equestris*). Not only were kinematics more strongly affected by alterations in perch diameter than incline, but both the level of effort (i.e. muscle recruitment) and the efficacy of force generation (i.e. potential force) was greater on the broad surface, where ankle extension has greater opportunity to contribute to propulsion, than on the narrow surface. Therefore, it appears that the gastrocnemius may be actively and anatomically tuned to function most effectively on the surfaces on which it can be put to the best use. Furthermore, increasing incline not only resulted in

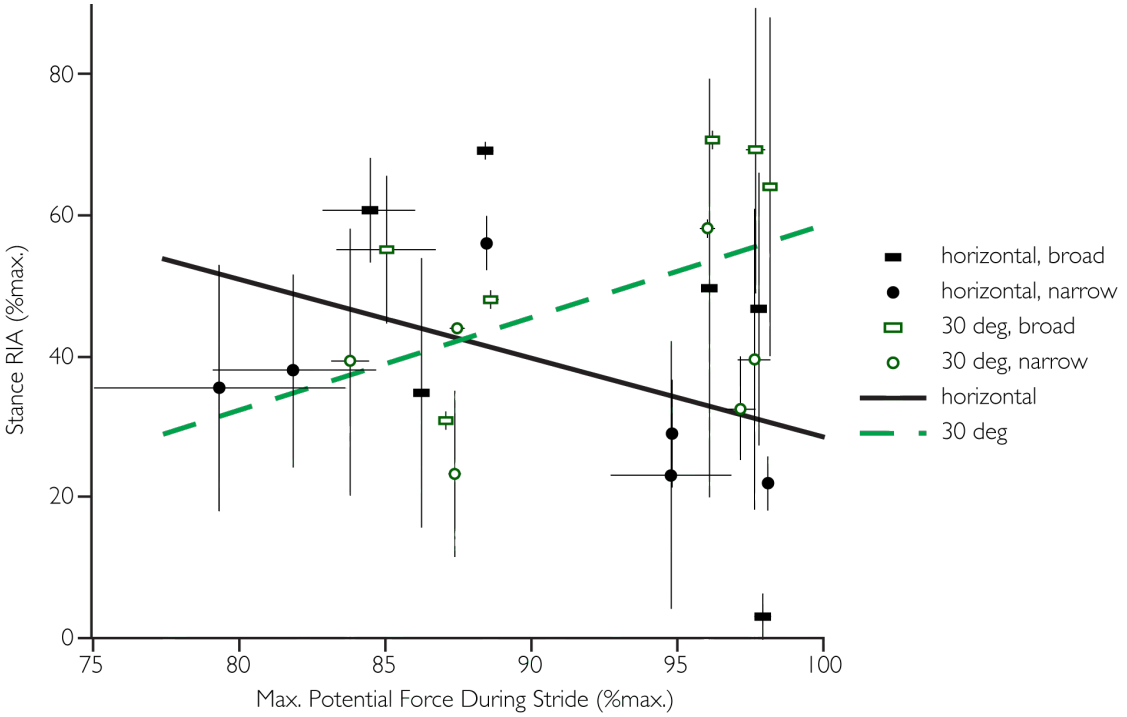

Figure 3.4. Regressions of maximum (max.) potential force during any period of muscle activity during the stride vs. rectified integrated area (RIA) during stance phase on horizontal (solid, black line) and 30 deg incline. Closed, black symbols, horizontal treatment; open, green symbols; 30 deg incline. Rectangles, broad perch; circles, narrow perch. Values are mean ± s.e.m.

familiar shifts in magnitude and timing of muscle activity to increase the muscle recruitment during the propulsive phase of the stride (Carlson-Kuhta et al., 1998; Gillis and Biewener, 2002; Daley and Biewener, 2003; Higham and Jayne, 2004b; Foster and Higham, 2014), but it altered the relationship between force-generating capacity and muscle recruitment. On horizontal conditions where muscles were operating over more optimal portions of the FLC and theoretically capable of generating greater forces, there was a corresponding drop in muscle recruitment. However, on inclined surfaces, there was a positive relationship between potential force and muscle recruitment. Thus, it appears that demands imposed by the physical environment have the potential to impact fundamental principles governing the interaction between behavioral and physiological aspects of muscle function.

Impact of perch diameter on kinematics and muscle function

The kinematics of *Anolis equestris* moving on simulated arboreal substrates coincides with patterns seen in other species of *Anolis* lizard (Spezzano and Jayne, 2004; Foster and Higham, 2012, 2014). As in these other species, alterations in perch diameter had a greater effect on limb kinematics than changes in incline, and the majority of the compensatory shifts in the magnitudes of angles occurred in the proximal rather than the distal joints. Differences in the geometry of the two perch surfaces explain the vast majority of the angular and angular velocity changes observed here. On the narrow perch, *A. equestris* places its hind limbs on the sides of the perch, primarily via increased femur depression. With the pes in this location, propulsion is characterized by rapid extension of the knee and ankle before the pes is allowed to abduct and fall away from the lateral sides of the perch to begin swing phase. Therefore, in order to recover and prepare for the next stance phase, the limb must be flexed during protraction to bring the foot back into a position to land on the perch surface. This contrasts with the broad perch, where the limb is forced to remain on the dorsal surface. In this situation, the entire foot, including digits, are in a position to remain in contact with the surface in an orientation that allows knee and ankle extension to contribute significantly to forward propulsion, as is common and well recognized in terrestrial animals (Brinkman, 1980; Gregersen et al., 1998; Russell and Bels, 2001b; McGowan et al., 2005; McGowan et al., 2008; Arnold et al., 2013). However, in order to prepare for the next stride, the limb must be elevated and extended during protraction, explaining the faster knee and ankle

extension (rather than flexion) velocities on these surfaces compared to the narrow perches.

The greater potential for ankle extension to contribute to propulsion on the broad surface also may explain the shifts in gastrocnemius function elicited by altering perch diameter. The gastrocnemius muscle activity had a greater RIA during stance, on the broad surface compared to the narrow surface, indicating that muscle recruitment was greater and the muscle was working "harder" on the broader surface. Further the minimum and maximum potential forces were greater and there was less change in MTU length during stance phase on the broad compared to the narrow surface. This suggests that the gastrocnemius was functioning more effectively, focused on a more optimal region of its FLC on the broader perch compared to the small diameter perch. Together, these results seem to suggest that the gastrocnemius was contributing more to propulsion on the broader conditions. On the flip side, this suggests that because the gastrocnemius may be ill equipped to function effectively on narrow surfaces, other muscles may have to take on a greater proportion of the propulsive effort in order to maintain a given level of locomotor performance, effectively reorganizing the locomotor system. The puboischiotibialis, a major limb depressor and knee flexor, is one of the more obvious muscles that we might expect to take on a more influential role during locomotion on narrow surfaces (Higham and Jayne, 2004b; Foster and Higham, 2014). Assuming an adaptive advantage to moving effectively on narrow surfaces, a reasonable assumption given that this animal lives primarily in the crowns of trees, we would expect that this

muscle would be functioning closest to the plateau region of its FLC when the limb is more depressed as it is on narrow perches.

Relationship between potential force and muscle recruitment

We propose that a fundamental mechanism by which ecological challenges can impact muscle function is by affecting the relationship between "how hard" muscles are working (i.e. muscle recruitment) and how efficient they are at generating force (i.e. active location on the FLC). If the lengths over which a muscle is active shift so that the forces it is capable of generating increase, one might consider it to be functioning more efficiently. Assuming no alteration in the demands placed on the animal, it is reasonable to expect that a muscle that is generating force more effectively would not need to recruit as many motor units to accomplish a given task than a muscle that is functioning on a less optimal position on the FLC, resulting in a negative relationship between potential force and muscle recruitment. This is analagous to the trade-off between muscle shortening velocity and motor unit recruitment necessary for a given force (Roberts and Azizi, 2011). Alternatively, if there is an increase in the demand placed on the animal, it is possible that muscle fiber recruitment will remain constant, or even increase, despite generating forces more effectively in order to meet those increased demands. This would result in a positive relationship between potential force and muscle recruitment. Interestingly, we saw both relationships in our data. Regardless of perch diameter, animals whose gastrocnemius muscles were functioning at more optimal portions on the FLC decreased motor unit recruitment during the stance phase on horizontal conditions

(negative relationship) but increased muscle fiber recruitment on 30 deg inclines (positive relationship; Fig 3.4). Thus, it appears that the increased muscle work required on inclined conditions, in which there is a greater component of gravity resisting forward locomotion (Cartmill, 1985; Preuschoft, 2002), disrupts the expected tradeoff between potential force and muscle recruitment observed on horizontal conditions.

The role of tendon in cyclical locomotion of small lizards

The morphological calculations and *in situ* experiments performed here provide strong evidence that neither the tendon of the gastrocnemius nor any other hind limb tendon is likely to stretch and store elastic energy during a cyclical locomotor task like running. This result is not surprising given that the combination of relatively constant tendon material properties (Bennett et al., 1986; Pollock and Shadwick, 1994b; but see Matson et al., 2012) and positive allometry of muscle cross-sectional area means that smaller animals are less likely to be able to generate the forces necessary to stretch their tendons (Biewener et al., 1981; Biewener and Blickhan, 1988; Pollock and Shadwick, 1994a).

Our calculations represented a worst-case scenario likely grossly overestimated the stresses the tendons could possibly be experiencing during running: not only were the muscle forces we used in our calculations estimated assuming maximal muscle fiber recruitment under isometric conditions, but the entirety of the mass of the animal was added to those forces such that each muscle was theoretically responsible for supporting and propelling the entirety of the body mass. Even though the elastic modulus of tendon

may not always be constant (Matson et al., 2012), the value used in the calculations here fell within the range of those reported in the literature (Bennett et al., 1986; Pollock and Shadwick, 1994b; Matson et al., 2012); halving the value for the elastic modulus and thereby doubling estimated values of tendon strain would still result in values of tendon strain well below 0.1% of MTU length. Further, our *in situ* experiments provided additional corroboration because the gastrocnemius tendon would not deform even in the face of a supramaximal tetanic contraction, which is not likely to be biologically relevant. Therefore, we are confident in concluding that, excluding ballistic behaviors, hind limb tendons are functioning as tethers to transmit, rather than store forces in this, and other, smaller, *Anolis* species, which have even less mass to help load tendons.

This result has the potential to transform future studies of *in vivo* muscle function in small terrestrial animals. In such cases, the small size of muscle and tendon is a barrier to understanding how muscles are functioning in active, naturally behaving animals because surgical techniques such as tendon buckles for measuring *in vivo* forces, and sonomicrometry crystals for measuring *in vivo* muscle lengths are either impractical or impossible. Therefore, knowing that changes in the length of the entire MTU reflects changing in length of the muscle itself permits the use of kinematic and morphological data to infer *in vivo* muscle lengths. This is a necessary step when trying to link *in vivo* muscle activation patterns to *in situ* FLC. Linking kinematics (i.e. curvature of the midline) with muscle lengths has proven very useful in the study of muscle function in swimming fishes (Katz and Shadwick, 1998; Shadwick et al., 1998; Donley and Shadwick, 2003), although this relationship becomes decoupled in lamnid/thunniform

swimmers that have a different muscle/tendon arrangement (Donley et al., 2005; Shadwick and Syme, 2008).

Biarticular muscles and isometric force production

The maximum change in gastrocnemius MTU length observed during stance phase in *Anolis equestris* ranged from an average of 4.77±0.5% resting MTU length on broad surfaces to 7.10±0.70% resting MTU length on narrow surfaces. These values are very similar to the changes in muscle length observed during the isometric contractions of the lateral gastrocnemius of the Tamar wallaby during hopping (average = 6±2.2% resting muscle length) and fall well below the length changes observed during flight in the pigeon pectoralis muscle (30-36% resting muscle length; Biewener, 1998). Therefore, gastrocnemius MTU strain in *A. equestris* appears to fall within the range expected for muscles that achieve economical force production (as opposed to high power) through isometric contraction. Interestingly, however, *A. equestris* appears to achieve this isometry via a different mechanism than the Tamar wallaby.

There are two ways to achieve isometric force production when joint angles are changing: 1) MTU length may change due to changes in joint angles but the MTU length change may be caused solely by deformation of a series elastic element (e.g. tendon), allowing the muscle to maintain a constant length during force production (tendon-driven isometry), or 2) MTU length may remain relatively constant if the muscle is biarticular because coincident changes in angle of the two joints may act to counteract each other

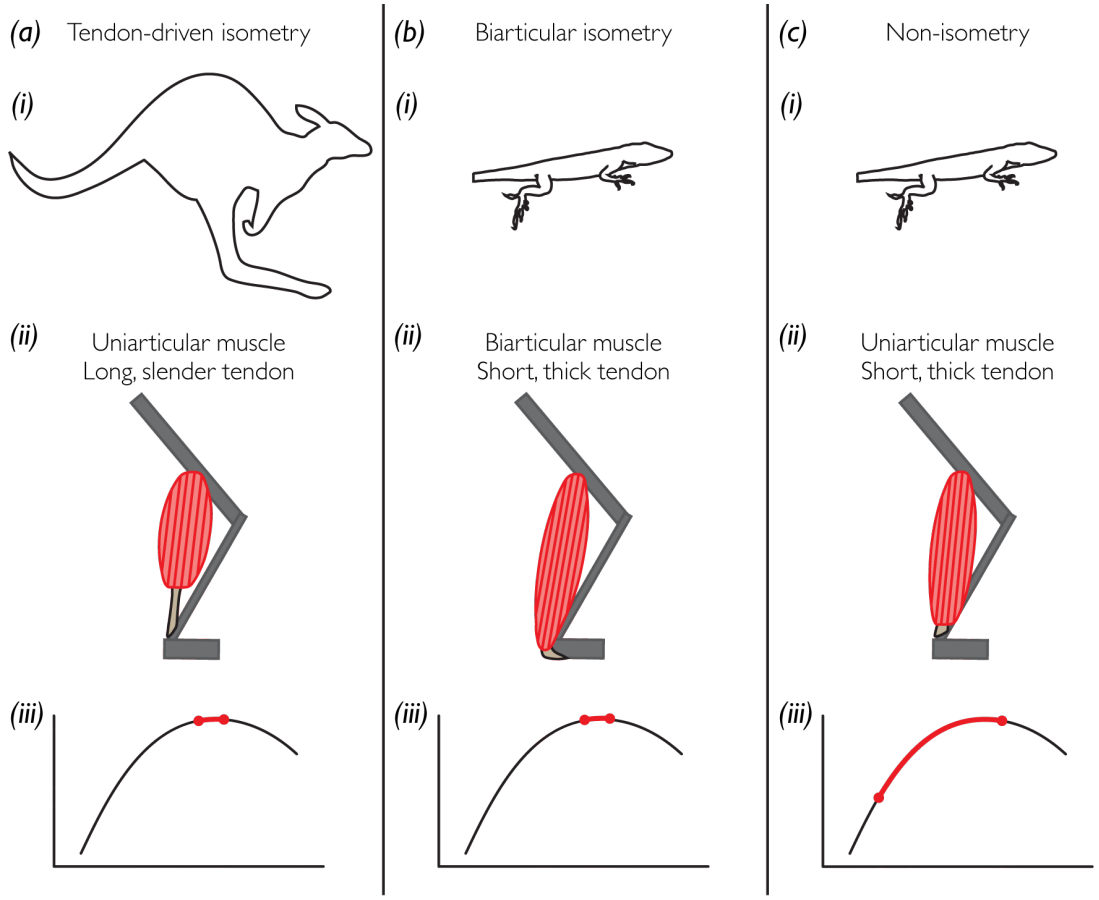

Figure 3.5. Comparison of muscles contracting via tendon-driven isometry (a), biarticular isometry (b), non-isometry (c). Tendon-driven isometry (a) likely occurs primarily in larger animals (i) that have sufficient body mass to deform long, comparatively slender tendons (ii), allowing the muscle fibers to function over a very narrow range of lengths (i.e. isometrically) on the force-length curve (iii). Biarticular isometry (b) is likely the predominant mechanism of achieving isometry in small animals (i) that lack the body mass/muscle force to stretch shorter, comparatively thicker tendons (ii). However, since the muscle is biarticular, simultaneous extension and flexion in the two joints allows the muscle to function over a very narrow range of lengths on the force-length curve (iii). Non-isometric contractions (c) likely occur in uniarticular (ii) muscle of small animals (i) because changes in muscle-tendon unit length caused by joint flexion/extension translate directly into large changes in muscle length on the force-length curve (iii) since the tendon cannot stretch.

(biarticular isometry; Fig. 3.5). These two mechanisms of achieving isometry relate to two behavioral modes (cyclical vs. ballistic locomotion) or two body sizes (small vs large; Fig. 3.5). Large animals have sufficient mass and are capable of generating sufficient muscle forces to stretch their tendons during both behavioral modes and so can utilize tendon-driven isometry (Alexander, 1974; Alexander and Vernon, 1975;

Biewener, 1998). In contrast, small animals that lack the body mass and muscle force capacity to stretch tendons (Biewener et al., 1981; Biewener and Blickhan, 1988; Pollock and Shadwick, 1994a) must rely on biarticular isometry when using a cyclical locomotor mode because, unlike in ballistic movements, there is insufficient time to employ a catch mechanism (Astley and Roberts, 2012) to help load the tendon in advance (Fig. 3.5). Therefore, as the gastrocnemius of *A. equestris* crosses both knee and ankle joints and the tendon of the gastrocnemius is unlikely to be deforming during running, it may be that biarticular isometry is the only mechanism by which it is able to achieve the efficient force production under conditions that require joints to move through large angular excursions.

Biarticularity may be considered disadvantageous in muscles doing positive work because contraction of a single muscle can cause movements at two joints, requiring additional antagonistic contributions from additional muscles to ensure actuation of only the desired movements. However, cases like this one, where the gastrocnemius is likely performing little work, the advantage of being able to generate force efficiently by functioning isometrically, near the plateau of the FLC, regardless of substrate, may partially explain the presence of biarticular muscles in animals that need to move effectively under many different conditions. Biarticular muscles are common in vertebrates and it is tempting to propose that isometric force production may be one of the driving forces behind the evolution of such a morphological arrangement. Although we cannot make such a statement based on a single muscle in a single species, investigation of the contractile properties and in vivo function of additional biarticular

muscles in additional species would undoubtedly provide valuable insight into the adaptive value of such muscular arrangements.

Conclusion

Together, the three studies in this dissertation demonstrate the profound impact substrate structure has on locomotor behavior and the muscles that power those behaviors. Despite adopting some of the common kinematic strategies for dealing with shifts in incline and perch diameter, *Anolis carolinensis* not only appears to adopt different kinematic strategies for dealing with these challenges than a species belonging to a different ecomorph (*A. sagrei*) but also modulates its forelimb movements differently from its hind limb movements. In part, this differential modulation of forelimb from hind limb may reflect shifts in the different contributions each limb makes to propulsion; our data suggest that the forelimbs may be adopting a more propulsive role not only on steeper inclines but also on narrower perch diameters, leaving the hind limbs to contribute more to stabilization on these surfaces.

However, despite the numerous shifts in kinematics elicited by altering perch diameter, there were relatively few changes in activity of the muscles generating those limb movements in *A. carolinensis*. This decoupled response of muscle activity from limb movement emphasize the complexity of the physiological determinants of locomotor behavior and the necessity of considering additional factors (e.g. muscle operating lengths and/or efficiency of force production) that can impact the link between muscle activity and kinematics.

Finally, by combining *in vivo* and *in situ* techniques, we found not only that both the recruitment and the force generation capacity of the gastrocnemius shifts to allow the muscle to contribute more to propulsion on broader surfaces than on narrower surfaces, but that incline impacts the relationship between those two variables. Thus, constraining foot placement has a profound impact on the function of this muscle. Further, we discovered that the biarticular nature of this muscle may be responsible for allowing it to contract isometrically and, therefore, function more efficiently. Finally, the combination of calculations based on morphological data and *in situ* experiments revealed that the tendons of *A. equestris* are not likely to be able to stretch and store elastic energy during cyclical locomotion, permitting the use of indirect methods to infer *in vivo* muscle length and force generation capacity and circumventing size-limiting surgical techniques. As this species is the largest species of anole, this methodology will likely be both relevant and useful in the investigation of muscle function in other, smaller *Anolis* species as well as other small lizards, transforming the field of muscle ecophysiology.

Literature Cited

Aerts, P., Van Damme, R., Vanhooydonck, B., Zaaf, A. and Herrel, A. (2000). Lizard locomotion: how morphology meets ecology. *Neth. J. Zool.* **50**, 261-277.

Alexander, R. M. (1974). The mechanics of jumping by a dog (*Canis familiaris*). *J. Zool.* **173**, 549-573.

Alexander, R. M. (1977). Allometry of the limbs of antelopes (Bovidae). *J. Zool.* **183**, 125-146.

Alexander, R. M. and Vernon, A. (1975). The mechanics of hopping by kangaroos (Macropodidae). *J. Zool.* **177**, 265-303.

Alföldi, J., Di Palma, F., Grabherr, M., Williams, C., Kong, L., Mauceli, E., Russell, P., Lowe, C. B., Glor, R. E., Jaffe, J. D. et al. (2011). The genome of the green anole lizard and a comparative analysis with birds and mammals. *Nature* **477**, 587-591.

Allen, V., Elsey, R. M., Jones, N., Wright, J. and Hutchinson, J. R. (2010). Functional specialization and ontogenetic scaling of limb anatomy in *Alligator mississippiensis*. *J. Anat.* **216**, 423-445.

Arnold, A. S., Lee, D. V. and Biewener, A. A. (2013). Modulation of joint moments and work in the goat hindlimb with locomotor speed and surface grade. *J. Exp. Biol.* **216**, 2201-2212.

Arnold, E. N. (1998). Structural niche, limb morphology and locomotion in lacertid lizards (Squamata, Lacertidae); a preliminary survey. *Bull. Nat. Hist. Mus. Lond. (Zool.)* **64**, 63-89.

Ashley-Ross, M. A. (1995). Patterns of hind limb motor output during walking in the salamander, *Dicamptodon tenebrosus*, with comparisons to other tetrapods. *J. Comp. Physiol. (A)* **177**, 273-285.

Astley, H. C. and Roberts, T. J. (2012). Evidence for a vertebrate catapult: elastic energy storage in the plantaris tendon during frog jumping. *Biol. Lett.* **8**, 386-389.

Autumn, K., Hsieh, S. T., Dudek, D. M., Chen, J., Chitaphan, C. and Full, R. J. (2006). Dynamics of geckos running vertically. *J. Exp. Biol.* **209**, 260-272.

Bennett, M. B., Ker, R. F., Imery, N. J. and Alexander, R. M. (1986). Mechanical properties of various mammalian tendons. *J. Zool.* **209**, 537-548.

Biewener, A. and Baudinette, R. (1995). In vivo muscle force and elastic energy storage during steady-speed hopping of tammar wallabies (*Macropus eugenii*). *J. Exp. Biol.* **198**, 1829-1841.

Biewener, A., Alexander, R. M. and Heglund, N. C. (1981). Elastic energy storage in the hopping of kangaroo rats (*Dipodomys spectabilis*). *J. Zool.* **195**, 369-383.

Biewener, A. A. (1998). Muscle function *in vivo*: a comparison of muscles used for elastic energy savings *versus* muscles used to generate mechanical power. *Amer. Zool.* **38**, 703-717.

Biewener, A. A. and Blickhan, R. (1988). Kangaroo rat locomotion: design for elastic energy storage or acceleration? *J. Exp. Biol.* **140**, 243-255.

Biewener, A. A. and Gillis, G. B. (1999). Dynamics of muscle function during locomotion: accommodating variable conditions. *J. Exp. Biol.* **202**, 3387-3396.

Biewener, A. A. and Roberts, T. J. (2000). Muscle and tendon contributions to force, work, and elastic energy savings: a comparative perspective. *Exerc. Sport Sci. Rev.* **28**, 99-107.

Birn-Jeffery, A. V. and Higham, T. E. (2014). Geckos significantly alter foot orientation to facilitate adhesion during downhill locomotion. *Biol. Lett.* **10**.

Blix, M. (1892). Die länge und die spannung des muskels. *Skand. Arch. Physiol.* **3**, 295-318.

Blix, M. (1893). Die länge und die spannung des muskels. *Skand. Arch. Physiol.* **4**, 399-409.

Blix, M. (1894). Die länge und die spannung des muskels. *Skand. Arch. Physiol.* **5**, 173-206.

Brainerd, E. L., Baier, D. B., Gatesy, S. M., Hedrick, T. L., Metzger, K. A., Gilbert, S. L. and Crisco, J. J. (2010). X-ray reconstruction of moving morphology (XROMM): precision, accuracy and applications in comparative biomechanics research. *J. Exp. Zool. A. Ecol. Genet. Physiol.* **313A**, 262-279.

Brinkman, D. (1980). The hind limb step cycle of *Caiman sclerops* and the mechanics of the crocodile tarsus and metatarsus. *Can. J. Zool.* **58**, 2187-2200.

Carlson-Kuhta, P., Trank, T. V. and Smith, J. L. (1998). Forms of forward quadrupedal locomotion. II. A comparison of posture, hindlimb kinematics, and motor patterns for upslope and level walking. *J. Neurophysiol.* **79**, 1687-1701.

Cartmill, M. (1985). Climbing. In *Functional Vertebrate Morphology*, eds. M. Hildebrand D. M. Bramble K. F. Liem and D. B. Wake), pp. 73-88. Cambridge, MA: Harvard University Press.

Collette, B. B. (1961). Correlations between ecology and morphology in anoline lizards from Havana, Cuba, and southern Florida. *Bull. Comp. Mus. Zool.* **125**.

Daley, M. A. and Biewener, A. A. (2003). Muscle force-length dynamics during level versus incline locomotion: a comparison of *in vivo* performance of two guinea fowl ankle extensors. *J. Exp. Biol.* **206**, 2941-2958.

De Leon, R., Hodgson, J. A., Roy, R. R. and Edgerton, V. R. (1994). Extensor- and flexor-like modulation within motor pools of the rat hindlimb during treadmill locomotion and swimming. *Brain Res.* **654**, 241-250.

Deban, S. M., Schilling, N. and Carrier, D. R. (2012). Activity of extrinsic limb muscles in dogs at walk, trot and gallop. *J. Exp. Biol.* **215**, 287-300.

Demes, B., Larson, S. G., Stern Jr, J. T., Jungers, W. L., Biknevicius, A. R. and Schmitt, D. (1994). The kinetics of primate quadrupedalism: "hindlimb drive" reconsidered. *J. Hum. Evol.* **26**, 353-374.

Donley, J. M. and Shadwick, R. E. (2003). Steady swimming muscle dynamics in the leopard shark *Triakis semifasciata*. *J. Exp. Biol.* **206**, 1117-1126.

Donley, J. M., Shadwick, R. E., Sepulveda, C. A., Konstantinidis, P. and Gemballa, S. (2005). Patterns of red muscle strain/activation and body kinematics during steady swimming in a lamnid shark, the shortfin mako (*Isurus oxyrinchus*). *J. Exp. Biol.* **208**, 2377-2387.

Farley, C. and Emshwiller, M. (1996). Efficiency of uphill locomotion in nocturnal and diurnal lizards. *J. Exp. Biol.* **199**, 587-592.

Filipe, V. M., Pereira, J. E., Costa, L. M., Maurício, A. C., Couto, P. A., Melo-Pinto, P. and Varejão, A. S. P. (2006). Effect of skin movement on the analysis of hindlimb kinematics during treadmill locomotion in rats. *J. Neurosci. Methods* **153**, 55-61.

Fischer, M. S., Krause, C. and Lilje, K. E. (2010). Evolution of chameleon locomotion, or how to become arboreal as a reptile. *Zoology* **113**, 67-74.

Foster, K. L. and Higham, T. E. (2012). How fore- and hindlimb function changes with incline and perch diameter in the green anole, *Anolis carolinensis*. *J. Exp. Biol.* **215**, 2288-2300.

Foster, K. L. and Higham, T. E. (2014). Context-dependent changes in motor control and kinematics during locomotion: modulation and decoupling. *Proc. R. Soc. B.* **281**, 20133331.

Fowler, E. G., Gregor, R. J., Hodgson, J. A. and Roy, R. R. (1993). Relationship between ankle muscle and joint kinetics during the stance phase of locomotion in the cat. *J. Biomech.* **26**, 465-483.

Franz, T. M., Demes, B. and Carlson, K. J. (2005). Gait mechanics of lemurid primates on terrestrial and arboreal substrates. *J. Hum. Evol.* **48**, 199-217.

Full, R. J., Blickhan, R. and Ting, L. H. (1991). Leg design in hexapedal runners. *J. Exp. Biol.* **158**, 369-390.

Gabaldón, A. M., Nelson, F. E. and Roberts, T. J. (2001). Gastrocnemius muscle mechanics in turkeys during uphill and downhill running. *Amer. Zool.* **41**, 1448.

Gabaldón, A. M., Nelson, F. E. and Roberts, T. J. (2004). Mechanical function of two ankle extensors in wild turkeys: shifts from energy production to energy absorption during incline versus decline running. *J. Exp. Biol.* **207**, 2277-2288.

Gálvez-López, E., Maes, L. D. and Abourachid, A. (2011). The search for stability on narrow supports: an experimental study in cats and dogs. *Zoology* **114**, 224-232.

Gans, C. and de Vree, F. (1987). Functional bases of fiber length and angulation in muscle. *J. Morphol.* **192**, 63-85.

Garland, T., Jr. and Losos, J. B. (1994). Ecological morphology of locomotor performance in squamate reptiles. In *Ecological Morphology: integrative organismal biology*, eds. P. C. Wainwright and S. M. Reilly), pp. 240-302. Chicago: University of Chicago Press.

Gillis, G. B. and Biewener, A. A. (2002). Effects of surface grade on proximal hindlimb muscle strain and activation during rat locomotion. *J. Appl. Physiol.* **93**, 1731-1743.

Gilman, C. A., Bartlett, M. D., Gillis, G. B. and Irschick, D. J. (2012). Total recoil: perch compliance alters jumping performance and kinematics in green anole lizards (*Anolis carolinensis*). *J. Exp. Biol.* **215**, 220-226.

Goldman, D. I., Chen, T. S., Dudek, D. M. and Full, R. J. (2006). Dynamics of rapid vertical climbing in cockroaches reveals a template. *J. Exp. Biol.* **209**, 2990-3000.

Gregersen, C. S., Silverton, N. A. and Carrier, D. R. (1998). External work and potential for elastic storage at the limb joints of running dogs. *J. Exp. Biol.* **201**, 3197-3210.

Haines, R. W. (1952). The shoulder joint of lizards and the primitive reptilian shoulder mechanism. *J. Anat.* **86**, 412-422.

Harmon, L. J. and Losos, J. B. (2005). The effect of intraspecific sample size on type I and type II error rates in comparative studies. *Evolution* **59**, 2705-2710.

Haxton, H. A. (1944). Absolute muscle force in the ankle flexors of man. *J. Physiol.* **103**, 267-273.

Hedrick, T. L. (2008). Software techniques for two- and three-dimensional kinematic measurements of biological and biomimetic systems. *Bioinspir. Biomim.* **3**, 034001.

Herrel, A., Vanhooydonck, B., Porck, J. and Irschick, D. J. (2008a). Anatomical basis of differences in locomotor behavior in *Anolis* lizards: a comparison between two ecomorphs. *Bull. Mus. Comp. Zool.* **159**, 213-238.

Herrel, A., Schaerlaeken, V., Ross, C., Meyers, J., Nishikawa, K., Abdala, V., Manzano, A. and Aerts, P. (2008b). Electromyography and the evolution of motor control: limitations and insights. *Integr. Comp. Biol.* **48**, 261-271.

Herzog, W. (2000). Muscle properties and coordination during voluntary movement. *J. Sports Sci.* **18**, 141-152.

Higham, T. E. and Jayne, B. C. (2004a). Locomotion of lizards on inclines and perches: hindlimb kinematics of an arboreal specialist and a terrestrial generalist. *J. Exp. Biol.* **207**, 233-248.

Higham, T. E. and Jayne, B. C. (2004b). *In vivo* muscle activity in the hindlimb of the arboreal lizard, *Chamaeleo calyptratus*: general patterns and the effects of incline. *J. Exp. Biol.* **207**, 249-261.

Higham, T. E. and Biewener, A. A. (2008). Integration within and between muscles during terrestrial locomotion: effects of incline and speed. *J. Exp. Biol.* **211**, 2303-2316.

Higham, T. E. and Nelson, F. E. (2008). The integration of lateral gastrocnemius muscle function and kinematics in running turkeys. *Zoology* **111**, 483-493.

Higham, T. E., Davenport, M. S. and Jayne, B. C. (2001). Maneuvering in an arboreal habitat: the effects of turning angle on the locomotion of three sympatric ecomorphs of *Anolis* lizards. *J. Exp. Biol.* **204**, 4141-4155.

Hill, A. V. (1922). The maximum work and mechanical efficiency of human muscles, and their most economical speed. *J. Physiol.* **56**, 19-41.

Hill, A. V. (1938). The heat of shortening and the dynamic constants of muscle. *Proc. R. Soc. B.* **126**, 136-195.

Hill, A. V. (1949). The onset of contraction. *Proc. R. Soc. B.* **136**, 242-254.

Hill, A. V. (1951). The transition from rest to full activity in muscle: the velocity of shortening. *Proc. R. Soc. B.* **138**, 329-338.

Hill, A. V. (1953). The mechanics of active muscle. *Proc. R. Soc. B.* **141**, 104-117.

Huey, R. B. and Hertz, P. E. (1982). Effects of body size and slope on sprint speed of a lizard (*Stellio* (*Agama*) *stellio*). *J. Exp. Biol.* **97**, 401-409.

Humphry. (1876). On the comparison of the fore and hind limbs in vertebrates. *J. Anat. Physiol.* **10**, 659-671.

Irschick, D. J. and Jayne, B. C. (1998). Effects of incline on speed, acceleration, body posture and hindlimb kinematics in two species of lizard *Callisaurus draconoides* and *Uma scoparia*. *J. Exp. Biol.* **201**, 273-287.

Irschick, D. J. and Jayne, B. C. (1999). A field study of the effects of incline on the escape locomotion of a bipedal lizard, *Callisaurus draconoides*. *Phys. Biochem. Zool.* **72**, 44-56.

Irschick, D. J. and Losos, J. B. (1999). Do lizards avoid habitats in which performance is submaximal? The relationship between sprinting capabilities and structural habitat use in Caribbean anoles. *Amer. Nat.* **154**, 293-305.

Irschick, D. J., Carlisle, E., Elstrott, J., Ramos, M., Buckley, C., Vanhooydonck, B., Meyers, J. A. Y. and Herrel, A. (2005). A comparison of habitat use, morphology, clinging performance and escape behaviour among two divergent green anole lizard (*Anolis carolinensis*) populations. *Biol. J. Linn. Soc.* **85**, 223-234.

Jayne, B. C. and Irschick, D. J. (1999). Effects of incline and speed on the three-dimensional hindlimb kinematics of a generalized iguanian lizard (*Dipsosaurus dorsalis*). *J. Exp. Biol.* **202**, 143-159.

Jenkins, F. A. and Goslow, G. E. (1983). The functional anatomy of the shoulder of the savannah monitor lizard (*Varanus exanthematicus*). *J. Morphol.* **175**, 195-216.

Johnston, I. A. (1991). Muscle action during locomotion: a comparative perspective. *J. Exp. Biol.* **160**, 167-185.

Katz, S. L. and Shadwick, R. E. (1998). Curvature of swimming fish midlines as an index of muscle strain suggests swimming muscle produces net positive work. *J. Theor. Biol.* **193**, 243-256.

Kimura, T., Okada, M. and Ishida, H. (1979). Kinesiological characteristics of primate walking: Its significance in human walking. In *Environment, Behavior and Morphology: Dynamic Interactions in Primates*, eds. M. Morbeck and H. Preuschoft), pp. 297-311. New York: Gustav Fischer.

Klopfer, P. H. and MacArthur, R. H. (1960). Niche size and faunal diversity. *Amer. Nat.* **94**, 293-300.

Kohlsdorf, T. and Biewener, A. A. (2006). Negotiating obstacles: running kinematics of the lizard *Sceloporus malachiticus*. *J. Zool. Lond.* **270**, 359-371.

Lammers, A. R. (2007). Locomotor kinetics on sloped arboreal and terrestrial substrates in a small quadrupedal mammal. *Zoology* **110**, 93-103.

Lammers, A. R. and Biknevicius, A. R. (2004). The biodynamics of arboreal locomotion: the effects of substrate diameter on locomotor kinetics in the gray short-tailed opossum (*Monodelphis domestica*). *J. Exp. Biol.* **207**, 4325-4336.

Lammers, A. R. and Gauntner, T. (2008). Mechanics of torque generation during quadrupedal arboreal locomotion. *J. Biomech.* **41**, 2388-2395.

Lammers, A. R. and Zurcher, U. (2011). Stability during arboreal locomotion. In *Theoretical Biomechanics*, (ed. V. Klika), pp. 319-334. Rijeka: InTech.

Lammers, A. R., Earls, K. D. and Biknevicius, A. R. (2006). Locomotor kinetics and kinematics on inclines and declines in the gray short-tailed opossum *Monodelphis domestica*. *J. Exp. Biol.* **209**, 4154-4166.

Larson, S. G., Schmitt, D., Lemelin, P. and Hamrick, M. (2000). Uniqueness of primate forelimb posture during quadrupedal locomotion. *Am. J. Phys. Anthropol.* **112**, 87-101.

Larson, S. G., Schmitt, D., Lemelin, P. and Hamrick, M. (2001). Limb excursion during quadrupedal walking: how do primates compare to other mammals? *J. Zool.* **255**, 353-365.

Lee, D. V. (2010). Effects of grade and mass distribution on the mechanics of trotting in dogs. *J. Exp. Biol.* **214**, 402-411.

Licht, P. (1968). Response of the thermal preferendum and heat resistance to thermal acclimation under different photoperiods in the lizard *Anolis carolinensis*. *American Midland Naturalist* **79**, 149-158.

Lieber, R. L. and Ward, S. R. (2011). Skeletal muscle design to meet functional demands. *Philos. Trans. R. Soc. Lond. B. Biol. Sci.* **366**, 1466-1476.

Loeb, G. E. and Gans, C. (1986). The organization of muscle. In *Electromyography for Experimentalists*, pp. 25-43. London: University of Chicago Press.

Losos, J. B. (1990a). Ecomorphology, performance capability, and scaling of West Indian *Anolis* lizards: an evolutionary analysis. *Ecol. Monogr.* **60**, 369-388.

Losos, J. B. (1990b). The evolution of form and function: morphology and locomotor performance in West Indian *Anolis* lizards. *Evolution* **44**, 1189-1203.

Losos, J. B. (1992). The evolution of convergent structure in Caribbean *Anolis* communities. *Syst. Biol.* **41**, 403-420.

Losos, J. B. (1994). Integrative approaches to evolutionary ecology: *Anolis* lizards as model systems. *Annu. Rev. Ecol. Syst.* **25**, 467-493.

Losos, J. B. (1995). Community evolution in Greater Antillean *Anolis* lizards: phylogenetic patterns and experimental tests. *Philos. Trans. R. Soc. Lond. B. Biol. Sci.* **349**, 69-75.

Losos, J. B. (2009). Lizards in an Evolutionary Tree: Ecology and Adaptive Radiation of Anoles. Berkeley, CA: University of California Press.

Losos, J. B. and Sinervo, B. (1989). The effects of morphology and perch diameter on sprint performance of *Anolis* lizards. *J. Exp. Biol.* **145**, 23-30.

Losos, J. B. and Irschick, D. J. (1996). The effect of perch diameter on escape behaviour of *Anolis* lizards: laboratory predictions and field tests. *Anim. Behav.* **51**, 593-602.

Losos, J. B., Gannon, M. R., Pfeiffer, W. J. and Waide, R. B. (1990). Notes on the ecology and behavior of *Anolis cuvieri* (Lacertilia: Iguanidae) in Puerto Rico. *Carib. J. Sci.* **26**, 65-66.

Mahler, D. L., Revell, L. J., Glor, R. E. and Losos, J. B. (2010). Ecological opportunity and the rate of morphological evolution in the diversification of Greater Antillean anoles. *Evolution* **64**, 2731-2745.

Matson, A., Konow, N., Miller, S., Konow, P. P. and Roberts, T. J. (2012). Tendon material properties vary and are interdependent among turkey hindlimb muscles. *J. Exp. Biol.* **215**, 3552-3558.

Mattingly, W. B. and Jayne, B. C. (2004). Resource use in arboreal habitats: structure affects locomotion of four ecomorphs of *Anolis* lizards. *Ecology* **85**, 1111-1124.

McGowan, C. P., Baudinette, R. V. and Biewener, A. A. (2005). Joint work and power associated with acceleration and deceleration in tammar wallabies (*Macropus eugenii*). *J. Exp. Biol.* **208**, 41-53.

McGowan, C. P., Neptune, R. R. and Kram, R. (2008). Independent effects of weight and mass on plantar flexor activity during walking: implications for their contributions to body support and forward propulsion. *J. Appl. Physiol.* **105**, 486-494.

Medler, S. (2002). Comparative trends in shortening velocity and force production in skeletal muscles. *Amer. J. Physiol. Reg. Integr. Comp. Physiol.* **283**, R368-R378.

Nakano, Y. (2002). The effects of substratum inclination on locomotor patterns in primates. *Z. Morphol. Anthropol.* **83**, 189-199.

Nelson, F. E., Gabaldón, A. M. and Roberts, T. J. (2004). Force-velocity properties of two avian hindlimb muscles. *Comparative Biochemistry and Physiology Part A: Molecular & Integrative Physiology* **137**, 711-721.

Olberding, J. P., McBrayer, L. M. and Higham, T.E. (2012). Performance and three-dimensional kinematics of bipedal lizards during obstacle negotiation. *J. Exp. Biol.* **215**, 247-255.

Olson, J. M. and Marsh, R. L. (1998). Activation patterns and length changes in hindlimb muscles of the bullfrog *Rana catesbeiana* during jumping. *J. Exp. Biol.* **201**, 2763-2777.

Payne, R. C., Crompton, R. H., Isler, K., Savage, R., Vereecke, E. E., Günther, M. M., Thorpe, S. K. S. and D'Août, K. (2006). Morphological analysis of the hindlimb in apes and humans. II. Moment arms. *J. Anat.* **208**, 725-742.

Perry, G., LeVering, K., Girard, I. and Garland, T., Jr. (2004). Locomotor performance and social dominance in male *Anolis cristatellus*. *Anim. Behav.* **67**, 37-47.

Peterson, J. A. (1971). Functional morphology of the shoulder in *Chamaeleo* and *Anolis*. *Am. Zool.* **11**, 704-705.

Peterson, J. A. (1973). Adaptation for arboreal locomotion in the shoulder region of lizards. In *Department of Anatomy*. Chicago, IL: University of Chicago.

Peterson, J. A. (1974). In *The Second Anolis Newsletter*, (ed. E. E. Williams). Cambridge, MA: Museum of Comparative Zoology, Harvard University.

Peterson, J. A. (1984). The locomotion of *Chamaeleo* (Reptilia: Sauria) with particular reference to the forelimb. *J. Zool.* **202**, 1-42.

Pollock, C. M. and Shadwick, R. E. (1994a). Allometry of muscle, tendon, and elastic energy storage capacity in mammals. *Amer. J. Physiol. Reg. Integr. Comp. Physiol.* **266**, R1022-R1031.

Pollock, C. M. and Shadwick, R. E. (1994b). Relationship between body mass and biomechanical properties of limb tendons in adult mammals. *Amer. J. Physiol. Reg. Integr. Comp. Physiol.* **266**, 1016-1021.

Pounds, J. A. (1988). Ecomorphology, locomotion, and microhabitat structure: patterns in a tropical mainland *Anolis* community. *Ecol. Monogr.* **58**, 299-320.

Preuschoft, H. (2002). What does "arboreal locomotion" mean exactly and what are the relationships between "climbing", environment and morphology? *Z. Morphol. Anthropol.* **83**, 171-188.

Rassier, D. E., MacIntosh, B. R. and Herzog, W. (1999). Length dependence of active force production in skeletal muscle. *J. Appl. Physiol.* **86**, 1445-1457.

Reynolds, T. R. (1985). Mechanics of increased support of weight by the hindlimbs in primates. *Am. J. Phys. Anthropol.* **67**, 335-349.

Richmond, F. J. R. (1998). Elements of style in neuromuscular architecture. *Amer. Zool.* **38**, 729-742.

Rivera, A. R. V. and Blob, R. W. (2010). Forelimb kinematics and motor patterns of the slider turtle (*Trachemys scripta*) during swimming and walking: shared and novel strategies for meeting locomotor demands of water and land. *J. Exp. Biol.* **213**, 3515-3526.

Roberts, T. J. and Gabaldón, A. M. (2008). Interpreting muscle function from EMG: lessons learned from direct measurements of muscle force. *Integr. Comp. Biol.* **48**, 312-320.

Roberts, T. J. and Azizi, E. (2011). Flexible mechanisms: the diverse roles of biological springs in vertebrate movement. *J. Exp. Biol.* **214**, 353-361.

Roberts, T. J., Marsh, R. L., Weyand, P. G. and Taylor, C. R. (1997). Muscular force in running turkeys: the economy of minimizing work. *Science* **275**, 1113-1115.

Roberts, T. J., Higginson, B. K., Nelson, F. E. and Gabaldón, A. M. (2007). Muscle strain is modulated more with running slope than speed in wild turkey knee and hip extensors. *J. Exp. Biol.* **210**, 2510-2517.

Russell, A. P. and Bauer, A. M. (2008). The appendicular locomotor apparatus of *Sphenodon* and normal-limbed squamates. In *Biology of the Reptilia*, vol. 21, Morphology I, The Skull and Appendicular Locomotor Apparatus of the Lepidosauria eds. C. Gans A. Gaunt, S. and K. Adler), pp. 1-466. Ithaca, New York: Society for the Study of Amphibians and Reptiles.

Russell, A. P. and Bels, V. (2001a). Biomechanics and kinematics of limb-based locomotion in lizards: review, synthesis and prospectus. *Comp. Biochem. Physiol. A. Physiol.* **131**, 89-112.

Russell, A. P. and Bels, V. (2001b). Digital Hyperextension in *Anolis sagrei*. *Herpetologica* **57**, 58-65.

Sacks, R. D. and Roy, R. R. (1982). Architecture of the hind limb muscles of cats: functional significance. *J. Morphol.* **173**, 185-195.

Sanderson, S. L. (1990). Versatility and specialization in labrid fishes: ecomorphological implications. *Oecologia* **84**, 272-279.

Schmidt, A. and Fischer, M. S. (2010). Arboreal locomotion in rats – the challenge of maintaining stability. *J. Exp. Biol.* **213**, 3615-3624.

Schmidt, A. and Fischer, M. S. (2011). The kinematic consequences of locomotion on sloped arboreal substrates in a generalized (*Rattus norvegicus*) and a specialized (*Sciurus vulgaris*) rodent. *J. Exp. Biol.* **214**, 2544-2559.

Schmitt, D. (1994). Forelimb mechanics as a function of substrate type during quadrupedalism in two anthropoid primates. *J. Hum. Evol.* **26**, 441-457.

Schmitt, J. and Bonnono, S. (2009). Dynamics and stability of lateral plane locomotion on inclines. *J. Theor. Biol.* **261**, 598-609.

Shadwick, R. E. and Syme, D. A. (2008). Thunniform swimming: muscle dynamics and mechanical power production of aerobic fibres in yellowfin tuna (*Thunnus albacares*). *J. Exp. Biol.* **211**, 1603-1611.

Shadwick, R. E., Steffensen, J. F., Katz, S. L. and Knower, T. (1998). Muscle dynamics in fish during steady swimming. *Amer. Zool.* **38**, 755-770.

Snyder, R. C. (1954). The anatomy and function of the pelvic girdle and hindlimb in lizard locomotion. *Am. J. Anat.* **95**, 1-45.

Spezzano, L. C. and Jayne, B. C. (2004). The effects of surface diameter and incline on the hindlimb kinematics of an arboreal lizard (*Anolis sagrei*). *J. Exp. Biol.* **207**, 2115-2131.

Taylor, C. R., Caldwell, S. L. and Rowntree, V. J. (1972). Running up and down hills: some consequences of size. *Science* **178**, 1096-1097.

Toro, E., Herrel, A. and Irschick, D. J. (2004). The evolution of jumping performance in Caribbean *Anolis* lizards: solutions to biomechanical trade-offs. *Am. Nat.* **163**, 844-856.

Vanhooydonck, B., Herrel, A. and Irschick, D. J. (2006a). Out on a limb: the differential effect of substrate diameter on acceleration capacity in *Anolis* lizards. *J. Exp. Biol.* **209**, 4515-4523.

Vanhooydonck, B., Aerts, P., Irschick, D. J. and Herrel, A. (2006b). Power generation during locomotion in *Anolis* lizards: an ecomorphological approach. In *Ecology and Biomechanics: A mechanical approach to the ecology of animals and plants*, eds. A. Herrel T. Speck and N. P. Rowe), pp. 253-269. Boca Raton, Florida: CRC Press.

Vilensky, J. A., Moore, A. M. and Libii, J. N. (1994). Squirrel monkey locomotion on an inclined treadmill: implications for the evolution of gaits. *J. Hum. Evol.* **26**, 375-386.

Walmsley, B., Hodgson, J. A. and Burke, R. E. (1978). Forces produced by medial gastrocnemius and soleus muscles during locomotion in freely moving cats. *J. Neurophysiol.* **41**, 1203-1216.

Wells, J. B. (1965). Comparison of mechanical properties between slow and fast mammalian muscles. *J. Physiol.* **178**, 252-269.

Williams, E. E. (1972). The origin of faunas. Evolution of lizard congeners in a complex island fauna: a trial analysis. *Evol. Biol.* **6**, 47-89.

Wilson, A. and Lichtwark, G. (2011). The anatomical arrangement of muscle and tendon enhances limb versatility and locomotor performance. *Philos. Trans. R. Soc. Lond. B. Biol. Sci.* **366**, 1540-1553.

Zaaf, A., Herrel, A., Aerts, P. and De Vree, F. (1999). Morphology and morphometrics of the appendicular musculature in geckoes with different locomotor habits (Lepidosauria). *Zoomorph.* **119**, 9-22.

Zaaf, A., Van Damme, R., Herrel, A. and Aerts, P. (2001). Spatio-temporal gait characteristics of level and vertical locomotion in a ground-dwelling and a climbing gecko. *J. Exp. Biol.* **204**, 1233-1246.

Zani, P. A. (2000). The comparative evolution of lizard claw and toe morphology and clinging performance. *J. Evol. Biol.* **13**, 316-325.

Zar, J. H. (1999). Biostatistical Analysis. Upper Saddle River: Prentice Hall.

Zihlman, A. L., McFarland, R. K. and Underwood, C. E. (2011). Functional anatomy and adaptation of male gorillas (*Gorilla gorilla gorilla*) with comparison to male orangutans (*Pongo pygmaeus*). *Anat. Rec.* **294**, 1842-1855.